

# SLOVAK GEOLOGICAL MAGAZINE

VOLUME 8 NO 2

ISSN 1335-096X

<i>Rapant, S.</i> : Foreword	107
<i>Ivan, P.</i> : Relict Magmatic Minerals and Textures in the HP/LT Metamorphosed Oceanic Rocks of the Triassic-Jurassic Meľjata Ocean (Inner Western Carpathians)	109
<i>Čurlík, J. and Šefčík, P.</i> : Soils and sediments testing for contamination by heavy metals – some case studies in Slovakia	123
<i>Rapant, S., Khun, M., Jurkovič, L. and Lelkovičová, M.</i> : Potential Influence of Geochemical Background on the Health State of Population of the Slovak Republic	137
<i>Kordík, J., van Lanen, H. A. J. and Dijkstra, R.</i> : Monitoring and the FLONET/TRANS model as tools to characterize the nitrate distribution and transport in the Noor catchment (the Netherlands)	147
<i>András, P., Kotulová, J., Haškova, A. and Luptáková, J.</i> : Origin and evolution of ore-forming fluids at Pezinok-Kolársky Vrch 86 deposit (Western Carpathians, Slovakia)	159
<i>Rapant, S., Bodiš, D., Mackových, D. and Pramuka, S.</i> : Distribution of Si in Stream Sediments of Slovakia – an Amendment to the Geochemical Atlas of the Slovak Republic	171



Geological Survey of Slovak Republic, Bratislava  
Dionýz Štúr Publishers

## 2/2002

## **SLOVAK GEOLOGICAL MAGAZINE**

Periodical journal of Geological Survey of Slovak Republic is a quarterly presenting the results of investigation and researches in a wide range of topics:

- regional geology and geological maps
- lithology and stratigraphy
- petrology and mineralogy
- paleontology
- geochemistry and isotope geology
- geophysics and deep structure
- geology of deposits and metallogeny
- tectonics and structural geology
- hydrogeology and geothermal energy
- environmental geochemistry
- engineering geology and geotechnology
- geological factors of the environment
- petroarcheology

The journal is focused on problems of the Alpine-Carpathian region.

---

### **Editor in Chief**

JOZEF HÓK

### **Editorial Board**

#### INTERNAL MEMBER

Vladimír <b>Bezák</b>	Jaroslav <b>Lexa</b>
Miroslav <b>Bielik</b>	Karol <b>Marsina</b>
Dušan <b>Bodiš</b>	Ján <b>Mello</b>
Pavol <b>Grecula</b>	Jozef <b>Michalík</b>
Vladimír <b>Hanzel</b>	Milan <b>Polák</b>
Juraj <b>Janočko</b>	Michal <b>Potfaj</b>
Michal <b>Kaličiak</b>	Martin <b>Radvanec</b>
Michal <b>Kováč</b>	Dionýz <b>Vass</b>
Ján <b>Král'</b>	Anna <b>Vozárová</b>

#### EXTERNAL MEMBERS

Dimitros <b>Papanikolaou</b>	Athens
Franz <b>Neubauer</b>	Salzburg
Jan <b>Veizer</b>	Bochum
Franco Paolo <b>Sassi</b>	Padova
Niek <b>Rengers</b>	Enschede
Géza <b>Császár</b>	Budapest
Miloš <b>Suk</b>	Brno
Zdeněk <b>Kukal</b>	Praha
Vladica <b>Cvetkovic</b>	Beograd
Nestor <b>Oszczypko</b>	Kraków

---

**Managing Editor:** G. Šipošová

**Language review and translation:** M. Ondrášik

**Technical Editor:** G. Šipošová

**Address of the publishers:** Geological Survey of Slovak Republic, Mlynská dolina 1, 817 04 Bratislava, Slovakia

**Printed at:** Gupress Bratislava

Ústredná geologická knižnica SR  
ŠGÚDŠ

**Annual subscrij**

© Geological Survey of Slovak Rept



3902001018508

clude the postage

, 817 04 Bratislava, SLOVAKIA

---

---

# SLOVAK GEOLOGICAL MAGAZINE

VOLUME 8 NO 2

ISSN 1335-096X

---



Geological Survey of Slovak Republic, Bratislava  
Dionýz Štúr Publishers

**2/2002**



## Foreword

Distribution of chemical elements on the Earth is not random, but related and controlled by a broad complex of conditions and processes, study of those is in focus of Geochemistry. Geochemistry, compared to other natural sciences about Earth, is relatively young scientific field. In their youth it came out of knowledge from other natural scientific areas, but nowadays the level of geochemical information already essentially influences the development and information virtually in all other branches of geological sciences. In last decades a trend of significant enforcement of Geochemistry in the subject of formation and protection of the environment was apparent. Obviously, no environmental information could be really unbiased without objective geochemical information about the level and grade of contamination of waters, soils, sediments and rocks.

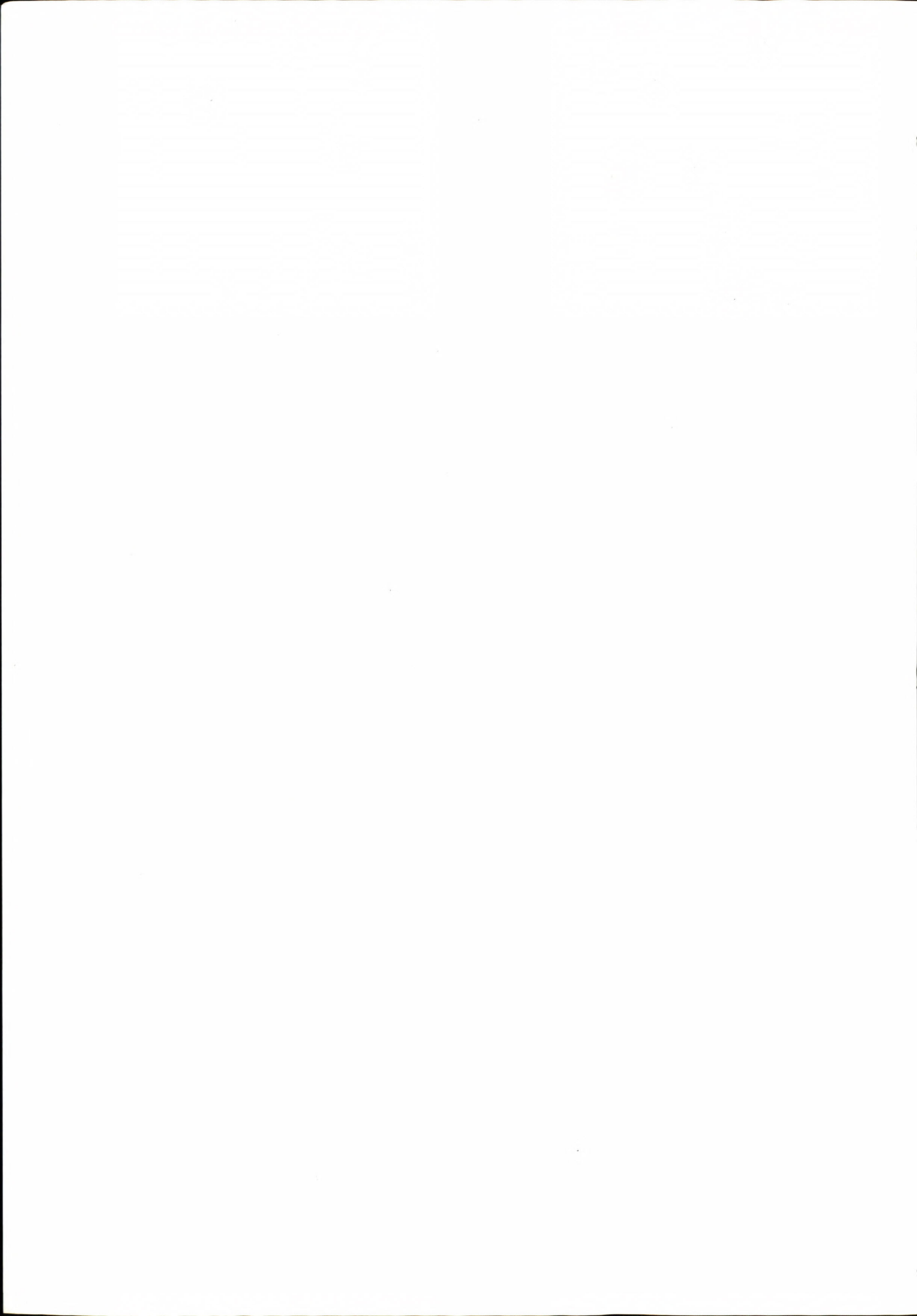
In Slovakia the beginning of geochemical information primarily of mineralogical-geochemical type is possible to trace predominantly in historical mining activity that in our country has a tradition since Middle Ages. The development of Geochemistry, as an independent branch of science, started in Slovakia only in the second half of 20<sup>th</sup> century. Gradually, all basic branches and trends of Geochemistry were elaborated, including theoretical, laboratory-experimental, as well as applied fixation.

In the last years in Slovakia the latest geochemical information is presented on professional seminars „*GEOCHÉMIA (GEOCHEMISTRY)*“, organised annually by the Geological Survey of the Slovak Republic, Bratislava and Faculty of Natural Sciences of the Comenius University, Bratislava.

In the current single-subject volume selected contributions from the years 2000 and 2001 are presented. Even the focus of individual published contributions obviously shows that in Slovakia nowadays studied geochemical problems are really manifold, from the scientific, subject-matter, as well as methodical point of view. It includes the problems of endogenous and exogenous geochemistry, geochemistry of ore deposits, furthermore broad problems of environmental geochemistry up to medical geochemistry.

Finally, I would like to express my gratitude to authors of individual contributions as well as to reviewers (anonymous) who read the manuscripts and suggested many helpful changes.

S. Rapant



## Relict Magmatic Minerals and Textures in the HP/LT Metamorphosed Oceanic Rocks of the Triassic-Jurassic Meliata Ocean (Inner Western Carpathians)

PETER IVAN

Department of Geochemistry, Comenius University, Mlynská dolina G, 842 15 Bratislava, Slovak Republic

*Abstract:* High-pressure low-temperature (HP/LT) metamorphosed rocks of the Meliatic Unit (inner Western Carpathians) were formed during the Middle/Upper Jurassic subduction of the Mesozoic Meliata Ocean. They have been found in the form of variable in size bodies (from dm to km) in the mélange-like formations of the Bôrka Nappe (Hačava and Kobeliarovo Fms.), in the Bodva Valley Ophiolite Formation and also as recycled material in the Upper Cretaceous Gosau-type conglomerates from Dobšinská Ľadová Jaskyňa settlement.

Their original magmatic textures are observable due to selective replacement of magmatic minerals by metamorphic mineral assemblage or distribution of fine pigment of Fe-Ti oxides (ghost textures). Preserved textures suggest that most of these rocks were originally represented by basalts and dolerites, rarely even by gabbro, formed in the upper part of the oceanic crust of the Meliata Ocean. Lava solidification speed and the contact with the specific environment as well were the cause of variability in textures. In the basalts ophitic and subophitic textures were most widespread, furthermore glomeroophitic, intersertal, variolitic and vitritic textures have been identified. Rapid cooling mostly on the contact with water or rocks chilled margins or autoclastic lava breccia originated whereas on the contact with carbonaceous mud peperites and hyaloclastites occurred. Intrusive magmatic rocks had originally doleritic or gabbroic textures. Relic clinopyroxene is only preserved magmatic mineral. Its composition in accordance with whole-rock geochemical data indicates back-arc basin basalt (BABB) signature of these HP/LT metamorphosed basaltic rocks. The comparison of the magmatic clinopyroxene compositions from subducted (HP/LT metamorphosed) and obducted (LP/LT metamorphosed) basalts of the Meliatic Ocean confirmed results of previous geochemical study, that the crust of initial and early stages of the Meliata Ocean opening had been subducted while crust of evolved stage with basalts close to normal mid-ocean ridge basalt (N-MORB) had been mostly obducted. Identification of basalts, dolerites and also gabbros among the HP/LT metamorphosed rocks suggests for normal oceanic crust already in the early stage of Meliata Ocean opening. Traces of the oceanic ridge type metamorphism in dolerites and gabbros support this assumption. Metamorphic alteration of oceanic rocks in the subduction zone evolved progressively to HP/LT conditions, relic minerals of previous low-pressure stages are rarely preserved. Only a part of them was retrogressed during exhumation.

*Key words:* Meliata Ocean, oceanic crust, blueschists, magmatic relicts

### Introduction

The origin, opening and subsequent subduction of the Triassic-Jurassic Meliata Ocean represents events that have markedly influenced the Alpine history of Western Carpathians. Despite the fact that the Meliata (or Meliata-Hallstatt) Ocean occurs in many schemes of Mesozoic geotectonic evolution (Stampfli, 1996; Channell and Kozur, 1997; Plašienka, 2000; Golonka et al., 2000; Neugebauer et al., 2001, and others) detailed data about its origin and texture are still missing. Our knowledge comes out mostly from lithological and facial studies of sedimentary rocks (Kozur and Mock, 1997; Channell and Kozur, 1997; Mello et al., 1997; Schweigl and Neubauer, 1997, and others). Less the knowledge is based on the understanding of the rocks, forming the sea-floor of this ocean – magmatic rocks of the oceanic crust. This is probably due to their relatively rare occurrence – oceanic crust rocks are preserved only as blocks of variable size

in melanges or as small tectonic slices (Ivan et al., 1994). Furthermore shortly after their formation in an oceanic rift as well as during following accretion, eventually subduction, metamorphic processes modified their original petrographic and partially also their geochemical characteristics. Despite of this fact, also in some of the mostly altered rocks experienced metamorphic alteration in high-pressure low temperature conditions, relics of magmatic minerals and textures have been preserved. The aim of this study is to summarised data about relicts of the magmatic stage of evolution in HP/LT metamorphosed relicts of the Meliata Ocean oceanic crust and so to contribute to better knowledge of its geological history.

### Geology of HP/LT metamorphosed oceanic rocks in the Meliaticum unit

Rock complexes of Inner Western Carpathians, related to the evolution of the Meliata oceanic basin, are

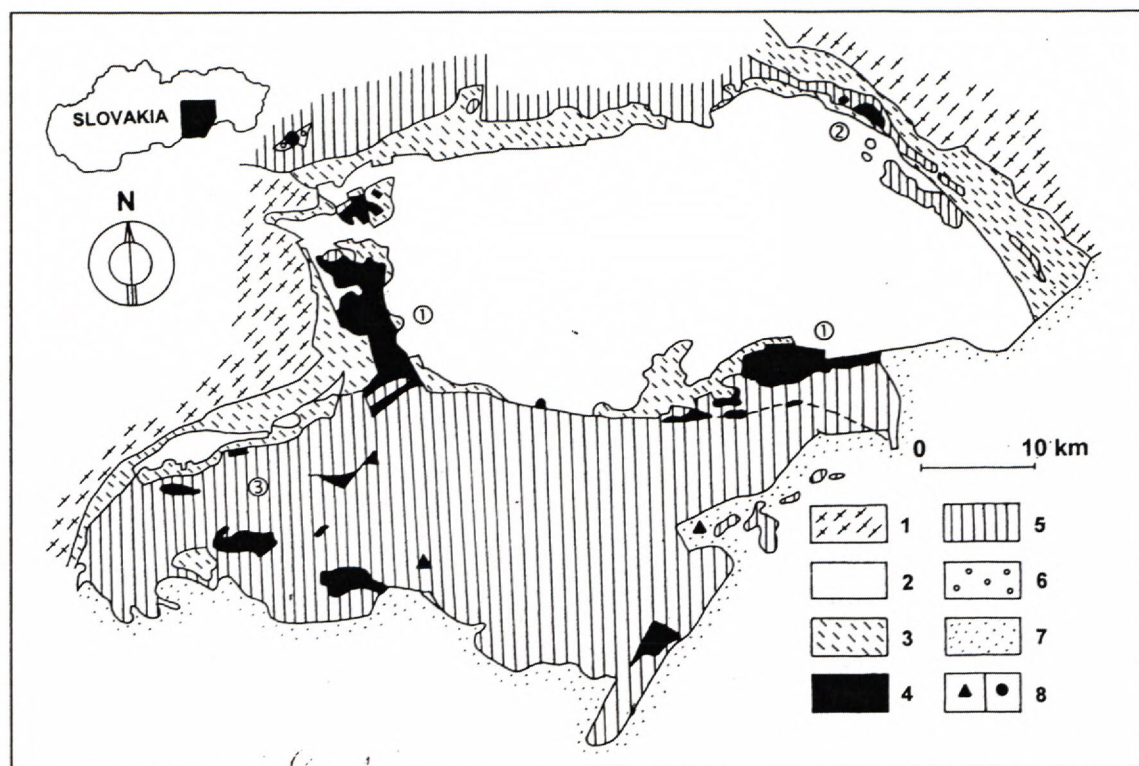


Fig. 1: Geological units with oceanic crust relicts of the Meliata Ocean in the Inner Western Carpathians.

Explanations: 1 – Veporicum unit, 2 – Early Paleozoic of the Gemicum unit, 3 – Late Paleozoic of the Gemicum unit, 4 – Formations with oceanic crust relicts of the Meliata Ocean (Meliatic Unit), 5 – other Mesozoic formations of the Inner Western Carpathians, 6 – Gosau-type Cretaceous conglomerates from Dobšinská ľadová jaskyňa settlement, 7 – Neogene, 8 – HP/LT metamorphosed oceanic rocks in boreholes (Bodva Valley Ophiolite Fm.; triangle) and in Cretaceous conglomerates (filled circle); 1 – Bôrka nappe, 2 – Meliata Fm., northern part in the neighbourhood of Jaklovce village, 3 – Meliata Fm.

referred as the Meliatic Unit. Relicts of the Meliata Ocean oceanic crust occur in two forms: either as (1) tectonic slices or blocks in nappe piles and melanges, or as (2) their redeposited material in the form of pebbles in conglomerates (Ivan, in press). Tectonic slices and blocks are a part of the Meliata unit s.s. in the area of Jaklovce and in broader surroundings of Meliata (Hovorka and Spišiak, 1998; Mock et al., 1998), Bodva Valley Ophiolite Formation (Harangi et al., 1996), Darnó Formation (Downes et al., 1990; Harangi et al., 1996) and Bôrka nappe (Ivan and Kronome, 1996; Mello et al., 1998). Oceanic crust rocks occur in the form of pebbles in Cretaceous Gosau-like conglomerates from the Dobšinská ľadová Jaskyňa settlement (Hovorka et al., 1990; Ivan et al., 1998). Relicts of the Meliata Ocean oceanic crust came over variable geotectonic evolution that caused differences in their metamorphic alteration. Following its origin and subsequent metamorphism in the oceanic rift zone, a part of the oceanic crust was subducted, metamorphosed in HP/LT conditions during closing of the ocean and thereafter exhumed, while other part escaped the subduction and it was obducted or peeled in an accretion prism setting without any important metamorphic alteration. Oceanic rocks affected by HP/LT metamorphic alteration occur predominantly in the Bôrka nappe, but also as a relatively rare rock in the Bodva Valley Ophiolite Formation and in Cretaceous Gosau-type conglomerates (Fig. 1).

Bôrka nappe is located in western and southern part of the Spišsko-Gemerské Rudohorie Mts. It was thrust over Gemicum Unit complexes, predominantly over the Early Paleozoic Gelnica Group or the Permian Gočaltovo Group. From the southern side the Bôrka nappe is limited by the Rožňava fault. The largest spread it reaches in western part, where it was saved from the erosion due to its position in the Nižná Slaná depression.

Bôrka nappe is built up by several lithostratigraphic units (Ivan and Mello, 2001). Although all units came over HP/LT metamorphic stage, relicts of the oceanic crust of the Meliata Ocean or magmatic rocks related to initial stages of its formation are located just in two formations (1) Hačava Fm. and (2) Kobeliarovo Fm.

Hačava Fm. builds an important part of the Bôrka nappe in its western as well as eastern parts. Probably it represents tectonically reworked melange, which was metamorphosed in bulk in HP/LT conditions and quickly exhumed, so it does not have signs of retrogression. Relicts of magmatic rocks form tiny enclaves, bodies and tectonic slices of the magnitude from a few centimetres up to first hundreds of meters. The most important localities are the Radzim Hill near Vyšná Slaná village, southwards from the Ježovec Saddle NE from the Kobeliarovo village, eastwards from Štítnik village, between Lúčka and Bôrka villages, in Zádiel Valley and between the Hačava village and Šugov Valley (Fig. 2). Except of the Ježovec

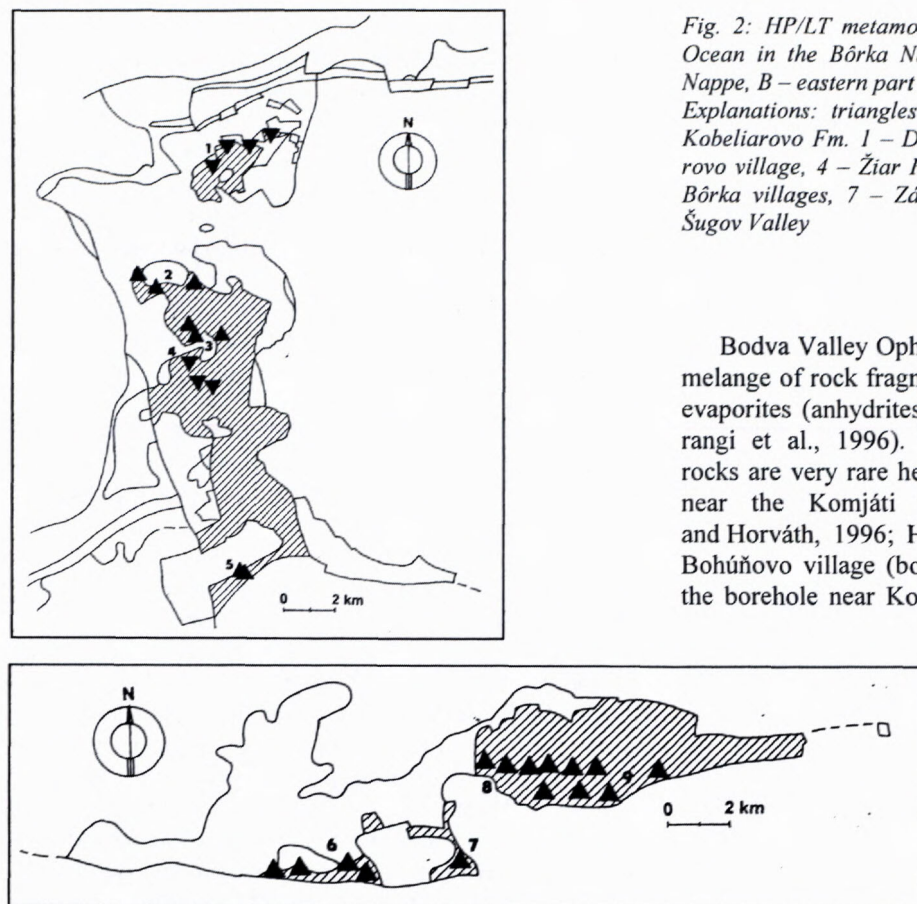


Fig. 2: HP/LT metamorphosed oceanic rocks of the Meliata Ocean in the Bôrka Nappe. A – western part of the Bôrka Nappe, B – eastern part of the Bôrka Nappe.

Explanations: triangles – Hačava Fm., inverted triangles – Kobeliarovo Fm. 1 – Dobšiná, 2 – Radzim Hill, 3 – Kobeliarovo village, 4 – Žiar Hill, 5 – Štítnik village, 6 – Lúčka and Bôrka villages, 7 – Zádiel Valley, 8 – Hačava village, 9 – Šugov Valley

Bodva Valley Ophiolite Formation represents salinary melange of rock fragments of the ophiolite association in evaporites (anhydrites) of Permian age (Réti, 1985; Harangi et al., 1996). HP/LT metamorphosed magmatic rocks are very rare here, identified just in two boreholes near the Komjáti village (borehole Ko-11; Józsa and Horváth, 1996; Horváth, 1997; 2000) and near the Bohúňovo village (borehole SA-6/82; Faryad, 1998). In the borehole near Komjáti, on the tectonic contact with underlying Perkupa Evaporite Fm. (Permian), about 200 m thick body of metamorphosed basic rocks has been found. In the borehole near Bohúňovo such a body sits directly in an evaporite melange and its thickness is just first tenths of meters.

Saddle and Zádiel Valley these rocks have been petrographically studied as glaucophanites in the classic study of Kamenický (1957). Occurrences are spatially (and in part also genetically) related to metamorphosed carbonates (middle part of the Šugov Valley, Bôrka) or to metapelites (Radzim, Ježovec Saddle, upper part of the Šugov Valley). At the Štítnik locality, apart from metamorphosed sediments, metamorphosed radiolarites have been also found in a close link to metamorphosed magmatic rocks.

Kobeliarovo Fm. builds the middle zone of western part of the Bôrka nappe, while in eastern part it is not present. Alike the Hačava Fm. it forms a melange of rigid blocks of metacarbonates (marbles) and metamorphosed magmatic rocks, predominantly in metapelitic matrix. It was metamorphosed in HP/LT conditions, but during exhumation it was subject to retrogression to greenschist facies. Metamorphosed magmatic rocks form tiny enclaves and thin layers (several centimeters thick) in carbonates, or small bodies (first tenths of meters) in metapelites in broader vicinity of the Žiar Hill. Identically metamorphosed magmatic rocks, that occur together with radiolarites in the form of bodies of the magnitude of first tenths up to hundreds of metres in the setting with various types of phyllites in the vicinity of Dobšiná, could also belong to the Kobeliarovo Fm. Hither to they have been regarded for a part of the Carboniferous of the Dobšiná Group of Gemericum (Rozložník, 1963). We have preliminary labelled them as a unique member (Steinberg member) of the Kobeliarovo Formation (Ivan and Mello, 2001).

In Cretaceous Gosau-type conglomerates near Dobšinská ľadová jaskyňa rare clasts of HP/LT metamorphosed basic rocks have been found in a unique type of conglomerates with prevailing rock clasts of the ophiolite sequence (Hovorka et al., 1990; Ivan et al., 1998).

#### Relict magmatic textures in HP/LT metamorphosed rocks of the Meliata Ocean

Already in the classic work of Kamenický (1957) the relict magmatic divergent-intersertal texture was ascribed to a part of the studied glaucophanites, although in the case of some the samples it was wrong (so called diabase porphyry). More recent studies (Reichwalder, 1973; Faryad, 1995a, 1997; Mazzoli and Vozárová, 1998), with exception of our study (Ivan and Kronome, 1996), do not present the phenomenon of relict magmatic textures.

Relict magmatic textures in the studied rocks are only rarely accompanied by original magmatic minerals. Usually, they are possible to identify just based on the distribution of secondary metamorphic minerals that specifically replace some of the original magmatic minerals, or they are preserved just as ghost, most often by distribution of fine pigment of Fe-Ti oxides. Abundance of rocks with preserved primary texture, as well as tiny details discernible in these rocks, indicate that in the HP/LT stage of metamorphism no significant deformation of rocks occurred and the signs of preferential orientation and veining reflect their previous metamorphic evolution. Metamorphosed magmatic rocks that associate with

metapelites preserved their primary texture usually better than those localised in carbonates.

Relict magmatic textures determined in HP/LT metamorphosed oceanic rocks of the Meliata Ocean are shown in figures 3, 4 and 5.

#### Bôrka Nappe – Hačava Fm.

Significant differences in types of primary textures and grades of their preservation occur among individual localities of the Hačava Formation.

#### Radzim Hill

In the area of the Radzim Hill (southwards from the Vyšná Slaná village), at its western (Široké Pole Saddle) and southern slopes the original magmatic textures are very well preserved. Metabasalts with primary subophitic texture prevail but metabasalts with fine-ophitic, intersertal and variolitic textures are also relatively widespread. Rarely, fine-grained metabasalts, brecciated during solidification and subsequently pervasively veined, are present. Macroscopically, metabasalts with primary subophitic texture are massive rocks with dark speckles of mafic minerals. Microscopically, the primary subophitic texture is difficult to identify because the mineral, which has preserved the original habit and composition, is clinopyroxene (Fig. 3A). The characteristic identification feature – laths of plagioclases – is absent. During metamorphic stages preceding HP/LT metamorphism (prehnite-pumpellyite, eventually prehnite-actinolite facies) plagioclase in basalt was either replaced by fine-grained aggregate of white mica or by fan-shaped aggregates of prehnite. Chlorite eventually actinolite also originated, partially at the expense of clinopyroxene. Mostly idiomorphic crystals of ilmenite have been replaced by leucoxene. The rock replaced in this way was subject to compression and preferred orientation of variable intensity, during those the leucoxenised ilmenites have been often flattened up to elongate lenses and aggregates of mica or prehnite, so deformed that they partially flow of the grains of clinopyroxene, suggestive of the mylonite texture. In the high-pressure stage the magmatic clinopyroxene was totally or partially replaced by Na-pyroxene,

prehnite by clinozoisite and subsequently by epidote, white mica obtained composition of fengite and chlorite and actinolite were replaced by glaucophane.

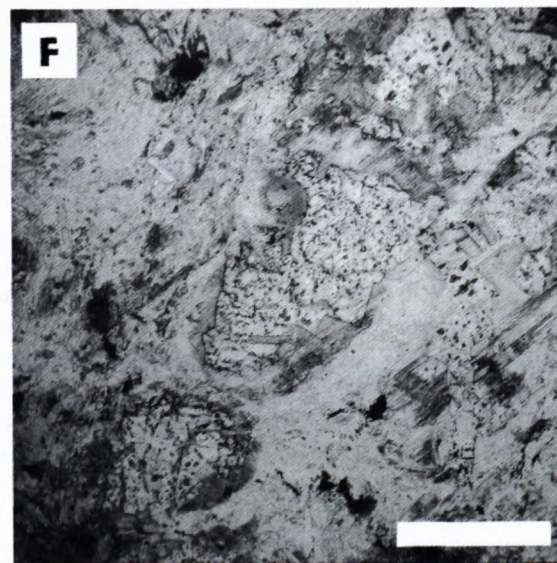
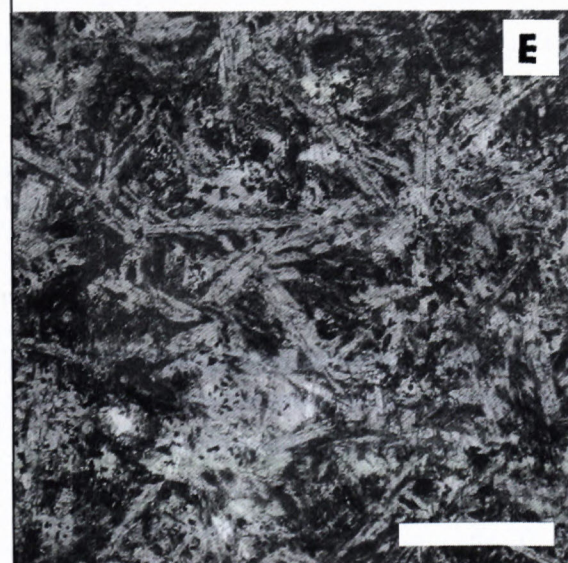
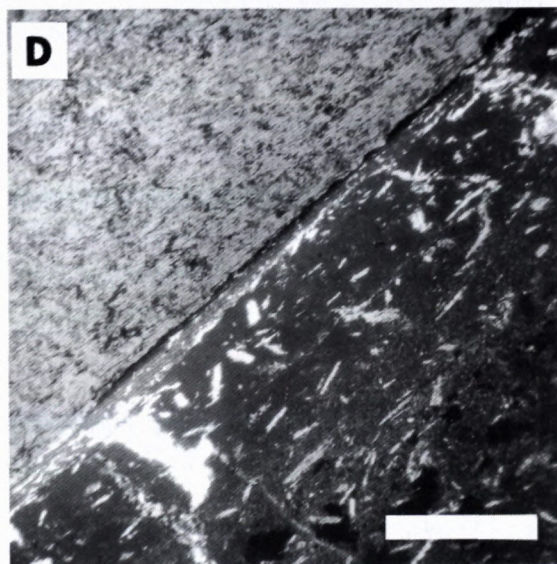
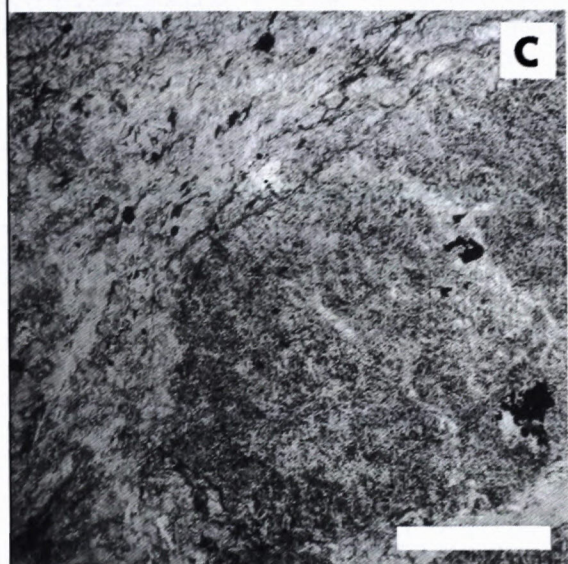
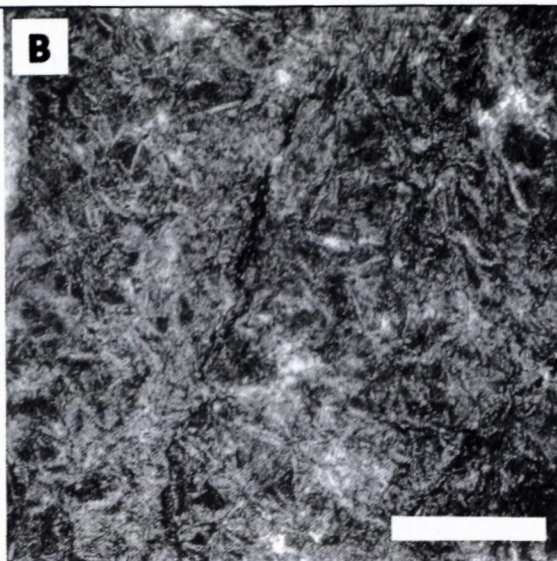
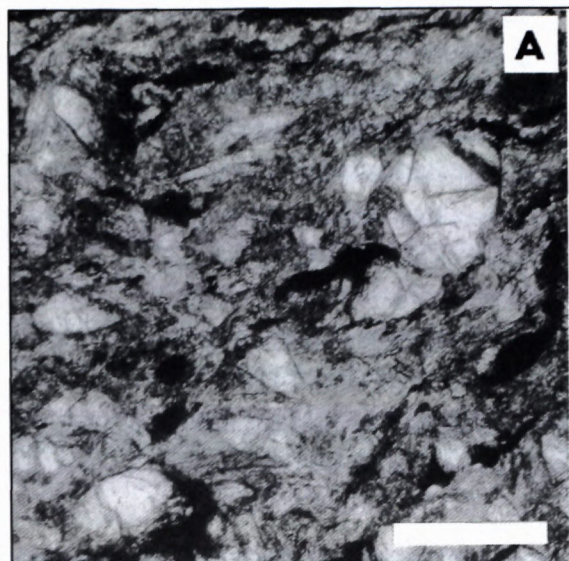
Glaucophanites with primary fine-ophitic to intersertal texture are markedly blue, fine-grained rocks, sometimes with isolated bright spots. In thin section they are characterised by preserved brown pigment after decomposed clinopyroxene or after volcanic glass, in which needles of the original plagioclase, arranged in ophitic texture, occur as ghosts (Fig. 3B). After solidification, the rocks with this texture were subject to low-grade alteration and pervasive veining with thin carbonate veinlets. In the proximity of veinlets they have been slightly replaced by albite and carbonate, while the remaining part was mostly chloritised. In the high-pressure stage of alteration chlorite was replaced by glaucophane, epidote. Fe-Ti pigment is also present. Relict clinopyroxene was altered through the intermediate stage of Na-pyroxene. Bright spots are composed of relict clinozoisite, less by albite and carbonate.

Variolitic texture in metabasalts from the Radzim Hill is preserved in the ghost form only. The original fan-shaped intergrowths of clinopyroxene and plagioclase are displayed by the distribution of Fe-Ti pigment. Chloritisation and pervasive veining of the rock by thin carbonate veinlets following the solidification are the reason why after HP/LT metamorphism the mineral composition is formed just by the pigment and by an aggregate of glaucophane, cut by a network of epidote veinlets.

Mechanical disintegration during solidification of metabasalts is manifested by the presence of rare meta-hyaloclastites to lava breccias, still with discernible ghost textures in individual fragments, such as fine-ophitic, intersertal and vitritic textures. The rock already contains just the assemblage of metamorphic minerals, where the fragments of the original basalt contain chlorite, albite and actinolite, minor glaucophane and carbonate, cemented by carbonate, albite, actinolite and glaucophane. Older actinolite is rimmed by glaucophane.

On the eastern end of the Radzim Hill (Hôra Saddle) and on the NE slope of the Spúšťadlo Hill (860.3m) a belt of HP/LT metamorphosed rocks is present, penetrated by a dense network of predominantly epidote veinlets. Microscopic study proved the preserved ghosts of primary vitritic

Fig. 3: Relict magmatic textures in metabasalts and metagabbro of the Hačava Fm. (Bôrka Nappe). Scale bar in all photos represents 1mm. A – Strongly deformed, formerly ophitic texture of metabasalt with preserved magmatic clinopyroxene (white crystals). Clinozoisite/epidote, glaucophane and leucoxenised ilmenite are other minerals composing this rock. Radzim Hill, sample VVS-6, II N. B – Relict intersertal texture in HP/LT metamorphosed fine-grained basalt. Radzim Hill, sample VVS-14, II N. C – Fine-grained basalt clast with originally intersertal texture in altered, strongly oriented, formerly mostly glassy basalt – probably quenched, most external part of a basaltic lava flow, metamorphosed in HP/LT conditions. Kobeliarovo village, 1 km N, sample VVS-127, II N. D – Basaltic lava chilled margin preserved on the contact of fine-grained basalt and probably altered surface of an older basalt, all metamorphosed in HP/LT conditions. Originally chilled margin with relict vitritic texture, containing sporadic plagioclase phenocrysts, is formed mostly by glaucophane. The rock on the contact is composed of glaucophane, epidote and white mica. Podježovec Saddle, sample VVS-142, II N. E – HP/LT metamorphosed basalt with ghost ophitic texture displayed mostly due to the fine Fe-Ti oxide pigment. Original magmatic assemblage was replaced by glaucophane, epidote and chlorite. Small amount of Na-Ca pyroxene as a transition metamorphic phase is also present. Štítik village, 2 km NE, sample VVS-173, II N. F – Relict gabbro texture of HP/LT metamorphosed gabbro. Relict magmatic clinopyroxene was replaced by Mg-chlorite with impregnation of small titanite crystals. Older amphiboles, created at the expense of clinopyroxene, were replaced by glaucophane as well as plagioclase, replaced by fine-grained glaucophane aggregate. Šugov Valley, sample VHA-37, II N.



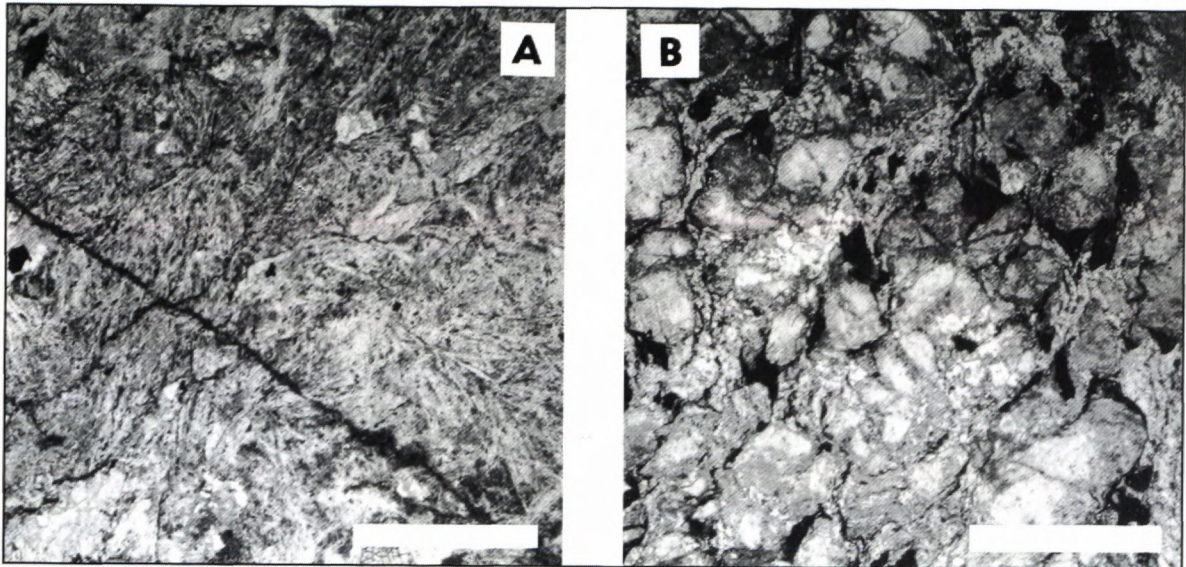


Fig. 4: Relict magmatic textures in metabasalts of the Hačava Fm. (Bôrka Nappe) formed on the contact with carbonaceous sediment. Scale bars in both photos represent 1 mm. A – Ghost variolitic texture in the basalt from the contact with carbonaceous sediment, fully replaced by carbonate. Lúčka village, 1 km E, sample FBO-40, II N. B – HP/LT metamorphosed peperite. Clasts of basaltic glass were chloritised (light grey) or devitrified (grey, pigmented) and then partly replaced by glaucophane (medium grey). Carbonate matrix was mostly replaced by epidote. Zádiel Valley, sample FBO-34, II N.

texture of basalt (mostly by the distribution of fine Fe-Ti pigment), locally with tiny fragments of fine-crystalline basalt. The subsequent hydrothermal alteration caused pervasive veining probably with carbonate veinlets and, in part, also the deformation of the rock. Glassy parts were replaced by chlorite. During high-pressure stage an aggregate of fine individuals of Na-amphibole (glaucophane) with divergent arrangement originated instead of chloritised glass. In fine-crystalline fragments albite, together with glaucophane, also originated. Carbonate in veinlets was prevailingly replaced by epidote. Similar rocks have been found as enclaves in sericite phyllites in the area northwards from the Kobeliarovo village (Fig. 3C).

#### Ježovec Saddle (NW of Kobeliarovo village)

Relict magmatic textures of HP/LT metamorphosed basalts from this locality are close to textures from the Radzim Hill. Medium- and fine-grained subophitic/ophitic texture, intersertal texture and chilled margin with vitritic texture and with tiny sporadic phenocrysts of plagioclase, originally formed at the contact with thin layer of sediment or heavily altered basalt, were identified (Fig. 3D). Textures of fine-grained rocks are preserved just as ghosts by the distribution of Fe-Ti pigment, more coarse-grained rocks also with a specific distribution of metamorphic minerals. Original clinopyroxenes were pseudomorphosed by chlorite, in which glaucophane crystals occur as blasts. Plagioclase laths were replaced by albite, clinozoisite/epidote and fine-grained aggregate of white mica. Compared to rocks from the Radzim Hill, in the period before high-pressure phase these rocks were metamorphosed in the greenschist facies coupled with moderate spilitisation.

#### Štítnik village

In the area eastward from the Štítnik village two small bodies of HP/LT metamorphosed basic rocks are known. The rocks of the more eastern body are represented by HP/LT basalts with the best preserved relict textures among the all studied localities. Glomeroophitic, intersertal and variolitic textures have been determined. They have been identified based on the distribution of Fe-Ti pigment as well as products, that replaced the original magmatic clinopyroxenes – e.g. relicts of Na-Ca pyroxenes. Basalts with glomeroophitic texture were composed of laths of skeletal plagioclase up to 3 mm long, among whose fan-shaped aggregates of clinopyroxene were present (Fig. 3E). More fine-grained varieties had analogous texture; however, they contained sporadically present phenocrysts of plagioclase. Even more fine-grained rocks were characterised by variolitic, locally also intersertal textures with sporadic phenocrysts of plagioclase and scattered gas cavities. Metamorphic texture, on which mostly glaucophane, less also epidote and chlorite participated, does not respect the original texture. HP/LT metamorphosed radiolarites also occur with metabasalts. It seems that before the high-pressure stage of metamorphism basalts were affected just by minimum alteration. In the more western body pervasive veining and alteration caused that magmatic textures were obliterated.

#### Lúčka and Bôrka villages

In the area between the Lúčka and Bôrka villages HP/LT metamorphosed magmatic rocks are represented by basalts, those effusions occurred in an environment with carbonate sedimentation. Extensive hydrothermal

alteration was the reason for an apparent recrystallisation and the origin of metamorphic textures during the HP/LT stage of alteration. Relict breccia-type texture of lavas or variolitic texture (Fig. 4A) were preserved just thanks to the nearly total replacement by hematite or carbonate on the contact of the lava with carbonaceous mud, probably immediately after solidification. Rarely identified primary ophitic or subophitic texture in the centre of bigger bodies can be predicted based on spatial distribution of albite and epidote crystals and white mica, partially following the original plagioclase.

#### *Zádiel Valley*

HP/LT metamorphosed rocks from this locality are a direct eastern continuation of the occurrences near the Bôrka village. From the relatively well preserved primary texture it is clear that peperite, pervasively veined and hydrothermally altered still before the high-pressure stage of metamorphism, was their protolith. Differences in the mode of crystallisation and alteration are the reasons for the current variable composition of individual clasts (Fig. 4B).

#### *Hačava village*

The biggest body of HP/LT metamorphosed magmatic rocks of the Meliatic Unit is located northwards from Hačava. Primary magmatic textures are preserved especially in its western part, while the recrystallisation and preferential orientation increase in direction to the east, so that the original textures can be difficult to identify. The body was originally composed mostly of doleritic basalts with subophitic texture. In massive varieties with relict subophitic texture also laths after original plagioclase, up to 3 mm large, are macroscopically observable. The texture is noticeable also macroscopically, despite its complex metamorphic evolution (Ivan and Kronome, 1996). The spaces after original laths of plagioclase are usually filled by aggregate of short columnar crystals of epidote, in some samples also by fine-laminar aggregate of mica. Spaces between the laths (also between the epidote crystals) are filled mostly by glaucophane. In a part of the epidote aggregates fan-shaped aligned pigment is preserved, indicating the original replacement of plagioclase by prehnite. Glaucophane among the original laths is extensively variably coloured. Dark blue parts rich in riebeckite often have subhedral habitus and enclose needles and pigment of Ti-minerals (originally sagenite). They probably originated after older, Ti-bearing, amphiboles and are enclosed or overgrown by pale blue glaucophane. Bright glaucophane also replaces older actinolite and chlorite. Magmatic clinopyroxene is preserved just rarely in the form of relicts, partially replaced by metamorphic pyroxene – aegirine (c.f. Faryad, 1997). Ilmenites usually preserved their primary magmatic shape, but they were totally replaced by leucoxene. Preferentially oriented types of glaucophanites originated by the deformation of basalts still in the time, when they contained plagioclase replaced by prehnite. They contain garnet, formed at the expense of clinozoisite which was created after prehnite during the metamorphic evolution.

Occasionally, metabasalts with primary vitritic texture, probably representing metamorphosed chilled margin of a basalt body, have been found. Petrographically, these rocks are identical to the above-described case. Chilled margins appear to have been created at the contacts with older basic magmatic rock.

#### *Šugov Valley*

The bodies of HP/LT metamorphosed rocks, located in the northern part of the Hačava Fm. belt, are represented by metabasalts that erupted into carbonate environment and similarly, as in the case of the locality Bôrka, the primary magmatic textures are not preserved due to the extensive hydrothermal alteration. Fine fragments and short lenses of basic material of centimetres size, conformably embedded in massive carbonates, were subject to extensive recrystallisation (Reichwalder, 1973). Just in rare cases, in samples heavily impregnated by hematite pigment, it was possible to find out that they originally represented strongly fractured and brecciated basalt with vitritic to intersertal texture.

In the southern part of the Hačava Fm. rock belt metamorphosed doleritic basalts occur with heavily deformed subophitic texture. They represent eastern continuation of the analogous rocks from Hačava. Relatively coarse-grained rocks (grain size 6 mm), originally with gabbroic texture, have been determined here too. Magmatic mineral assemblage in this rock was originally composed of pyroxene, plagioclase and ilmenite. Relicts of brown, green and colourless amphibole are the result of rock alteration accompanied by decreasing temperature during the oceanic ridge type of metamorphism, still before the high-pressure stage of metamorphism. The crystallisation of amphiboles occurred on intergranulars and fissures in direction towards the interior of clinopyroxene crystals. The relicts of clinopyroxenes were finally chloritised. During the HP/LT metamorphism a part of the amphiboles (actinolites) were replaced by glaucophane. The aggregate of fine needles of glaucophane together with brownish pigment, replaces also the original plagioclase (Fig. 3F). The rock also contains small grains of ilmenite, replaced by leucoxene, and accessory zonal tourmaline. In the belt of HP/LT metamorphosed phyllites and black shales also a small body of fine-grained metabasalt with well-preserved subophitic texture was found. Plagioclase laths were replaced by fine-grained aggregate of clinozoisite/epidote. Clinopyroxene was replaced by glaucophane.

#### *Bôrka Nappe – Kobeliarovo Fm.*

Primary textures of metamorphosed magmatic rocks of the Kobeliarovo Fm. are usually well identifiable, although these rocks, compared to Hačava Fm. rocks, were furthermore affected by retrogression up to the greenschist facies conditions. Their characteristic features are massive texture, blue-green to green colour and impregnation by magnetite octahedrons up to 1 mm in size.

## Žiar Hill

Relict magmatic textures of majority of the studied basic rocks from this area are manifested also macroscopically (Fig. 5A). Subophitic and doleritic textures are dominant, but hyaloclastites have been also found. Metabasalts to dolerites, that had primary clinopyroxene-plagioclase composition with abundant content of ilmenite, have also a similar association of metamorphic minerals. Original plagioclase laths are replaced by aggregate of randomly oriented epidote columns of no preferential orientation, albite and white mica in interstices. On the place of the original clinopyroxene, aggregate of bluish actinolite, rich in Na, with minor chlorite and relict riebeckite, are present. Primary euhedral ilmenite is totally replaced by leucoxene. Small aggregates of albite grains, rare stilpnomelane and carbonate are also present. Magnetite forms individual octahedrons of various sizes, less often their aggregates (Fig. 5B). Some rocks were subject to more extensive albitisation or carbonatisation probably still before the HP/LT metamorphism. Metamorphosed basic rocks located in carbonates did not preserve relicts of primary magmatic textures. Hyaloclastites with ghost texture, formed by tiny crystals of magnetite, are an exception (Fig. 5C).

## Dobšiná town

Unlike the Žiar Hill area, relict magmatic textures preserved in rocks from the vicinity of the Dobšiná town are more variegated and indicate an important abundance of fine-grained basalts. Subophitic, glomeroophitic and vario-litic textures have been determined. Similarly as in the above cases, they are usually preserved just as ghost textures, displayed by the distribution of Fe-Ti pigment as well as by metamorphic minerals. The metamorphic mineral assemblage is identical to the previous case, but instead of riebeckite, relict glaucophane is present. Basalts were metamorphosed together with associated radiolarites.

## Bodva Valley Ophiolite Fm.

Mineralogical, petrographical and metamorphic characteristics of multistage metamorphosed basic rocks of this formation were published by of Horváth (1997; 2000). Primary magmatic textures, such as gabbrodoleritic, doleritic and subophitic, are well preserved despite complex relations among associations of metamorphic minerals, produced by several metamorphic stages (Fig. 5D). Laths and columns of magmatic plagioclase consist of relicts of prehnite and fine-grained clinzoisite to epidote replacing the prehnite, further accompanied by albite. Aggregate of urallite, impregnated by small grains of magnetite, is probably the result of direct alteration of clinopyroxene relicts. However still before, during the oceanic ridge metamorphism, clinopyroxene was extensively overprinted by several generations of amphibole (brown, green, greenish) in direction from intergranular grains. The growth of amphiboles continued also during the HP/LT metamorphic stage, but owing to the retrogression just riebeckite was preserved and glaucophane was replaced by bluish actinolite with higher Na content. Mainly at contacts of the original plagioclase and pyroxene newly formed chlorite, epidote and titanite are present. Abundant euhedral crystals of primary ilmenite are totally replaced by leucoxene.

## Gosau-type conglomerates

In Cretaceous conglomerates from the Dobšinská Ľadová Jaskyňa settlement eight pebbles of HP/LT metamorphosed basic rocks have been already found, from which only two have preserved the primary magmatic texture. Ophitic texture of the first one is possible to identify based on the arrangement and unequal size of original plagioclase laths, replaced by fine-grained aggregate of clinzoisite/epidote, albite and glaucophane in variable ratio (Fig. 5F). Clinopyroxene was replaced by amphibole still before the high-pressure stage of alteration, because between original plagioclase laths zoned

Fig. 5: Relict magmatic textures in metabasalts of the Kobeliarovo Fm., Bodva Valley Ophiolite Fm. and Gosau-type Cretaceous conglomerates from Dobšinská Ľadová Jaskyňa settlement. Scale bars in all photos (except A) represent 1 mm.

A – Macroscopic visible relict doleritic texture of multi-stage metamorphosed dolerite of the Kobeliarovo Fm. Žiar Hill, sample VVS-47. B – relict ophitic texture preserved in HP/LT metamorphosed basalt, retrogressed into LP/LT conditions. Original plagioclase laths are replaced by aggregate of albite and plenty of small columnar crystals of epidote. Bluish actinolite, chlorite, white mica, leucoxene and magnetite are also present. Žiar Hill, sample VVS-46, II N. C – Metahyaloclastite composed of originally glassy clasts with sporadic plagioclase and/or clinopyroxene phenocrysts in carbonaceous matrix, fully transformed into magnetite-chlorite-albite-carbonate rock. Žiar Hill, sample VVS-99, II N. D – Multi-stage metamorphosed gabbro-dolerite of the Bodva Valley Ophiolite Fm. with relict dolerite texture. Magmatic plagioclase laths or columns were replaced by prehnite which is further transformed into clinzoisite/epidote and albite. Clinopyroxene is replaced by several types of amphibole and partly also by chlorite. Szögliget, borehole Szö-4, 154.8 m, sample VM-21, II N. E – HP/LT metamorphosed fine-grained basalt with ghost intersertal texture, displayed by distribution of Fe-Ti oxide pigment. Small laths of original plagioclase are still discernible. Clast in Cretaceous conglomerate. Dobšinská Ľadová Jaskyňa settlement, sample DLJ-52, II N. F – HP/LT metamorphosed basalt with relict ophitic texture. Clinopyroxene was replaced by chlorite and actinolite, and then actinolite was rimmed by glaucophane during high-pressure metamorphic stage. Plagioclase laths were replaced by glaucophane, clinzoisite/epidote and albite. Primary ilmenite crystals were leucoxenized (black). Clast in Cretaceous conglomerate, Dobšinská Ľadová Jaskyňa settlement, sample DLJ-63, II N.

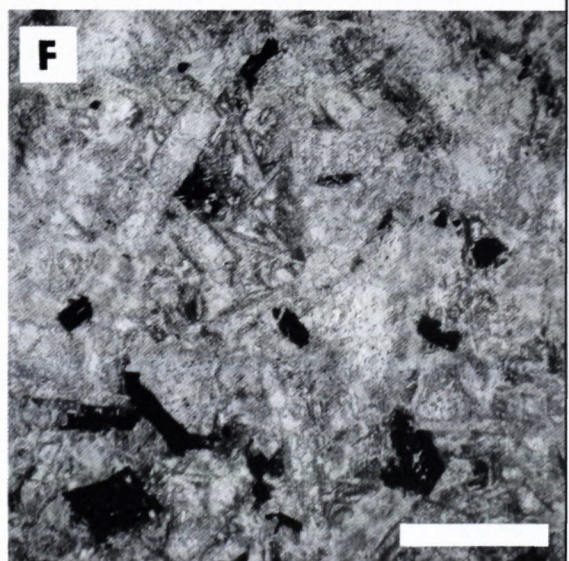
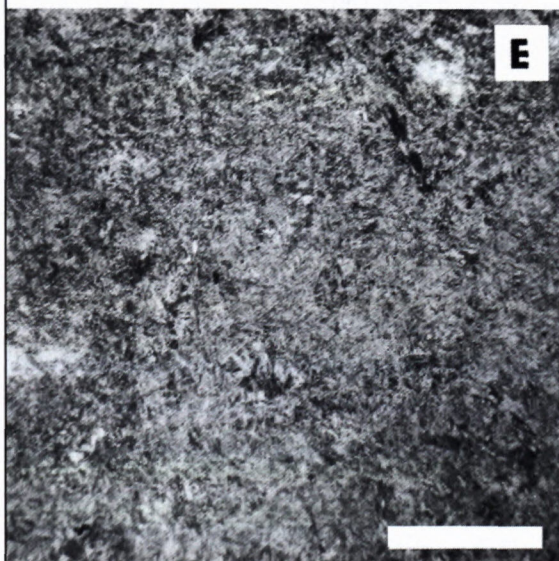
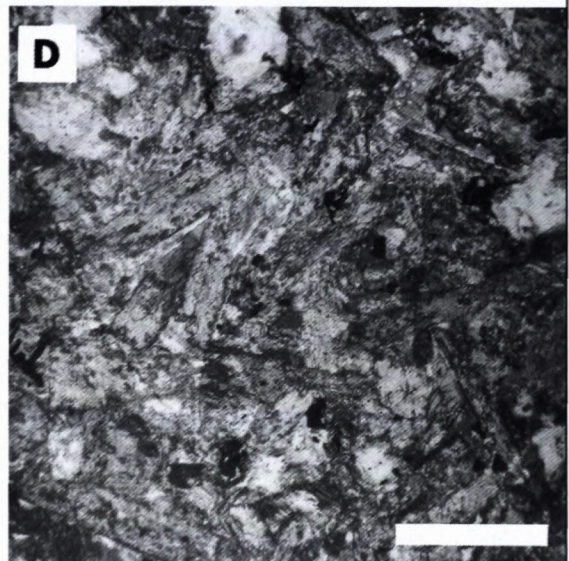
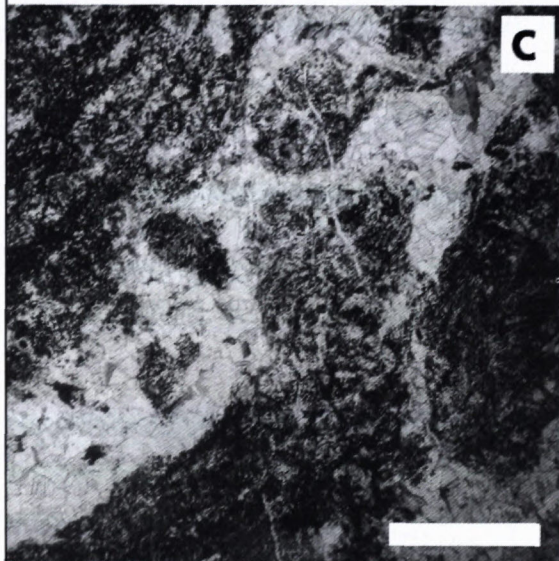
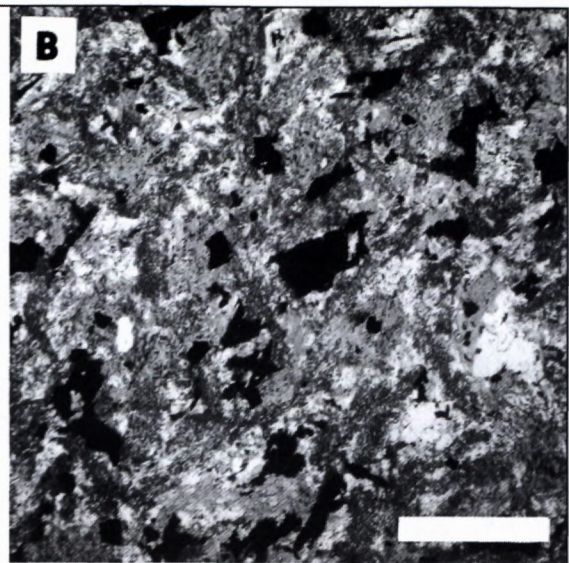
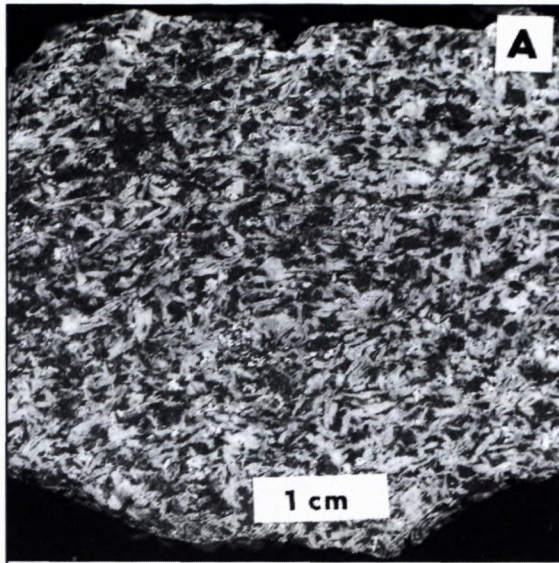


Table 1: Analyses of relict magmatic clinopyroxenes from HP/LT metamorphosed basalts from the Radzim Hill (Hačava Fm., Bôrka Nappe). Analysis of a metamorphic Na-Ca pyroxene is added for comparison (analysis no. 15).

Sample Analysis	VVS-6								VVS-16						
	1	2	3	4	5	6	7	8	9	10	11	12	13	14	15
SiO <sub>2</sub>	54.42	51.46	53.02	51.02	51.22	50.96	50.90	53.17	53.03	49.60	52.90	54.12	54.31	53.30	56.13
TiO <sub>2</sub>	0.46	1.06	0.35	0.84	0.94	1.07	0.83	0.41	0.55	1.52	0.78	0.36	0.54	0.59	0.08
Al <sub>2</sub> O <sub>3</sub>	1.68	3.33	1.91	3.82	3.67	4.17	4.15	2.21	1.68	3.74	3.59	1.90	1.62	1.74	6.76
FeO <sup>t</sup>	7.43	8.60	6.16	6.98	7.85	7.07	6.74	6.60	8.62	10.90	5.98	5.72	8.83	9.89	9.95
MnO	0.20	0.21	0.24	0.00	0.00	0.00	0.00	0.00	0.27	0.27	0.13	0.22	0.29	0.31	0.15
MgO	18.22	15.23	18.22	15.56	15.66	15.58	15.68	17.52	16.52	13.94	16.66	17.78	17.14	16.20	6.94
CaO	17.88	19.13	18.14	21.20	20.69	20.91	20.73	19.64	18.28	18.62	20.18	19.67	17.83	16.56	12.34
Na <sub>2</sub> O	0.26	0.46	0.49	0.61	0.43	0.53	0.54	0.46	0.32	0.49	0.33	0.28	0.34	0.39	8.17
K <sub>2</sub> O	0.00	0.00	0.00	0.08	0.12	0.09	0.09	0.11	0.00	0.00	0.00	0.00	0.00	0.00	0.00
Cr <sub>2</sub> O <sub>3</sub>	0.00	0.00	0.22	0.00	0.00	0.00	0.00	0.00	0.00	0.00	0.12	0.00	0.00	0.00	0.00
Total	100.55	99.48	98.75	100.11	100.58	100.38	99.66	100.12	99.27	99.08	100.67	100.05	100.90	98.98	100.52
Si	1.973	1.913	1.956	1.884	1.887	1.876	1.883	1.945	1.966	1.876	1.920	1.968	1.976	1.982	2.004
Al <sup>IV</sup>	0.027	0.087	0.044	0.116	0.113	0.124	0.117	0.055	0.034	0.124	0.080	0.032	0.024	0.018	0.000
Al <sup>VI</sup>	0.045	0.059	0.039	0.050	0.046	0.057	0.064	0.040	0.039	0.043	0.073	0.049	0.045	0.058	0.285
Ti	0.012	0.030	0.010	0.023	0.026	0.030	0.023	0.011	0.015	0.043	0.021	0.010	0.015	0.017	0.002
Fe <sup>t</sup>	0.225	0.267	0.190	0.216	0.242	0.218	0.209	0.202	0.267	0.345	0.182	0.174	0.269	0.307	0.297
Mn	0.006	0.006	0.008	0.000	0.000	0.000	0.000	0.000	0.009	0.009	0.004	0.007	0.009	0.010	0.005
Mg	0.985	0.844	1.002	0.857	0.860	0.858	0.865	0.955	0.913	0.786	0.901	0.964	0.929	0.898	0.369
Ca	0.695	0.762	0.717	0.839	0.816	0.825	0.822	0.770	0.726	0.755	0.785	0.766	0.695	0.660	0.472
Na	0.019	0.033	0.035	0.044	0.031	0.038	0.039	0.033	0.023	0.036	0.023	0.020	0.024	0.028	0.566
K	0.000	0.000	0.000	0.004	0.005	0.004	0.004	0.005	0.000	0.000	0.000	0.000	0.000	0.000	0.000
Cr	0.000	0.000	0.006	0.000	0.000	0.000	0.000	0.000	0.000	0.000	0.003	0.000	0.000	0.000	0.000

Note: Analyses were performed by electron microprobe Jeol 733 (Geological Survey of the Slovak Republic) using following conditions for measuring: 15 kV, 2 · 10<sup>-8</sup> A, ZAFO; standards Na,Al- albite, Ca- wollastonite, Mg- MgO, Mn- willemitte, Fe,Cr- chromite, Ti- TiO<sub>2</sub>.

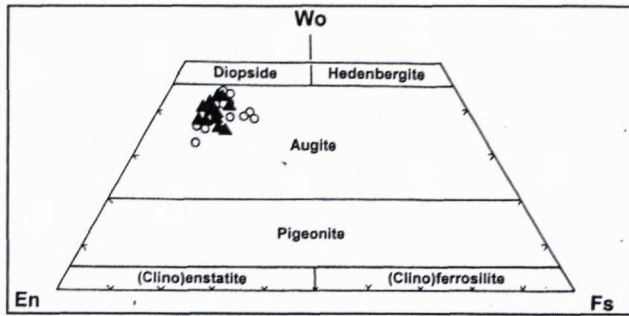


Fig. 6: Relict magmatic clinopyroxenes from HP/LT metamorphosed oceanic basalts of the Bôrka Nappe in the classification diagram by Morimoto et al. (1988). Clinopyroxenes from LP/LT metamorphosed oceanic basalts of the Meliata Unit from Jaklovce (Hovorka and Spišiak, 1988) are displayed for comparison (empty circles).

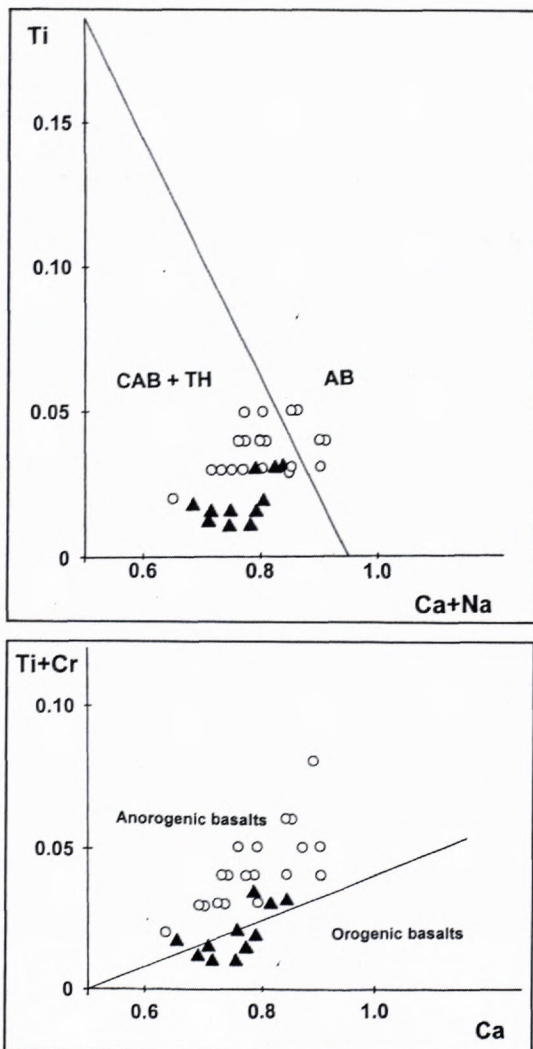


Fig. 7: Relict magmatic clinopyroxenes from HP/LT metamorphosed oceanic basalts of the Bôrka Nappe in discriminative diagrams by Leterrier et al. (1982). Clinopyroxenes from LP/LT metamorphosed oceanic basalts of the Meliata Unit from Jaklovce (Hovorka and Spišiak, 1988) are displayed for comparison (empty circles). A – Diagram Ca+Na vs. Ti (p.f.u.) discriminating clinopyroxenes from alkali basalts (AB) and calc-alkaline/ tholeiitic basalts (CAB/TH). B – Diagram Ca vs. Ti+Cr (p.f.u) for discrimination of clinopyroxenes from anorogenic and orogenic basalts.

amphibole crystals are predominantly presented. Actinolite in the centre rimmed by darker glaucophane with small inclusions of titanite is fringed by pale glaucophane without inclusions. Euhedral magmatic ilmenites were cataclastically deformed and affected by decomposition to leucoxene and magnetite.

Basic rock, forming the other rounded pebble, has preserved intersertal ghost texture (Fig. 5E). Major part of the rock is formed by metamorphic glaucophane.

**Relict magmatic minerals in HP/LT metamorphosed rocks of the Meliata Ocean**

Clinopyroxene is the only preserved magmatic mineral in HP/LT metamorphosed rocks of the Meliata Ocean. It was found on the localities Radzim Hill (Ivan and Kronome, 1996; Mazzoli and Vozárová, 1998) and Hačava village (Faryad, 1997). We have studied it in detail on the locality Radzim Hill.

Analyses of selected clinopyroxenes are shown in table 1. According to the classification of Morimoto et al. (1988) pyroxenes display augite composition (Fig. 6) identical to the composition of clinopyroxenes from the best preserved LP/LT metamorphosed oceanic basalts of the Meliata Ocean from Jaklovce (Meliata Fm.). Some of the clinopyroxene grains shows zoning; slightly increased contents of Al<sub>2</sub>O<sub>3</sub> and TiO<sub>2</sub> are typical for grain margins.

The application of discriminative diagrams by Leterrier et al. (1982) showed that pyroxenes from both compared localities have composition closer to pyroxenes

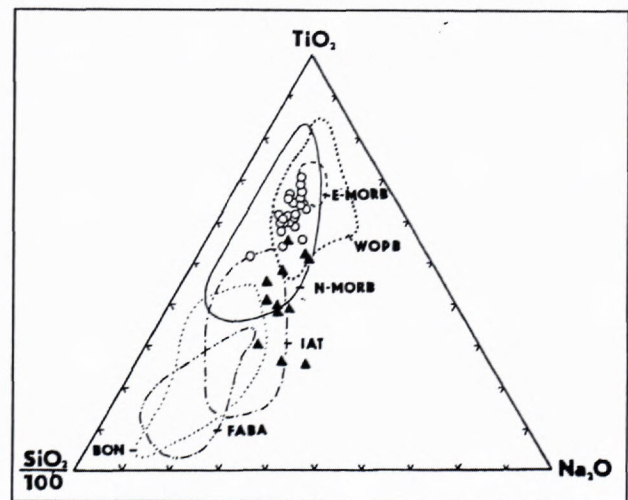


Fig. 8: Relict magmatic clinopyroxenes from HP/LT metamorphosed oceanic basalts of the Bôrka Nappe in TiO<sub>2</sub>-SiO<sub>2</sub>/100-Na<sub>2</sub>O discriminative diagram (Beccaluva et al., 1989). Clinopyroxenes from LP/LT metamorphosed oceanic basalts of the Meliata Unit from Jaklovce (Hovorka and Spišiak, 1988) are displayed for comparison (empty circles). More „arc-like“ character of metabasalts from the Bôrka Nappe seems to be apparent. Explanations: E-MORB- enriched mid-ocean ridge basalts, N-MORB- normal mid-ocean ridge basalts, WOPB- within oceanic plate basalts, IAT- island arc tholeiites, FABA- intraoceanic fore-arc basaltic andesites and andesites

from tholeiite or calc-alkaline basalts than to pyroxenes from alkaline basalts (Fig. 7A). In a similar way, pyroxenes from the Radzim Hill appear to be closer in composition to pyroxenes from orogenic basalts, in comparison to clinopyroxenes from the Meliata Fm. which are similar respond to pyroxenes of anorogenic basalts (Fig. 7B).

In the discriminative diagram of Beccaluva et al. (1989) clinopyroxenes from the Radzim Hill are projected more to the field of island-arc tholeiites (IAT), while clinopyroxenes from the Meliata Fm. respond to normal basalts of mid-oceanic ridges, although an overlap with the field of within-ocean plateau basalts (E-MORB) occurs here too.

Differences in composition between relict magmatic augites and metamorphic acmites are apparent from table 1 and they are most evident in Na and Ti contents.

## Discussion

HP/LT metamorphosed rocks, as a reliable indicator of subduction, have been extensively studied especially during the last three decades. Despite of that, references about preserved primary magmatic textures and minerals in these rocks are not very frequent. For instance, they are known from Franciscan melange (California), already described by Coleman and Lee (1963) and later also by Maruyama and Liou (1987, 1988) and Liou and Maruyama (1987). According to Coleman and Lee (1963), in the HP/LT metamorphosed rocks, pillow structures are preserved with hyalophitic to subophitic texture in the centre of pillows and variolitic and tachylitic texture on their rims. In Sanbagawa belt (Japan) Maruyama and Liou (1985) found well preserved not only the original volcanic rocks (pillow lavas, hyaloclastites and feeding dykes) but also original textures (ophitic, subophitic, intersertal and intergranular). Similar phenomenons are also known from HP/LT metamorphosed rocks from Mikabu and Chichibu belts (Japan; Suzuki and Ishizuka, 1998), from Susunai complex (SE Sachalin, Sakakibara et al., 1997), from Betic cordillera (Spain, Morata et al., 1994) and others. Furthermore, similar textures were also preserved in HP/LT rocks from Mariana forearc, that are the only example of high-pressure metamorphosed rocks in recent subduction zones so far Yamamoto et al. (1995). In all the above mentioned examples relict magmatic clinopyroxenes are also presented.

Relict magmatic textures, well preserved in most of the HP/LT metamorphosed basic rocks of the Hačava and Kobeliarovo Formations of the Bôrka Nappe, allow exact characteristic of the magmatic protolith of these rocks, the setting where they cooled and also their positions in the original Meliata Ocean basin. The composition of relict pyroxenes together with whole-rock geochemical data specify the geodynamic setting of magma generation. These data together with the determined details on metamorphic evolution significantly contribute to solving of complicated problems of origin, evolution and cessation of the Meliata Ocean.

Based on the above data the studied HP/LT metamorphosed rock can be divided into two different groups, formed in two different stages of opening of the

Meliata Ocean. Metabasalts from the localities Šugov Valley, Zádiel Valley, Lúčka and Bôrka and occurrences on the western slope of the Žiar Hill belong to the first group that erupted synchronously with carbonates sedimentation. Magma extrusions into the environment of carbonaceous mud caused mechanical disintegration of the quickly cooling lava and the generation of hyaloclastites. Carbonaceous setting was the reason for extensive subsolidus alteration, related to the crystallisation of hematite. These basalts appear formed in initial stages of opening of the Meliata Ocean to be which was interpreted as a back-arc basin (c.f. Stampfli, 1996; Ivan and Kronome, 1996). This is also supported by their geochemical characteristics that suggest the origin from a fractionated basaltic lava of arc signature (Ivan, 2000; Ivan, in print).

The second group is formed by rocks that originated in more advanced (early) stage of opening of the back-arc basin, when the basin already started to be deeper, probably below to the level of CCL. In the basin they originated as a component of the upper part of a magmatic crust which was similar by its features to the typical oceanic crust produced in oceanic rifts. Metabasalts at the localities Radzim Hill, Ježovec Saddle, Štítňik and Dobšiná originated as the uppermost part of the oceanic crust rock sequence of the Meliata Ocean basin. Variegated magmatic textures, preserved in relicts in HP/LT metamorphosed basalts in the western part of the locality Radzim Hill, and their changes observable within a single sample indicate that these basalts were probably extruded as pillow lavas. Vitritic to breccia-type textures in the eastern part of this locality would suggest that thin lava floods and/or ropy lavas were also probable. The composition of relict pyroxenes, compared to pyroxenes from LP/LT metamorphosed basalts of the Meliata Fm. from Jaklovce, indicate a still apparent influence of the arc-like mantle source on the composition of the parent rock. Identical results have been also obtained based on the study of the distribution of trace elements: while metabasalts from Radzim Hill can be still classified as BABB, those from Jaklovce are already close to typical oceanic N-MORB (Ivan, 2000; Ivan, in print). Similar conclusions are valid also for the other mentioned localities. While on the localities Radzim Hill and Ježovec Saddle no sedimentary rocks, originated simultaneously with metabasalts, have been proved, at the localities Štítňik and Dobšiná they accompany metamorphosed radiolarites that prove deep-sea setting of their origin.

Metamorphosed doleritic basalts from the area of Hačava originated in subvolcanic conditions. Sporadic occurrence of samples, representing original chilled margins, indicates that these basalts could originate as a part of a sheeted-dyke complex. This assumption is also supported by indications of the metamorphism of oceanic ridge type. Geochemically, they can be characterised as close to BABB (Ivan, 2000; Ivan, in print). Metadolerites from the area of Žiar Hill also crystallised in subvolcanic conditions from a fractionated basaltic magma, but necessary data for a closer identification of the setting of their origin are still missing.

Among the studied samples, metagabbros from Šugov Valley represent the relatively deepest part of the oceanic rock sequence of the Meliata Ocean crust. Their relict texture and composition remind of isotropic ophiolite gabbros from the upper part of the gabbro complex. Such an origin is also suggested by the well-preserved manifestations of the metamorphism of oceanic ridge type.

All the presented differences among individual occurrences of HP/LT metamorphosed magmatic rocks of the Hačava and Kobeliarovo Formations of the Bôrka nappe confirm that they represent independent fragments of the Meliata Ocean basin floor. The presence of just the upper parts of the oceanic crust in these fragments can be the result of their peeling in an accretion prism by a mechanism similar to that described by Kimura and Ludden (1995). In both formations not only magmatic rocks but also all other rocks i.e. pelitic sediments, carbonates or radiolaritic cherts were affected by HP/LT metamorphism (c.f. Faryad, 1995b). Therefore it seems to be probable that in this case a melange, formed in an accretion prism, was subject to metamorphism in the subduction zone. Then, different conditions of exhumation caused that a part of the melange does not take any signs of retrogression (Hačava Fm.), while another part was equilibrated in greenschist facies conditions (Kobeliarovo Fm.).

Fragments of metamorphosed dolerites to gabrodolerites from the Bodva Valley Ophiolite Formation, incorporated into evaporites, differ from metamorphosed basic rocks from the Bôrka nappe by their geochemical characteristics – they represent the products of a fractionated magma close to the enriched, mid-oceanic rift basalts (E-MORB). Furthermore, geochronological data from analogous rocks of this formation, that do not contain relicts of high-pressure phase minerals, suggest an older age of metamorphism than it is the supposed Middle Triassic age of the opening and spreading of the Meliata Ocean (Horváth, 2000). It can not be excluded that they represent initial stage products of the origin of this ocean.

Clasts of HP/LT metamorphosed rocks from the Cretaceous Gosau-type conglomerates occur together with clasts of rocks of virtually complete ophiolite sequence, but also with rhyolites and calc-alkaline basaltic andesites. The nappes of the Jurassic melange of an analogous type as it represents the Meliata Fm. were probably the source of this recycled material (Ivan et al., 1999).

## Conclusions

Based on the detailed study of HP/LT metamorphosed basic magmatic rocks, regarded as relicts of oceanic crust of the Triassic-Jurassic Meliata Ocean, the following conclusions have been attained:

- Relicts of primary magmatic textures in HP/LT metamorphosed basic rocks of the Hačava and Kobeliarovo Formations of the Bôrka Nappe, Bodva Valley Ophiolite Formation and pebbles of these rocks from Cretaceous conglomerates near Dobšinská Ľadová Jaskyňa are mostly well preserved.

- In these rocks magmatic textures are preserved as ghost textures, mainly formed by distribution of fine Fe-Ti pigment, less often by a specific distribution and orientation of metamorphic minerals.
- The obliteration of magmatic textures is the result of extensive hydrothermal alteration and pervasive veining shortly after the solidification or deformation during initial low-pressure stages of metamorphism in the subduction zone.
- The identified relict textures (gabbroic, doleritic, ophitic, subophitic, glomeroophitic, intersertal, vario-litic, vitritic) reflect exclusively the variable speed of solidification of basaltic magma, while breccia-type and hyaloclastite textures are the result of the contact with a specific environment.
- The Bôrka Nappe contains two groups of magmatic rocks, originally related to the origin of the Meliata Ocean: (1) volcanic rocks, syngenetic with the carbonate sedimentation, related to the initial stage of the oceanic basin opening and (2) magmatic (volcanic, subvolcanic and intrusive) rocks, related to the more advanced (early) stage of the opening; volcanic rocks can be accompanied by radiolarites.
- Magmatic rocks of the more advanced stage probably already formed an oceanic type of crust with common magmatic stratification.
- Magmatic rocks of the Bôrka Nappe related to the Meliata Ocean formation were metamorphosed in HP/LT conditions in the form of blocks in mélangé and were exhumed by two different ways.

The research was supported by the grant VEGA 1/6000/99. Author acknowledges Dr. S. Józsa from the Eötvös Lóránd University, Budapest, for the provision of samples of metamorphosed basalts from drill holes located in the Bodva Valley Ophiolite Fm.

## References

- Beccaluva L., Macciotta G., Piccardo G.B. & Zeda, O., 1989: Clinopyroxene composition of the ophiolite basalts as petrogenetic indicator. *Chem. Geol.*, 77, 165-182.
- Channell J.E.T. & Kozur H.W., 1997: How many oceans? Meliata, Vardar, and Pindos oceans in Mesozoic Alpine paleogeography. *Geology*, 25, 183-186.
- Coleman R.G. & Lee, D.E., 1963: Glaucophane-bearing metamorphic rock types of the Cazadero area, California. *J. Petrology*, 4, 260-301.
- Downes H., Pantó G., Árkai P. & Thirlwall, M.F., 1990: Petrology and geochemistry of Mesozoic igneous rocks, Bükk Mountains, Hungary. *Lithos*, 24, 201-215.
- Faryad, S.W., 1995a: Phase petrology and P-T conditions of mafic blueschists from the Meliata Unit, West Carpathians. *J. metamorph. Geol.*, 13, 701-714.
- Faryad S.W., 1995b: Petrology and phase relations of low-grade high-pressure metasediments from the Meliata unit, Western Carpathians, Slovakia. *Eur. J. Mineral.*, 7, 71-87.
- Faryad S.W., 1997: Lithology and metamorphism of the Meliata unit high-pressure rocks. In: Geological evolution of the Western Carpathians. Grečula P., Hovorka D. & Putiš M. (eds.): Bratislava, Mineralia slov., Monogr., 131-144.
- Faryad W.S. (1998): High-pressure metamorphic rocks of the Meliata Unit vs. Bôrka Nappe: Their correlation with blueschist pebbles in conglomerates from the Klape Unit of the Klippen Belt. (In Slovak with English summary). *Mineralia slov.*, 30, 235-240.

- Golonka J., Oszczytko N. & Ślącza, A., 2000: Late Carboniferous-Neogene geodynamic evolution and paleogeography of the circum-Carpathian region and adjacent areas. *Ann. Soc. Geol. Polon.*, 70, 107-136.
- Harangi S., Szabó C., Józsa S., Szoldán Z., Árva-Sós E., Balla M. & Kubovics, I., 1996: Mesozoic igneous suites in Hungary: Implications for genesis and tectonic setting in the northwestern part of Tethys. *Int. Geol. Rev.*, 38, 336-360.
- Horváth P., 1997: High-pressure metamorphism and p,T-path of the metabasic rocks in the borehole Komjáti-11, Bódva Valley area, NE Hungary. *Acta Mineral. Petrogr. Szeged*, 38, 151-163.
- Horváth P., 2000: Metamorphic evolution of gabbroic rocks of the Bódva Valley Ophiolite Complex, NE Hungary. *Geologica carpath.*, 51, 121-129.
- Hovorka D., Ivan P., Mock R., Rozložník L. & Spišiak, J., 1990: Sediments of Gosau type near Dobšiná Ice Cave: ideas for their non-traditional interpretation. (In Slovak). *Mineralia slov.*, 22, s. 519-525.
- Hovorka D. & Spišiak J., 1988: Mesozoic volcanism of the Western Carpathians. (In Slovak with English summary). Bratislava, Veda, 264 p.
- Hovorka D. & Spišiak J., 1998: Mesozoic Meliata ocean dismembered ophiolites. In: *Geodynamic development of the Western Carpathians*. M. Rakús edit. Bratislava, Geol. Survey Slovak Rep., 81-88.
- Ivan P., 2000: Geochemical types of the basic metavolcanic rocks in the Meliatic Unit (inner Western Carpathians). (In Slovak). In: *Geochemistry 2000*. O. Ďurža a S. Rapant (eds). *Konf. Symp. Sem.*, Bratislava, D. Štúr Publ., 31-34.
- Ivan P., in print: Relicts of the Meliata ocean crust: An overview of the results of mineralogical, petrological and geochemical data and their geodynamic implications. *Geologica carpath.*
- Ivan P., Hovorka D. & Spišiak J., 1998: Complete ophiolites as clasts in the Gosau-type Cretaceous conglomerates from Dobšinská Ladová Jaskyňa (Gemic Unit, inner Western Carpathians). In: *Carpath.-Balcan Geol. Assoc. XVI. Congress. Abstracts*. Geol. Survey Austria, Vienna, 233.
- Ivan P. & Kronome B., 1996: Protolith and geodynamic setting of the HP/LT metamorphosed basic rocks from the northern margin of the Bôrka nappe (Meliatic Unit, Inner Western Carpathians). *Slovak geol. Mag.*, 3-4/96, 331-334.
- Ivan P. & Mello J., 2001: Tectonic subunits in the Bôrka Nappe (inner Western Carpathians): Their lithostratigraphy and original position in the structure of the ancient Meliata ocean basin. *Geolines*, 13, 64-65.
- Ivan P., Méres Š. & Hovorka D., 1994: Oceanic crust in geological history of the Western Carpathian orogeny. *Acta geol. Hung.*, 37, 19-32.
- Józsa S. & Horváth P., 1996: Preliminary report on the metamorphic evolution of the Vardar-Meliata ophiolites, Bódva Valley area, NE Hungary. Abstract. In: *Terranes of Serbia. The formation of the geologic framework of Serbia and adjacent regions*. V. Knezević & B. Krstić eds., Belgrade, 227-228.
- Kamenický J., 1957: Serpentinities, diabases a glaukophanitic rocks from the Triassic of the Spišsko-gemerské rudohorie Mts. (In Slovak). *Geol. Práce, Zoš.*, 45, 5-108.
- Kimura G. & Ludden J., 1995: Peeling oceanic crust in subduction zones. *Geology*, 23, 217-220.
- Kozur H. & Mock R., 1997: New paleogeographic and tectonic interpretations in the Slovakian Carpathians and their implications and correlations with the Eastern Alps and other parts of the Western Tethys. Part II: Inner western Carpathians. *Mineralia slov.*, 29, 164-209.
- Leterrier, J., Maury, R.C., Thoron, P., Girard, D. & Marchal, M. 1982: Clinopyroxene composition as a method of identification of the magmatic affinities of paleovolcanic series. *Earth planet. Sci. Lett.*, 59, 139-154.
- Liou J.G. & Maruyama, S., 1987: Parageneses and compositions of amphiboles from Franciscan jadeite-glaucophane type facies series metabasites at Cazadero, California. *J. metamorph. Geol.*, 5, 371-395.
- Maruyama S. & Liou J.G., 1985: The stability of Na-Ca pyroxene in low-grade metabasites of high-pressure intermediate facies series. *Amer. Mineralogist*, 70, 16-29.
- Maruyama S. & Liou J.G., 1987: Clinopyroxene – a mineral telescoped through the processes of blueschist facies metamorphism. *J. metamorph. Geol.*, 5, 529-552.
- Maruyama S. & Liou J.G., 1988: Petrology of franciscan metabasites along the jadeite-glaucophane type facies series, Cazadero, California., *J. Petrology*, 29, 1-37.
- Mazzoli C. & Vozárová A., 1998: Subduction related processes in the Bôrka Nappe (inner Western Carpathians): a geochemical and petrological approach. In: *Rakús M. (edit.): Geodynamic development of the Western Carpathians*. Bratislava, Geol. Survey Slovak Rep., 89-106.
- Mello J., Elečko M., Pristaš J., Reichwalder P., Snopko L., Vass D., Vozárová A., Gaál L., Hanzel V., Hók J., Kováč P., Slavkay M. & Steiner A., 1997: Explanations to the geological map of the Slovenský kras Mts. 1: 50 000. (In Slovak). Bratislava, D. Štúr Publ., 1-255.
- Mello J., Reichwalder P. & Vozárová A., 1998: Bôrka Nappe: high-pressure relict from the subduction-accretion prism of the Meliata ocean (Inner Western Carpathians, Slovakia). *Slovak geol. Mag.*, 4, 261-273.
- Mock R., Sýkora M., Aubrecht R., Ožvoldová L., Kronome B., Reichwalder P. & Jablonský J., 1998: Petrology and petrography of the Meliaticum near the Meliata and Jaklovce Villages, Slovakia. *Slovak geol. Mag.*, 4: 223-260.
- Morata D., Puga E. & Aguirre, L., 1994: Na-metamorphic pyroxenes in low-grade metabasites from the External Zones of the Betic Cordilleras (southern Spain): influence of rock chemical composition on their formation. *Rev. geol. Chile*, 21, 269-283.
- Morimoto, N. et al., 1980: Nomenclature of pyroxenes. *Mineral. Petrology*, 39, 55-76.
- Neugebauer J., Greiner B. & Appel E., 2001: Kinematics of the Alpine-West Carpathian orogen and palaeogeographic implications. *J. geol. Soc.*, 158, 97-110.
- Plašienka D., 2000: Paleotectonic controls and tentative palinspastic restoration of the Carpathian realm during the Mesozoic. *Slovak geol. Mag.*, 6, 200-204.
- Reichwalder P., 1973: Geology of the Late Paleozoic of the southwestern part of the Spišsko-gemerské rudohorie Mts. (In Slovak). *Západné Karpaty*, 18, 99-139.
- Réti Z., 1985: Triassic ophiolite fragments in an evaporitic melange, northern Hungary. *Ophioliti*, 10, 411-422.
- Stampfli G.M., 1996: The-Intra Alpine terrain: A Paleotethyan remnant in the Alpine Variscides. *Eclogae geol. Helv.*, 89, 13-42.
- Sakakibara M., Ofuka H., Kimura G., Ishizuka H., Miyashita S., Okamura M. & Melnikov O.A., 1997: Metamorphic evolution of the Susunai metabasites in southern Sakhalin, Russian Republic. *J. metamorph. Geol.*, 15, 565-580.
- Suzuki S. & Ishizuka H., 1998: Low-grade metamorphism of the Mikabu and northern Chichibu belts in central Shikoku, SW Japan: implications for the areal extent of the Sanbagawa low-grade metamorphism. *J. metamorph. Geol.*, 16, 107-116.
- Schweigl J. & Neubauer F., 1997: Structural evolution of the central Northern Calcareous Alps: Significance for Jurassic to Tertiary geodynamics in the Alps. *Eclogae geol. Helv.*, 90, 303-323.
- Yamamoto K., Asahara Y.m, Maekawa H. & Sugitani K., 1995: Origin of blueschist-facies clasts in the Mariana forearc, Western Pacific. *Geochem. J.*, 29, 259-275.

## Soils and sediments testing for contamination by heavy metals – some case studies in Slovakia

ČURLÍK, J. and ŠEFČÍK, P.

Geological Survey of Slovak Republic, Mlynská dolina 1, 817 04 Bratislava, Slovak Republic

*Abstract.* Soil (sediment) testing and determination of various chemical forms of metals is important in evaluating their mobility and bioavailability. It can be perceived as an evolving process aimed at improving the assessment of risk associated with heavy metals in soils and plants. Especially the determination of an „available„ fraction of metals, based on single or sequential extraction and soil (pore) solution analyses is now gaining widespread acceptance, as a means to characterise hazards from contaminated soil.

The main task of this contribution is to summarise current testing methodologies illustrated by new analytical results obtained from some case studies in Slovakia. This paper examines new concepts and procedures used for the assessing hazard from metal contamination, including some limitations (analytical, soil) that produce testing results, weakening the relationship between higher content of metals in soil and actual environmental and human health hazards.

*Key words:* soil/sediment testing, metal speciation, single extraction, sequential extraction, soil solution, plant available metal fraction, soil contamination

### Introduction

The accumulation of heavy metals and metalloids in soils and sediments possess many risks to human and ecosystem health. Risks may be expressed either through the food chain or through the groundwater contamination. The evaluation of soils, stream and overbank sediments contamination is an evolving process aimed at improving the assessment of environmental and human health hazards associated with the content of potentially toxic elements in plants and water.

Risks due to soils and sediments pollution by metals are well recognized and major texts have been published by several authors (Alloway, 1990; Kabata - Pendias and Pendias, 1992; Salomons et al., 1995).

Many researches have tried to find out a relation between the concentration of potentially toxic elements in soil/plants system and their effect on organisms (plants and humans) based on total element content or extractable forms of elements (Fergusson, 1990). The most biological effects in soils are rather closely related to the soil solution concentration than to the total metal content. Because of most national inventories of metal concentrations in soils are based on the total metal content a preliminary approach is to find out how this data can be transformed to understand a real effect. This effect-based approach is aimed at elaboration of critical limits based on adverse effect on ecosystems. The implicit assumption is that (ecotoxicological) effects are due to the metal accumulation. However, in most cases, toxic effects are mainly due to the elevated bioavailable (mobile) concentration (de Vries and Bakker, 1998).

A big amount of work has been done in attempting to quantify metals held in different soil/sediment fractions, particularly those thought to be mobile and bioavailable, since these fractions can potentially adversely effect on the ecosystem. The most widely used approach is to choose a chemical extractant (single extraction) or series of extractants (sequential extraction) to remove particular chemical phases (species) of metals from soil and sediments (Tessier et al., 1979; Shuman and Hargrove, 1985; Keefer et al., 1984; Miller et al., 1985).

In most cases, however, toxic effects on micro-organisms and soil fauna is mostly due to an elevated bioavailable concentration in soil (pore) solution (Van Straalen and Bergema, 1995). But physico-chemical properties of solids control activities and concentrations of metals in the solution, therefore, directly affect their availability to plants. In spite of the fact that modern instrumental technique has made possible to analyse most elements in small concentrations in pore solution, there are still many limitations that hamper wider use of the results of pore solution analysis. Those limitations are theoretical, analytical and methodological (Gregor et al., 1997, 1999; de Vries and Bakker, 1998).

The aim of this paper is to illustrate on concrete results, obtained from studies of contaminated soils in Slovakia, mostly within INCO-COPERNICUS project „Long term risk of inadequate management practices on the sustainability of agricultural soils„ (co-ordinated by W. de Vries), the possibility of using soil (and sediments) testing and summarise soil testing methodologies and concepts. The evaluation of different tests and results, towards the hazards involved, is out of the scope of this paper. How-

ever, some theoretical and methodological problems are also tackled, to point out some new trends and concepts which might be useful to apply in geochemical and environmental studies of soils, sediments and sewage sludges.

### Methodology

For this study analytical results (single extraction and soil solution) of twenty contaminated soils were chosen. Their soil characteristics are presented in Tab. 1. Sequential analyses were performed on another set of contaminated soil samples from the Hron river basin. The basic characteristics of these soils are presented in Tab. 4.

**Sampling.** Sampling was done by augering that enabled us to take samples at fixed depths of a plough layer. The spatial variability of soil required to take 25 subsamples at one point in order to prepare composite sample from a plot area of 25 x 25 m.

**Soil properties analyses.** Fraction < 2 mm was arbitrary used for soil properties analyses by routine methods. Soil reaction was measured potentiometrically in suspensions. For determination of potential soil reaction 1M KCl solution and 20 g sample was used, for determination of active soil reaction redistilled water and 20 g of soil was used. Carbonates were determined by Janko in a lime - meter, in 10 % solution HCl and from 20 g of soil sample. The classical pipette method for soil texture was used (fraction < 2 mm, after the sample dispersion by sodium hexametaphosphate).

**Chemical analyses.** Soil extraction methods were used followed handbook by Houba et al. (1996) and hence, only principal methods are mentioned here:

**Soil extraction with 0.01 M CaCl<sub>2</sub>.** Soil samples dried at 40°C were extracted at 20°C with 0.01 M CaCl<sub>2</sub>. The suspension was stirred for 2 hours and centrifuged. Supernatant was taken for analysis.

**Soil extraction with aqua regia.** Soil samples were dried at 40°C and extracted with aqua regia at room temperature for 16 hours, followed by boiling under a reflux for 2 hours. Then the extract was filtered. The extracted solution was fulfilled to the standard volume by adding of nitric acid.

**Soil extraction with 0.05 M EDTA.** Soil samples were dried at 40 °C and extracted with 0.05 M EDTA solution by stirring the suspension for 1 hour at room temperature (20 °C). The extract was filtrated into a polyethylene bottle.

**Soil extraction with 0.05 M ammonium oxalate and oxalate acid mixture.** Soil samples, dried at 40°C, were extracted with ammonium acetate and acetic acid mixture (pH = 3.0 ± 0.1). The suspension was stirred for 2 hours in a dark room at 20 ± 1 °C. The extract was filtered into a polyethylene bottle.

**Methods for soil solution analysis.** 25 g of air-dried sample were extracted with 50 ml of 0.002 M CaCl<sub>2</sub>.

**Sequential extraction scheme** used in this work is based on Community Bureau of Reference method (1987) tested in 18 EU laboratories (Mackových et al., 1999). The following metal fractions are distinguished:

- i – exchangeable and carbonate fraction (0.11M acetic acid),
- ii – reducible fraction (Fe and Mn oxides bound) fraction (0.1M hydroxylamine hydrochloric),
- iii – organically (sulphide) bound fraction (8.8 M peroxide + 1M ammonium acetate),
- iv – residual fraction (total decomposition with inorganic acids mixture - HNO<sub>3</sub>, HF, HClO<sub>4</sub>).

### Metal speciation and metal fractions in soils/sediments

Metals, both naturally occurring and inputted to soils and sediments are present in an extremely large range of forms. They may be distributed among many components of soils or sediments and may be associated with them in many different ways. The nature of this association is often referred to as *speciation*. Soil scientists, geochemists and biologists have attempted to extract and quantify these fractions held in different soil/sediment fractions, particularly those which are thought to be mobile (chemical *species* or *forms*), since they can potentially pollute the groundwater or can get in to the food chain from a plant uptake. In soils and sediments this generally means to identify metals held in any of the following fractions:

- a) soluble
- b) extractable (adsorbed)
- c) organically bound
- d) Mn oxides occluded
- e) amorphous and crystalline oxyhydroxides Fe occluded
- f) bound in carbonates
- g) residual (total)

The potential availability (mobility) of elements in different fractions of soil/sediments is illustrated in Fig.1.

A big effort has been expended in attempting to quantify metals held in different fractions, particularly those fractions that are thought to be mobile and bioavailable. The most common and single physical separation technique is to filter solution through micropore membranes of the pore size 0.45 µm, thus it is rather a coarse differentiation between „soluble,, and „particulate,, metals.

The fundamentals and concepts of soil testing have been reviewed by McLaughlin et al. (2000). Basically two main groups of procedures are used at present:

- a) single chemical extraction,
- b) sequential chemical extraction.

### Assessing „plant available,, or „mobile,, amounts of metals in soils (sediments) by single extraction methods

For many years chemical extractants have been tested by soil scientists and geochemists to estimate „plant available,, („mobile,,) fractions of metals.

The development of these tests was mainly in response to the needs to monitor the metal uptake by plants in contaminated soils, in bottom sediments, soils loaded with sewage sludges and pesticides. Single extractions are generally used to extract the following fractions of potentially toxic metals (Berrow and Buridge, 1980):

- a) metals in soil solution (ionic, molecular, chelated and colloidal forms),
- b) exchangeable forms (readily exchangeable),
- c) in adsorption complexes (firmly bound),
- d) reducible-easily bound in sesquioxides (coprecipitated) and in hardly soluble salts,
- e) fixed in crystal lattices of secondary minerals (predominantly clay minerals).

In order to extract metals from the soil/sediments, the basic dissolution, chelation, desorption/ion exchange and oxidation/reduction processes are used prior to elemental determination.

Metals present in the solid phase as discrete phases (sulphides, carbonates, phosphates, oxides, or coprecipitated with sesquioxides) can be released by *dissolution processes*. Usually less soluble compounds require more vigorous extractant (usually inorganic acids).

Table 1: Selected soil characteristics

Sample	Site	Soil unit FAO (1970)	pH/CaCl <sub>2</sub> (1 : 5)	Carbonates (%)	Humus (%)	Clay (%)	CEC (cmol.kg <sup>-1</sup> )
ICSK-1	Slovenská Ľupča	Fluvisol	6.63	0.4	5.46	14.22	20.45
ICSK-2	Gemerská Poloma	Gleyic Fluvisol	6.92	1.6	4.17	3.84	17.39
ICSK-3	Družstevná pri Hornáde	Fluvisol	6.74	0.3	3.08	17.89	20.20
ICSK-4	Veľká Lodina	Fluvisol	7.14	6.4	2.99	4.61	14.49
ICSK-5	Kluknava	Cambisol	5.51	0	3.33	13.01	15.40
ICSK-6	Markušovce	Fluvisol	6.35	0.12	4.08	7.54	16.45
ICSK-7	Gelnica	Fluvisol	5.70	0	7.08	2.74	14.05
ICSK-8	Fiačice - Ľubňa	Fluvisol	6.87	0.5	3.99	7.78	17.40
ICSK-9	Kozárovce	Fluvisol	7.05	7.3	3.17	14.64	20.29
ICSK-10	Starý Tekov	Fluvisol	5.82	0	3.12	21.89	22.90
ICSK-11	Hontianske Tesáre	Fluvisol	5.54	0	1.65	17.51	15.85
ICSK-12	Domaniky	Fluvisol	6.13	0	2.17	11.35	17.95
ICSK-13	Iľija	Pseudogley	5.46	0	6.67	17.50	35.65
ICSK-14	Stará Kremnička	Fluvisol	6.70	0.52	2.17	9.69	13.75
ICSK-15	Bzenica	Fluvisol	6.03	0	5.99	11.34	20.50
ICSK-16	Tekovská Breznica	Fluvisol	7.00	4.2	2.32	7.17	14.49
ICSK-17	Kalná nad Hronom	Fluvisol	6.66	0.1	3.74	19.37	25.35
ICSK-18	Pezinok	Phaeozem	6.75	0.4	5.67	12.32	23.90
ICSK-19	Limbach	Cambisol	7.08	4.5	6.17	6.07	14.49
ICSK-20	Slovenský Grob	Fluvisol	7.06	0.3	4.64	17.47	20.80

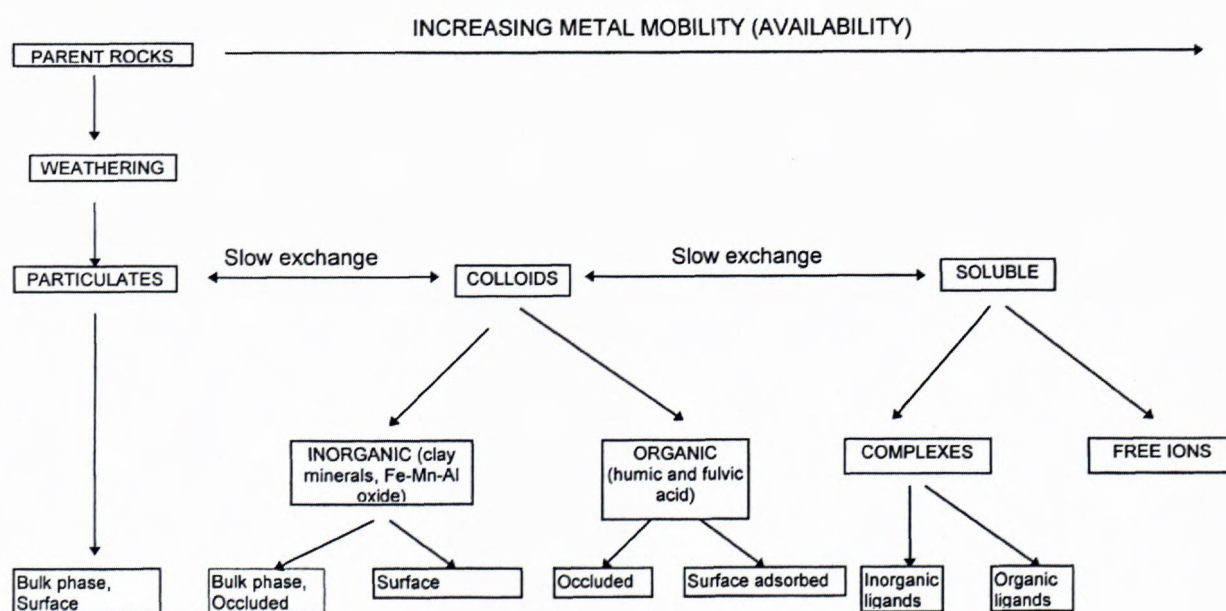


Fig. 1 The potential metal mobility (availability) of different fractions of soil/sediments.



Table 2: Heavy metal concentrations ( $\text{mg}\cdot\text{kg}^{-1}$ ) in contaminated soils obtained by different (single) extraction methods: i - the total (pseudototal) content obtained by aqua regia extraction, ii - the mobile fraction concentration obtained by 0.05 M EDTA, iii - the mobile fraction concentration obtained by ammonium oxalate and oxalate acid, iv - the „mobile“ (available) fraction concentration obtained by 0.01 M  $\text{CaCl}_2$ .

Sample	Extraction method	As	Cd	Cr	Cu	Hg	Ni	Pb	Zn
ICSK-1	i	20.95	0.5	30	57	0.080	26	62	123
	ii	0.35	0.3	< 0.1	23	< 0.005	2	25	9
	iii	5.85	0.1	1.6	32	< 0.005	4	4	18
	iv	0.05	< 0.05	< 0.1	< 0.5	< 0.005	< 0.5	< 0.5	< 0.3
ICSK-2	i	54.80	0.2	35	135	0.050	44	24	123
	ii	0.10	0.2	< 0.1	40	0.019	7	8	9
	iii	19.30	0.2	1.6	56	< 0.005	9	2	18
	iv	< 0.01	< 0.05	< 0.1	< 0.5	0.005	< 0.5	< 0.5	< 0.3
ICSK-3	i	18.80	0.4	33	113	0.110	36	33	110
	ii	0.40	0.2	< 0.1	44	< 0.005	5	11	10
	iii	10.00	0.1	1.4	74	< 0.005	7	3	25
	iv	0.03	< 0.05	< 0.1	< 0.5	< 0.005	< 0.5	< 0.5	< 0.3
ICSK-4	i	46.80	0.4	29	228	0.100	46	50	137
	ii	1.50	0.2	< 0.1	137	0.030	3	20	15
	iii	29.30	0.1	1.0	192	< 0.005	5	3	37
	iv	0.03	< 0.05	< 0.1	< 0.5	< 0.005	< 0.5	< 0.5	< 0.3
ICSK-5	i	36.80	0.6	38	70	0.200	40	43	177
	ii	1.80	0.3	< 0.1	29	0.009	3	18	30
	iii	19.20	0.2	1.0	39	< 0.005	3	3	45
	iv	0.09	< 0.05	< 0.1	< 0.5	< 0.005	< 0.5	< 0.5	0.6
ICSK-6	i	20.10	0.3	28	76	0.940	26	17	70
	ii	0.50	0.2	< 0.1	35	0.061	3	7	7
	iii	9.50	0.1	1.2	49	< 0.005	4	1	14
	iv	0.02	< 0.05	< 0.1	< 0.5	< 0.005	< 0.5	< 0.5	< 0.3
ICSK-7	i	87.50	0.7	17	589	0.180	25	170	243
	ii	0.60	0.3	< 0.1	260	0.048	2	58	30
	iii	50.50	0.2	1.3	372	< 0.005	3	29	61
	iv	0.05	< 0.05	< 0.1	< 0.5	< 0.005	< 0.5	< 0.5	0.6
ICSK-8	i	12.50	0.3	28	21	0.080	27	16	67
	ii	0.20	0.2	< 0.1	11	0.009	5	6	6
	iii	6.40	< 0.1	1.8	12	< 0.005	6	< 1	12
	iv	< 0.01	< 0.05	< 0.1	< 0.5	< 0.005	4.6	< 0.5	< 0.3
ICSK-9	i	39.20	0.7	25	117	0.120	17	62	158
	ii	1.00	0.5	< 0.1	59	0.024	3	22	35
	iii	23.70	0.1	0.8	71	< 0.005	3	3	46
	iv	0.03	< 0.05	< 0.1	< 0.5	< 0.005	< 0.5	< 0.5	< 0.3
ICSK-10	i	42.70	0.6	29	130	0.140	19	72	119
	ii	0.50	0.4	< 0.1	60	0.038	3	25	12
	iii	21.50	0.1	1.3	76	< 0.005	2	9	19
	iv	0.05	< 0.05	< 0.1	< 0.5	< 0.005	< 0.5	< 0.5	< 0.3
ICSK-11	i	17.50	13.7	23	201	0.030	14	1303	1704
	ii	0.10	8.4	< 0.1	81	0.019	< 1	467	400
	iii	9.20	2.2	0.4	135	< 0.005	< 2	243	595
	iv	< 0.01	1.16	< 0.1	< 0.5	< 0.005	< 0.5	< 0.5	52.3
ICSK-12	i	16.90	20.5	19	236	0.030	11.0	1301	2445
	ii	0.10	16.8	< 0.1	140	< 0.005	< 1	585	853
	iii	9.70	3.7	0.4	178	< 0.005	< 2	373	994
	iv	< 0.01	1.59	< 0.1	< 0.5	< 0.005	< 0.5	< 0.5	165.6

Table 2: to be continued

Sample	Extraction method	As	Cd	Cr	Cu	Hg	Ni	Pb	Zn
ICSK-13	i	119.50	1.1	19	39	0.030	8	220	178
	ii	0.90	0.7	< 0.1	9	0.006	1	102	26
	iii	45.70	0.1	0.7	12	< 0.005	< 2	24	31
	iv	0.04	< 0.05	< 0.1	< 0.5	< 0.005	< 0.5	< 0.5	< 0.3
ICSK-14	i	102.50	0.2	15	42	0.560	6	68	76
	ii	1.10	0.1	< 0.1	14	0.088	< 1	17	9
	iii	53.70	0.1	1.5	19	< 0.005	< 2	12	19
	iv	0.04	< 0.05	< 0.1	< 0.5	< 0.005	< 0.5	< 0.5	< 0.3
ICSK-15	i	62.00	2.0	15	90	0.060	12	322	427
	ii	1.10	1.3	< 0.1	43	0.054	2	147	94
	iii	28.30	0.2	0.8	52	< 0.005	3	29	128
	iv	0.05	< 0.05	< 0.1	< 0.5	< 0.005	< 0.5	< 0.5	< 0.3
ICSK-16	i	39.20	1.9	22	107	0.090	10	134	339
	ii	1.40	1.2	< 0.1	44	0.046	1	69	65
	iii	22.50	0.2	3.5	63	< 0.005	3	11	117
	iv	0.11	< 0.05	< 0.1	< 0.5	< 0.005	< 0.5	< 0.5	< 0.3
ICSK-17	i	48.50	1.2	27	193	0.140	19	122	215
	ii	0.60	0.9	< 0.1	105	0.076	4	56	40
	iii	31.40	0.1	1.7	131	< 0.005	4	15	51
	iv	0.03	< 0.05	< 0.1	< 0.5	< 0.005	< 0.5	< 0.5	< 0.3
ICSK-18	i	68.90	0.9	66	49	0.010	77	28	173
	ii	3.00	0.6	0.2	21	0.001	21	10	14
	iii	49.10	0.2	3.1	24	< 0.005	22	3	21
	iv	0.05	< 0.05	< 0.1	< 0.5	< 0.005	< 0.5	< 0.5	< 0.3
ICSK-19	i	4.70	0.3	9	138	0.010	7	33	81
	ii	0.30	0.1	0.2	103	< 0.005	1	12	13
	iii	1.50	< 0.1	0.7	94	< 0.005	< 2	1	16
	iv	0.01	< 0.05	< 0.1	< 0.5	< 0.005	< 0.5	< 0.5	< 0.3
ICSK-20	i	61.80	0.3	51	26	0.020	30	21	80
	ii	0.50	0.1	< 0.1	6	< 0.005	4	4	2
	iii	39.70	< 0.1	1.1	11	< 0.005	5	2	9
	iv	0.07	< 0.05	< 0.1	< 0.5	< 0.005	0.7	< 0.5	< 0.3

The mechanism of *complexation* is following: a metal is paired with a ligand supplied by a metal ligand salt, allowing metal desorption and helping to retain the metal ion in a solution in a complex form (McLaughlin et al., 2000). The weak chelating agents (EDTA, DTPA, TEA) are used most often. It seems reasonable that at least the more widespread use of DTPA reagent for testing „availability„ of Ni, Zn, Cu and Cd in contaminated soils is based on an internationally standardised method.

The *desorption/ion exchange processes* for extraction of metals from soil/sediments has not been used until now due to the very low analytic concentration, resulting from the extraction based on these processes. With the improvement of analytical instrumentation the detection limits were considerably lowered which allowed to detect very low concentration in the extracted solution. Mostly neutral salt solutions are used (NaNO<sub>3</sub>, Ca(NO<sub>3</sub>)<sub>2</sub>, Mg(NO<sub>3</sub>)<sub>2</sub>, NH<sub>4</sub>NO<sub>3</sub>, MgCl<sub>2</sub>, CaCl<sub>2</sub>). Generally, concentration of metals extracted by Cl salts are higher, than those extracted by corresponding nitrate salts.

Oxidation processes (with peroxide or acid solution of HNO<sub>3</sub>, HCl, HClO<sub>4</sub>, HF or aqua regia) can release metal sulphides and metals bound to organic materials. For heavy metals bound to (co-precipitated with) secondary sesquioxides (Fe, Mn, Al), *reducing agents* are used such as acidified hydroxylamine hydrochloride (NH<sub>2</sub>OH.HCl), acidified ammonium oxalate and dithionite/citrate solution (see also sequential extraction schemes).

The heavy metal concentrations in Slovakian contaminated soils obtained by different (single) extraction methods are presented in Tab. 2. It is clear from presented results that concentration of metals in different extractants is mainly a function of metal ability to be bound in different soil compounds. Higher concentration of several studied elements (As, Cu, Cr, Hg and Zn) in the ammonium acetate (+oxalate acid) fraction is due to selective binding of these elements to secondary Fe oxides. Especially high concentration of As in this fraction, as compared to the total content, points to the high selectivity of As to Fe oxides. Predominantly in alluvial soils redox

processes may partly deliberate As which can be than transported to the groundwater. Similar tendencies are evident for zinc (Tab. 2).

Very high portion of extractable Cd in contaminated soils is present in the fraction obtained by 0.05 M EDTA extraction. This extractant is used for extracting „available,, forms of the metal in soil to predict plant metal uptake. Our study, supported also by sequential extraction, points to the fact that Cd usually enters the highly „mobile,, fraction in contaminated soils independent of pH (our soils were mostly neutral - see Tab. 1). Cd contaminated soils show a good correlation between the total content and EDTA extractable concentration (Fig. 2). There have been assumptions, supported by some findings, that the behaviour of Cd in soil and its bioavailability differ according to Cd origin. Cd added to soils from anthropogeneous sources is more bioavailable (Kabata-Pendias and Pendias, 1992). Similar results were obtained also for lead contaminated soils in which both EDTA extractable and the fraction thought to be bind in Fe oxides are high.

CaCl<sub>2</sub> extraction has been suggested as the best predictor of phytoavailable metals in soils (Houba et al., 1996). A good correlation has been found only in limited number of soil types. Soils tested in our experiments are hardly to evaluate, as different soil types have been used, and no correlation between soil and plants has been detected. Anyhow, in some cases high concentrations of available Cd have been detected in soils (ICSK-11, 12).

Many authors have reported a good correlation between extractable metal content and metals uptake by

plants. However, the comparison between positive and negative results of such tests revealed in some cases insignificant correlation between extracted metals and metal content in tested plants. Some extractants are useful to extract metals and predict metal availability in neutral and calcareous soils (DTPA) but not in acid soils. Davies (1992) found a good correlation between the plant uptake and the amount of potentially toxic metals in contaminated soils using a strong extractant such as EDTA.

An overview of different results (positive or negative) published by Ross (1994) has shown that it is extremely difficult to summarise these findings since so many test solutions, different bioassay test plants, different soils and different extraction techniques have been used. Our results show that the prediction of plant metal content based on a single extraction is very questionable. Single extractants can neither give a useful information on the metal speciation in soils/sediments.

#### Selective sequential extraction (dissolution) procedures

Metal fractionations using sequential extraction techniques have been used to extract heavy metals from contaminated stream sediments (Tessier et al., 1979) and metals applied in waste sludge. Such extraction usually starts with the weakest, least aggressive and ends with strongest and most aggressive extractant. Sequential extractants are generally used to characterise five or six of the above stated fractions (see part: Metal speciation...). The weakest extractants in the system are the most spe-

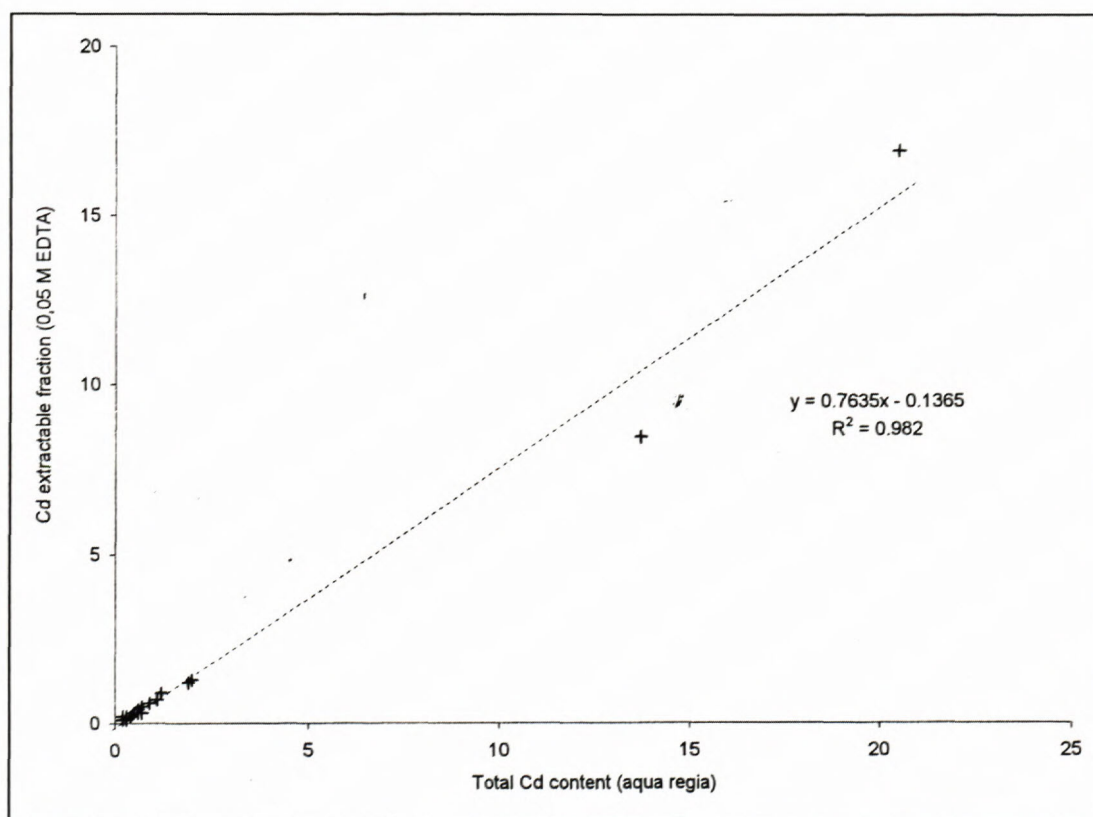


Fig. 2 Relationship between total and EDTA Cd contents in soils ( $\text{mg.kg}^{-1}$ )

cific, the later, stronger extractants, the least specific, but because they come later in the sequence, only one or two groups of compounds may remain that they can dissolve (Becket, 1989; Ross, 1994). A very large number of sequential extraction schemes have been used. The principal schemes of sequential chemical extractions are presented in Tab. 3.

It is clear from the table, that there are some differences in opinions concerning appropriate use of extractants. There is some agreement only about the *kinds* of extractants needed for each fraction. For example, soluble and easily exchangeable fractions are often extracted using dilute salt solutions replacing cations, while organically bound fractions are released using oxidising agents. Reducing agents are used to release metals bound in Fe and Mn oxides. Strong acids are used to assess residual or occluded metals in soils.

Up to now a range of problems and limitations were associated with sequential extraction. The major problem results from the fact that extractants are not as selective as it is stated. Another problem is related to a large number of different extracting techniques which make difficult to compare results from different studies.

Apart from those problems Salomons and Forstner (1984) pointed to three another serious problems that must be considered when using selective sequential extraction procedures:

- labile metal phases could be transformed during sample preparation,
- readsorption or precipitation processes could occur during extraction,
- the duration of extraction and the soil/solution ratios play important roles as far as the quantity of extracted metals.

Metal fractionation using sequential extraction techniques (Community Bureau of Reference, 1987) has been used in our study to identify the metals fate in contaminated alluvial soils of the Hron river basin. Results presented in Tab. 4 emphasise the possibility to predict the groundwater contamination through the soils (Čurlík et al., 2000). In the cited work soil characteristics are described in more details. Based on this study, only simple postulates are made here.

Mainly the soil organic matter and secondary Fe and Mn oxides are responsible for the soil metal retention. These soil components are unevenly distributed down the

Table 3: Five principal sequential extraction schemes for assessing metal fraction in soils/sediments. Numbers refer to stages in the extraction scheme

Fraction	Tessier et al. (1979)	Miller et al. (1986)	Sposito et al. (1982)	McLaren and Crawford (1973)	* BCR (1987)
Soluble		1 H <sub>2</sub> O			
Exchangeable	1 1 M MgCl <sub>2</sub>	2 0.5 M Ca(NO <sub>3</sub> ) <sub>2</sub>	1 0.5 M KNO <sub>3</sub>	1 0.05 M CaCl <sub>2</sub>	1 0.11 M Acetate acid
Acid Soluble		4 HOAc 0.1 M Ca(NO <sub>3</sub> ) <sub>2</sub>			
Adsorbed		3 Pb(NO <sub>3</sub> ) <sub>2</sub>	2 H <sub>2</sub> O	2 2.5% HOAc	
Organic	4 0.02 M HNO <sub>3</sub> 30 % H <sub>2</sub> O <sub>2</sub> 3.2 M NH <sub>4</sub> OAc	5 0.1M K <sub>4</sub> P <sub>2</sub> O <sub>7</sub>	3 0.5 M NaOH	3 1M K <sub>4</sub> P <sub>2</sub> O <sub>7</sub>	3 8.8 M H <sub>2</sub> O <sub>2</sub> 1 M NH <sub>4</sub> OAc
Fe Mn oxide	3 0.04 M NH <sub>2</sub> OH.HCl in 25 % HOAc				2 0.1 M Hydroxylamine + hydrochloric
Mn oxide		6 0.01 M NH <sub>2</sub> OH.HCl + 0.1 M HNO <sub>3</sub>			2 0.1 M Hydroxylamine + hydrochloric
Fe oxide		7 Ammonium Oxalate Acid in UV light		4 Ammonium Oxalate Acid	2 0.1 M Hydroxylamine + hydrochloric
Carbonate	2 1 M NaOAc		4 0.05 M Na <sub>2</sub> - EDTA		1 0.11 M Acetate acid
Residual	5 2 x 70 % HNO <sub>3</sub> 40 % HF/72 % HClO <sub>4</sub>	8 HNO <sub>3</sub> + HF	5 4 M HNO <sub>3</sub>	5 Conc. HF	4 HNO <sub>3</sub> +HF+HClO <sub>4</sub>

\* BCR – Community Bureau of Reference (1987)

Table 4: Results of heavy metals concentrations ( $\text{mg}\cdot\text{kg}^{-1}$ ) in different soil fractions obtained by sequential extraction analyses: i-exchangeable (carbonate) fraction (0.11 M Acetic acid), ii-fraction held in Fe-Mn oxide (0.1 M Hydroxylamine + hydrochloric), iii-organically bound (sulphidic) fraction ( $8.8 \text{ M H}_2\text{O}_2 + 1 \text{ M NH}_4\text{Oac}$ ), iv-residual fraction (soil samples decomposition with inorganic acid mixture  $\text{HNO}_3 + \text{HF} + \text{HClO}_4$ ).

Elements	Extraction method	Samples					
		LV-1		LV-2		LV-3	
		A hor.	C hor.	A hor.	C hor.	A hor.	C hor.
As	i	0.2	< 0.1	0.1	< 0.1	0.1	< 0.1
	ii	17.1	8.3	5.8	2.2	11.9	3.6
	iii	1.2	1.0	1.1	0.7	1.7	1.1
	iv	32.3	20.1	11.8	11.4	30.9	22.1
Cd	i	1.28	0.18	0.38	0.14	0.42	0.15
	ii	0.36	0.18	0.22	0.13	0.22	0.16
	iii	0.06	< 0.01	0.03	0.02	0.04	0.02
	iv	< 0.05	< 0.05	< 0.05	< 0.05	< 0.05	< 0.05
Cr	i	< 1	< 1	< 1	< 1	< 1	< 1
	ii	2	4	4	2	2	2
	iii	3	2	4	3	4	3
	iv	55	60	49	57	61	44
Cu	i	14	3	3	< 1	12	1
	ii	54	18	19	7	57	13
	iii	34	5	10	2	32	5
	iv	37	14	33	18	52	26
Hg	i	< 0.001	0.002	0.003	0.001	< 0.001	0.001
	ii	0.001	< 0.001	< 0.001	0.001	0.002	< 0.001
	iii	0.933	0.174	0.357	0.007	0.877	0.120
	iv	0.486	0.144	0.260	0.131	0.281	0.129
Ni	i	3	2	2	2	2	1
	ii	3	6	2	4	4	5
	iii	2	< 1	1	< 1	2	1
	iv	9	9	10	9	11	8
Pb	i	< 2	< 2	< 2	< 2	< 2	< 2
	ii	58	58	47	10	55	13
	iii	7	7	8	4	10	4
	iv	14	14	13	11	15	9
Sb	i	0.4	< 0.1	0.1	0.3	0.2	< 0.1
	ii	1.0	0.3	0.2	0.1	0.6	0.2
	iii	0.6	0.1	0.2	0.1	0.3	0.2
	iv	34.2	11.5	11.2	4.3	25.8	8.4
Zn	i	82	9	16	3	13	4
	ii	121	23	28	12	27	17
	iii	31	10	14	17	17	10
	iv	63	47	61	46	78	49
As	i	0.3	< 0.1	0.4	0.1	0.2	0.1
	ii	13.1	12.9	14.1	8.5	0.9	1.6
	iii	1.0	1.2	1.0	0.6	1.0	0.4
	iv	22.7	28.2	13.6	9.7	20.2	22.6
Cd	i	1.62	1.69	0.15	0.12	0.09	0.08
	ii	0.73	1.35	0.26	0.11	0.17	0.06
	iii	0.05	0.08	0.03	0.03	0.03	0.01
	iv	< 0.05	< 0.05	< 0.05	< 0.05	< 0.05	< 0.05
Cr	i	< 1	< 1	< 1	< 1	< 1	< 1
	ii	2	4	2	2	1	1
	iii	3	2	5	3	3	1
	iv	40	38	48	49	46	37
Cu	i	7	10	< 1	< 1	< 1	< 1
	ii	35	55	10	7	2	2
	iii	18	16	5	2	2	2
	iv	23	23	19	15	19	8

Table 4 (continued)

Elements	Extraction method	Samples					
		LV-1		LV-2		LV-3	
		A hor.	C hor.	A hor.	C hor.	A hor.	C hor.
Hg	i	< 0.001	0.006	0.003	< 0.001	0.002	< 0.001
	ii	0.002	0.003	< 0.001	0.001	0.001	< 0.001
	iii	0.592	0.617	0.035	0.009	0.104	0.021
	iv	0.146	0.174	0.092	0.130	0.093	0.079
Ni	i	2	1	1	1	1	< 1
	ii	4	5	7	5	6	4
	iii	3	< 1	3	2	< 1	< 1
	iv	9	10	10	10	11	7
Pb	i	2	< 2	< 2	< 2	< 2	< 2
	ii	75	102	23	11	14	6
	iii	7	7	4	3	5	4
	iv	16	17	10	8	11	8
Sb	i	0.5	0.3	0.1	0.2	0.1	0.5
	ii	0.5	0.7	0.2	0.1	< 0.1	0.1
	iii	0.2	0.1	< 0.1	< 0.1	0.1	< 0.1
	iv	18.1	20.0	10.5	5.8	4.5	4.7
Zn	i	71	63	3	3	2	< 1
	ii	130	152	23	15	12	7
	iii	27	32	10	9	6	7
	iv	66	73	58	49	51	39

LV-1 – Kozárovce (Gleyic Fluvisol, pH/KCl – 6.72), LV-2 – Hronský Beňadik (Fluvisol, pH/KCl – 6.41), LV-3 – Starý Tekov (Fluvisol, pH/KCl – 5.4), LV-5 – Tekovský Hrádok (Fluvisol, pH/KCl – 7.31), LV-6 – Mýtne Ludany (Phaeozem, pH/KCl – 6.93), LV-8 – Hronské Kľačany (Phaeozem, pH/KCl – 7.04).

soil profiles depending on the soil processes. But metal affinities to different soil fractions may play an important role for the proportion of metals held in so called „mobile„ forms.

As it was stated above, *arsenic* is mostly present in the residual fraction. Second place belongs to the fraction held in Fe and Mn oxides. Hence, the distribution of As in soil profiles partly corresponds to the formation (cumulating) of secondary oxyhydroxides within the depth.

*Cadmium* shows marked tendency to concentrate in the most mobile (exchangeable) fraction and partly in the reducible fraction (in Fe, Mn-oxides).

*Chromium* is mostly present in the residual fraction which points to the low mobility of his element in the soil (mostly Cr<sup>3+</sup>).

*Copper*, which is able to form chemical compounds of different solubility, can be present in different soil fractions, as it is apparent from the sequential extraction. Highly mobile (soluble) forms of copper are usually present in small amounts in the soil solution. Copper is also fixed to secondary sesquioxides.

*Mercury* is strongly held in organic matter. Therefore in all contaminated soils the highest concentration of mercury has been revealed in the organically bound fraction. Fortunately, this is the reason for the low potential toxicity of mercury in soils (except of methylated forms).

*Nickel* can be partly mobile in soils. Small portion of nickel in exchangeable fraction points to a possibility that this metal can be transferred from sources of contamination to the groundwater or from soils to plants.

*Lead* is concentrated mostly in secondary sesquioxes (Fe, Mn, Al), humus and clay. It is postulated that potential of lead toxicity related to the soil is low. The results point to the high portion of Pb concentrated in secondary oxides.

*Antimony* is usually dispersed in soil. In contaminated soils of the Hron river basin Sb is distributed to a long distance from known contamination sources (Nízke Tatry Mts., Štiavnické vrchy Mts. and Kremnické vrchy Mts.). Antimony is a weak migrant when oxidised. But its concentration in plants, and small concentration in the very mobile fraction (exchangeable), far from primary contamination sources, point to a possible water transport of Sb similarly to As, to which it is geochemically linked (Alloway, 1990; Fergusson, 1990).

*Zinc* is present in soil in several fractions (Alloway, 1990): water-soluble, exchangeable, fixed to organic matter, clay and nonsoluble metal oxides. From the sequential extraction it is clear that higher proportion of Zn is bound to secondary oxides (Fe, Al?, oxides).

Various sequential extraction schemes have been developed, including the one of the European Commission (formerly BCR) which was used in our study. This

scheme can be improved only in the presented way to be predictable for a plant uptake of metals or for an adverse effect on human health or eco-toxicity, but such results are still missing (McLaughlin et al., 2000).

### Metal concentration in pore (soil) solution

Apart from the occurrence of elements in the solid phase of soil/sediment little is known about their concentration and speciation in a pore (soil) solution. The knowledge about pore solution concentration and the solubility of elements is of a great importance in studies of their biogeochemical cycles and their availability to plants. Plants essentially take up heavy metals from soil via solution. On the other hand, heavy metals from the

solution may be transferred (leached) to the groundwater and cause its contamination.

The pore solution is the most important constituent influencing chemical and biological activities in soils/sediments. Soil organisms without water die or become dormant. Mineral transformation becomes slow and chemical weathering is limited.

In spite of the overall acceptance of these general statements there is no meaningful definition of the pore solution. From the viewpoint of soil chemistry the pore (soil) solution is defined as „the aqueous liquid phase in whose the composition is influenced by flows of matter and energy between it and its surroundings and by the gravitational field of the Earth (Sposito, 1989).

Table 5: Major inorganic components in pore (soil) solution (Sumner, 2000).

Category	Major component ( $10^{-4}$ to $10^{-2}$ mol.l $^{-1}$ )	Minor components ( $10^{-6}$ to $10^{-4}$ mol.l $^{-1}$ )	Others
Cations	Ca $^{2+}$ , Mg $^{2+}$ , Na $^{+}$ , K $^{+}$	Fe $^{2+}$ , Mn $^{2+}$ , Zn $^{2+}$ , Cu $^{2+}$ , NH $_4^{+}$ , Al $^{3+}$	Cr $^{3+}$ , Ni $^{2+}$ , Cd $^{2+}$ , Pb $^{2+}$
Anions	HCO $_3^{-}$ , Cl $^{-}$ , SO $_4^{2-}$	H $_2$ PO $_4^{-}$ , F $^{-}$ , HS $^{-}$	CrO $_4^{2-}$ , HMoO $_4^{+}$
Neutral	Si(OH) $_4^0$	B(OH) $_3^0$	

Table 6: Major organic components found in pore (soil) solution (Sumner, 2000).

Source	Major components ( $10^{-5}$ to $10^{-3}$ mol.l $^{-1}$ )	Minor components ( $<10^{-5}$ mol.l $^{-1}$ )
Natural	carboxylic acids, amino acids, simple sugars	carbohydrates, phenols, proteins, alcohols, sulfhydryls
Anthropogenic		herbicides, fungicides, insecticides, PCBs, PAHs, petroleum, hydro- carbons, surfactants, solvents

By this definition the pore solution is an open system that exchanges matter and energy with other subsystems (air, water, biota). Also, because the solution is defined as a phase it implies that the pore solution has uniform properties and can be isolated from soils (sediments). These requirements of uniformity (stable composition, temperature) can be met only on small time-space area because of the variable nature of the pore solution. The pore solution is not a distinct entity but rather it is a continuum of phases, ranging from that held in colloids, through the immobile water in micropores, to free water percolating through macropores.

As the pore solution is highly variable its composition can be discussed only in general terms. The concentration of inorganic constituents in the pore solution is controlled by pH, Eh and solid phase composition.

Commonly found inorganic components in pore solution are given in Tab. 5. Trends in composition are similar but natural and anthropogenic factors can have big influences on this composition. The composition of soluble organic components in the pore solution reflects the composition of organic matter in the solid phase. Major organic components found in pore (soil) solution are present in Tab. 6. All studies of metals in pore solution suffer from two major problems:

- finding suitable techniques for detecting extremely low concentrations,
- differentiation between free metal ions in solution and soluble organo/metallic complexes.

Other problems are associated with obtaining of an unaltered solution. The moisture of field soils and fresh sediments can range from air dried to saturated over short period of time. Most techniques for obtaining samples of solutions function poorly when water content is below the saturation.

Methods for obtaining the pore solution can be broadly categorised in three groups: *aqueous extracts*, *column displacements* and *pressure extraction*. An alternative method is to use saturated soil paste (USDA, 1954).

Obtaining *aqueous extract* includes adding water to samples, to the point of saturation or beyond, equilibrating and removing solution.

*Column displacement* consists of forcing a fraction of pore solution to move from the soil (sediment) by leaching by an aqueous solution or with nonsoluble organic solvent. This procedure can be modified to include pressure from the top or vacuum applied to the bottom of the column.

Neither the variation in the total electrolyte concentration nor the activity ratios of specific ion components

Table 7: Soil solution concentrations (soil solution extraction by 0.002 M CaCl<sub>2</sub>)

Sample	pH	EC mS/m	Cl <sup>-</sup> µg/l	(SO <sub>4</sub> ) <sup>2-</sup> µg/l	(HCO <sub>3</sub> ) <sup>-</sup> µg/l	N-NO <sub>2</sub> µg/l	N-NO <sub>3</sub> µg/l	N-NH <sub>4</sub> µg/l	N-tot. µg/l	Ca µg/l	Mg µg/l	Na µg/l	K µg/l	Al µg/l	Fe µg/l	As µg/l	Cd µg/l	Cr µg/l	Cu µg/l	Hg µg/l	Ni µg/l	Pb µg/l	Zn µg/l
ICSK-1	6,7	21,95	13570	5200	183	378	< 90	3885	13945	90,374	19480	2700	20040	37	62	20	2	< 2	48	0,1	14	< 10	93
ICSK-2	7,3	21,47	14810	9400	153	566	4179	2139	13583	121,45	8530	2090	3010	< 20	20	2,7	5	3	74	0,1	152	< 10	720
ICSK-3	6,8	18,63	12340	3400	122	2750	2146	1926	18576	63,735	31410	3480	13340	< 20	20	6,7	3	< 2	77	0,1	44	13	210
ICSK-4	7,4	16,74	9880	3800	122	798	2733	1148	10342	86,229	17010	610	9550	< 20	10	12,6	< 2	2	62	< 0,1	35	12	110
ICSK-5	6,0	21,47	17280	11200	37	1684	6438	1829	15441	84,610	10090	3430	37290	35	40	18,1	2	< 2	129	< 0,1	52	< 10	300
ICSK-6	6,8	16,74	9880	4600	122	1236	2485	1193	8618	109,19	12690	1340	1790	< 20	30	2,4	< 2	< 2	31	0,1	16	< 10	80
ICSK-7	6,4	14,38	9880	13400	37	1833	9849	4053	16354	81,736	7910	1630	5240	32	60	10,4	2	2	269	0,3	44	< 10	270
ICSK-8	7,1	16,74	14810	4000	153	1784	3840	1779	18243	95,655	26880	870	3419	< 20	40	1,4	< 2	2	26	< 0,1	21	< 10	110
ICSK-9	7,2	21,5	11110	6600	183	1964	1694	2252	6715	107,21	18510	4070	7680	46	10	40,8	2	3	73	< 0,1	13	< 10	68
ICSK-10	6,3	12,91	20980	6800	37	1145	474	1548	7924	74,775	15570	9450	4550	95	20	10,5	< 2	< 2	66	0,3	17	< 10	58
ICSK-11	6,5	11,56	23450	5400	18	37	< 90	676	7356	81,204	9520	5860	15770	47	16	1,5	7	< 2	50	0,3	10	< 10	466
ICSK-12	6,1	8,84	20980	11200	37	37	1649	1070	5795	63,177	1383	4960	14420	27	22	1,1	32	2	86	0,9	19	< 10	2790
ICSK-13	6,7	34,28	13570	8600	183	< 6	< 90	5348	9458	118,78	15480	1350	31860	125	67	11,1	26	< 2	40	1,3	35	26	209
ICSK-14	6,8	12,97	11110	5000	37	79	836	1070	14257	65,199	22550	2660	20940	< 20	283	2,9	138	8	56	1,2	36	< 10	189
ICSK-15	7,2	28,51	13570	6400	214	1322	565	1661	10444	96,263	22160	2280	29670	53	41	11,9	19	3	68	1,0	< 10	< 10	75
ICSK-16	6,9	17,85	16040	2400	122	1023	3569	1126	15851	93,912	15940	5980	6780	< 20	20	26,7	5	< 2	46	1,3	< 10	< 10	106
ICSK-17	6,8	39,61	18510	87500	183	1065	9510	760	22341	126,98	24750	7930	4920	< 20	42	6,5	7	2	77	0,7	< 10	< 10	101
ICSK-18	6,9	31,62	25920	19200	183	1309	2259	1126	17248	112,89	21400	16810	2480	176	99	13,3	8	< 2	46	0,9	17	< 10	137
ICSK-19	7,0	20,07	6170	2000	122	956	2711	2167	8114	101,12	5290	985	40960	224	103	7,0	3	4	97	0,4	< 10	12	57
ICSK-20	6,8	21,85	25920	3800	122	518	271	1281	5799	97,471	14770	9000	3180	56	43	6,7	5	4	33	0,6	16	< 10	46

of the pore solution can be adequately resolved when water to sample ratios vary from field moisture contents to ratio >1. This is the main limitation to the use of water extracts as models for pore solution (Sumner, 2000).

*Pressure extraction* is defined as the use positive pressure or vacuum, eventually centrifugation, to remove the pore solution.

*Field methods* include several types of lysimetric studies.

From above stated it is obvious that at least:

- the definition of pore solution is idealised and more functional definition is needed before the concentration/activities of free metal ions in pore solution will be used for the assessment of critical limits;
- the adjustment of design, execution and interpretation of pore solution study methods is strongly recommended;
- the derivation of the total dissolved metal concentration from the total pore concentration should be based on clear understanding of the pore solution. The partition of metals concentration between solid phase and solution should be clearly related to transfer functions.

The solubility of heavy metals under field conditions is strongly linked to soil parameters such as pH, SOM and DOC (Romkens and Salomons, 1998).

The studied soils have acidic to neutral character (pH 5.51 – 7.14) with CEC ranging from 13.75 – 35.65 cmol.kg<sup>-1</sup> (Tab. 1). As it was stated in methodological part of this paper, in this study the soil solution was extracted by 0.002 M CaCl<sub>2</sub>.

It should be noted that the obtained results (Tab. 7) have very high concentrations of Ca<sup>2+</sup> and Cl<sup>-</sup>. It is clear that the results are influenced by the background solution. This conclusion is supported also by the relatively low HCO<sub>3</sub><sup>-</sup> concentration which should be related to Ca<sup>2+</sup> content in these soils.

The content of SO<sub>4</sub><sup>2-</sup> is relatively high and points to the fact that some elements in solution were leached due to acid sulphate weathering of sulphides (and hence, sulphatic complexation of metals may play some role in metals transfer).

The nutrient element concentrations in soil solution (K, Mg, Na) show some relation to the parent rocks or to the application of fertilisers (agricultural soils).

The Al and Fe concentration in soil solution does not give clear evidence to soil properties. Higher Fe concentration occurs in soils with some gleyic features.

The potential toxic elements (As, Cd, Cr, Cu, Hg, Ni, Pb and Zn) show relatively high concentrations in soil solution. The limit value for As in the groundwater (5 µg.l<sup>-1</sup>) is exceeded in more than half of the samples. Arsenic, which occurs as oxoanions in soils, may show an increase in concentration in soil solution with rising pH. This might be the case of soils with gleyic carbonatic processes.

The total content of Cd in studied soils ranges from 0.3 to 20.5 mg.kg<sup>-1</sup>. Cd solution concentrations range from < 2 (detection limit) to 138 µg.l<sup>-1</sup>, which is extremely high. The critical limit proposed for Cd concen-

tration in soil solution (precautionary principle) is 10 µg.l<sup>-1</sup> (Čurlík et al. 2000) and it is exceeded in several soils contaminated by Zn-Pb (ICSK 11-16). As it was stated by Romkens and Salomons (1998) no single relation appears to exist between the total Cd content and the solution concentration. In the forest soils frequently higher Cd content in soil solutions is due to lower pH values and higher soluble organic fraction content.

The concentration of Cr in soil solution is relatively low and point to known aspects of low solubility/mobility of Cr<sup>3+</sup> compounds.

The Cu solution concentrations range from 31 to 269 µg.l<sup>-1</sup>. These concentrations are high and may have an adverse effect to plants (de Vries and Romkens, 2000; In Čurlík et al. 2000). Higher Cu concentrations in pore solutions may be controlled by DOC (dissolved organic carbon), as pointed by Romkens and Salomons (1998), and in alkaline soils (Fotovat and Naidu, 1998). Cu solution concentration in studied contaminated soil is above the limit for groundwater quality standard (20 µg.l<sup>-1</sup>).

Suggested critical limit for mercury concentration in soil solutions is 0.1 µg.l<sup>-1</sup> (Čurlík et al., 2000). In spite of the fact that studied soils are not Hg - contaminated (see Tab. 2 – total content) its solution concentrations are mostly above the limit.

In several soils the solution concentrations for nickel are above the current groundwater quality standards (20 µg.l<sup>-1</sup>). This may lead to leaching of Ni to groundwater.

The proposed critical limit for lead in soil solution is 50 to 80 µg.l<sup>-1</sup> (Čurlík et al., 2000). The results show that lead is a bad migrant and its concentrations in soil solutions are not high.

Current Dutch groundwater quality standard for Zn is 65 µg.l<sup>-1</sup> (Romkens and Salomons, 1998). The solution concentrations of Zn in soils are much above the standard.

The solubility of potentially toxic elements under field conditions is thought to be linked to soil parameters (Romkens and Salomons, 1998). To obtain more reliable estimates more results related to metal solubility and leaching still need to be obtained.

## Conclusions

Recent advance in soil and sediment testing for potentially toxic elements is due to the improvement of analytical methods, especially the detection of low element concentrations, but also due to better understanding of the behaviour of metals related to soil (sediment) properties.

Recent developments of the testing methods continue in three directions: *single extraction* with soft extractant, *sequential extraction* with multi-solution extraction and *soil (pore) solution testing*, which is thought to be the best predictor of plant available metals. For all the mentioned methods, which are widely used, no meaningful measures exist for metal bioavailability till now. An improvement of these methods needs first of all an increase of the information level on the mobility (toxicity) of extracted species of elements.

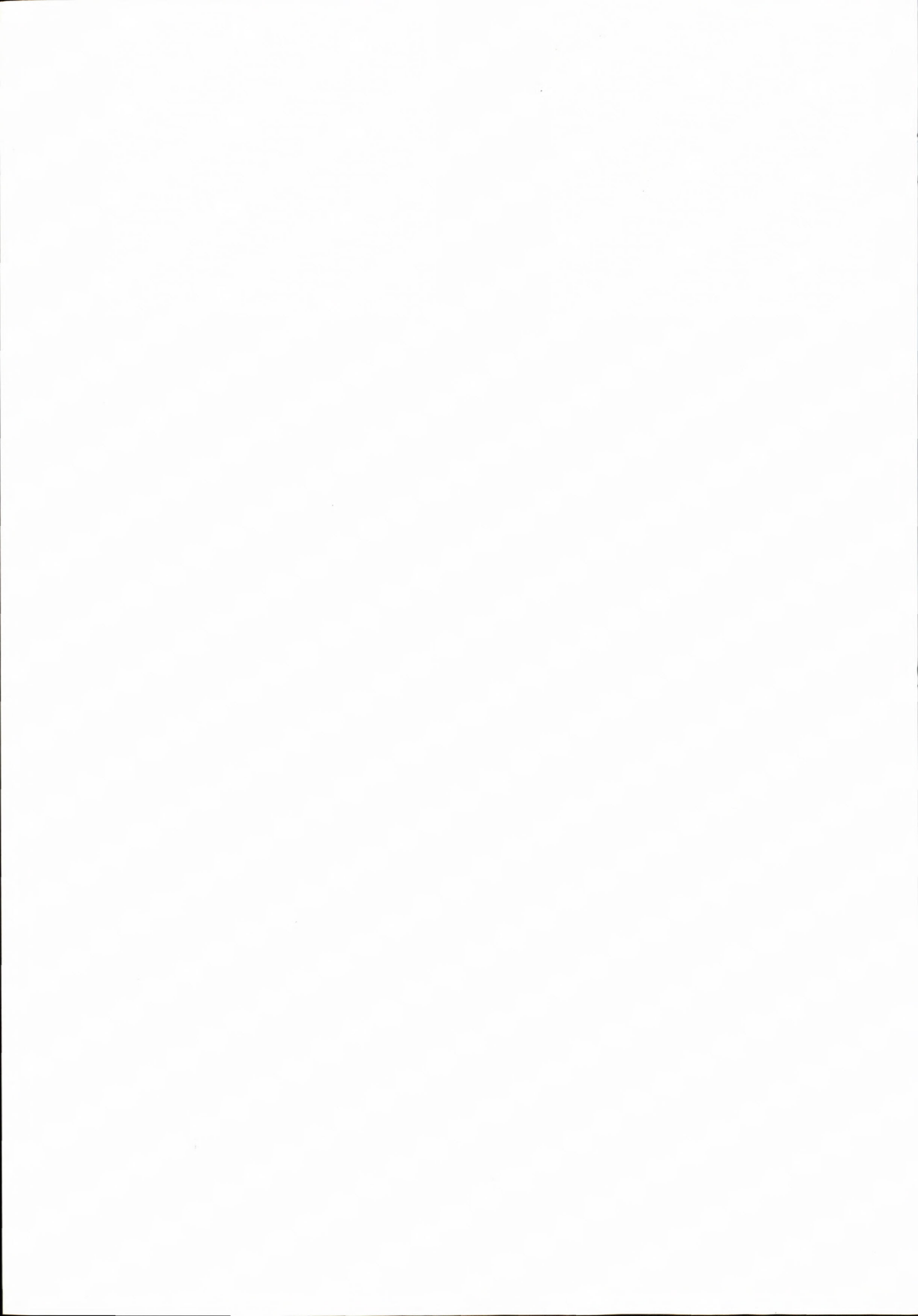
The results presented in this work show that contaminated soils may possess some danger for plants in topsoils and for the enhanced leaching towards to the groundwater in subsoils. Mobile fraction concentrations of different contaminated Slovakian soils, obtained by single extractant, are high for heavy metals (Cd, As, Cu, Zn) but no calibration data exists as far as the real toxicity to plants. The mobile Cd fraction concentration is clearly not related to soil properties (pH) but more closely to the total Cd content or to the form of Cd occurrence in soils (anthropogenic).

The results of sequential extraction analyses of contaminated alluvial soils of the river Hron basin show that some potentially toxic elements (Cd, Cu, Zn and possibly As, Sb) are present in most mobile fractions. These elements are brought from different remote sources (mining areas). This gives some evidence about a possible adverse effect for plants and groundwater (groundwater - soil interaction).

Soil (pore) solution testing results based on the soil solution extraction method show that As, Cd, Cu, and partly Zn and Hg exceeded current groundwater quality standards or critical limits (for Cd, Hg) proposed during the Bratislava meeting (Čurlík – Šefčík and Viechová, 2000). High concentrations of potentially toxic elements in soil (pore) solutions can be harmful for plants and the groundwater. The acidification of diffusely contaminated soils may speed up the mobility (leaching) of these elements and their transfer to plants (or groundwater).

## References

- Alloway, B. J., 1990: Heavy metals in Soils, London, 342 p.
- Becket, P.H.R.T., 1989: The use of extractants in studies on trace metals in soils. *Advances in Soil Science*, 9, pp. 143-176
- Berrow, M. L. and Burrige, J. C., 1980: Trace elements level in soil: effect of sewage sludge. In: *Inorganic Pollution and Agriculture*, pp. 159 - 190. MAFF Reference Book No. 326. HMSO, London
- Čurlík, J., Šefčík, P. and Vojtek, R., 2000: Set of regional maps of environmental geological factors of NE part of Levice district in scale of 1: 50 000 - Soil and soilgeochemical maps. (in Slovak) Final report, VÚPOP, Bratislava, 76 p.
- Čurlík, J., Šefčík, P. and Viechová, Z., (Edits) 2000: Ad Hoc International Expert Group on Effect-based Critical Limits for Heavy Metals. Proceedings, SSCRI Bratislava, Slovak Republic, 164 p.
- de Vries, W., and Romkens, P., 2000: Critical limits for heavy metals. In: *Ad Hoc International Expert Group on Effect-based Critical Limits for Heavy Metals*. Proceedings, SSCRI Bratislava, Slovak Republic, pp. 84 - 86
- Davies, B.E., 1992: Inter-relationships between soil properties and the uptake of cadmium, copper, lead and zinc from contaminated soil by radish (*Raphanus sativus* L.). *Water, Air, Soil Pollut.*, 63, pp. 331 - 342
- de Vries, W. and Bakker, D.J., 1998: Manual for calculating critical loads of heavy metals for terrestrial ecosystems. Guidelines for critical limits, calculation methods and input data. Wageningen, the Netherlands, DLO Winand Staring Centre, Report 166, 144 pp.
- Fergusson, J.E., 1990: *The Heavy Elements. Chemistry, Environmental Impact and Health effects*. Pergamon Press, 614 p.
- Fotovat, A, Naidu, R., 1998: Changes in composition of soil aqueous phase influence chemistry of indigenous heavy metals in alkaline sodic and acidic soils. *Geoderma*, 84, pp. 213 - 234
- Gregor, H. D., Spranger, T. and Honerbach, F., 1997: Critical limits and Effect based Approaches for Heavy Metals and Persistent Organic Pollutants. Proceedings of the Workshop Texte 5/98, Bad Harzburg, Umweltbundesamt, Berlin, pp. I-1 - I-352
- Gregor, H. D., Mohaupt-Jahr, B. and Honerbach, F., 1999: Workshop on Effect- Based Approaches for Heavy Metals. Proceedings of the Workshop Texte 87/99, Schwerin, Umweltbundesamt, Berlin, 157 p.
- Houba, V.J.G., Lexmond, T.M., Novozamsky, I. and van der Lee, J.J., 1996: State of the art and future developments in soil analysis for bioavailability assessment. *Science of the Total Environment*, 178, pp. 21 - 28
- Kabata-Pendias, A., Pendias, H., 1992: *Trace elements in Soils and Plants*, CRC Press London, 2<sup>nd</sup> edition, 365 p.
- Keefer, R.F., Codling, E.E. and Singh, R.N., 1984: Fractionation of metal-organic components extracted from a sludge-amended soil. *Soil Science Society of America*, 48, pp. 1054 - 1059
- Mackových, D., Nováková, J. and Šoltýsová, H. 1999: Experimental works in heavy metal speciation of stream sediments. (in Slovak), *Geochémia 1999*, Department of geochemistry of Nat. Scie. Faculty of Comenius University Bratislava, pp. 67 - 71
- McLaughlin, M.J., Zarcinas, B.A., Stevens, D.P. and Cook, N., 2000: Soil testing for heavy metals. *Commun. Soil Sci. Plant. Anal.*, 31(11-14): pp. 1661-1700
- Miller, W.P., Martens, D.C. and Zelazny, L.W., 1985: Effect of sequence in extraction of trace metals from soils. *Soil Science Society of America*, 50, pp. 579 - 584
- Ross, S. M., et al., 1994: *Toxic Metals in Soil - Plant Systems*. J. Willey & Sons, 469 p.
- Romkens, P.F.A.M. and Salomons, W., 1998: Cd, Cu and Zn solubility in arable and forest soils: consequences of land use changes for metal mobility and risk assessment. *Soil Science*, Vol. 193, No. 11, pp. 859 - 871
- Salomons, W. and Forster, U., 1984: *Metals in the Hydrocycle*. Springer-Verlag, New York
- Salomons, W., Forster, U. and Mader, P., (eds), 1995: *Heavy Metals*. Springer-Verlag, Berlin, Germany.
- Shuman, L.M. and Hargrove, W.L., 1985: Effect of tillage on the distribution of magnese, copper, iron and zinc in soil fractions. *Soil Science Society of America*, 49, pp. 1117 - 1121
- Sposito, G., 1989: *The Chemistry of Soils*. Oxford University Press, New York - Oxford, 279 p.
- Sumner, M.E. (Edit.), 2000: *Handbook of Soil Science*. CRC Press London, New York
- Tessier, A., Campell, P. G. C. and Bisson, M., 1979: Sequential extraction procedure for the speciation of particulate trace metals. *Anal. Chem.*, 51 (7), pp. 844 - 851
- Van Straalen, N.M. and Bergema, W.F., 1995: Ecological risk of increased bioavailability of metals under soil acidification. *Pedobiologia*, 39, pp. 1-9



## Potential Influence of Geochemical Background on the Health State of Population of the Slovak Republic

RAPANT, S.<sup>1</sup>, KHUN, M.<sup>2</sup>, JURKOVIČ, Ľ.<sup>2</sup> and LETKOVIČOVÁ, M.<sup>3</sup>

<sup>1</sup>Geological Survey of the Slovak Republic, Mlynská dolina 1, 817 04 Bratislava

<sup>2</sup>Department of Geochemistry, Faculty of Natural Sciences, Comenius University, Mlynská dolina, 842 15 Bratislava

<sup>3</sup>ENVIRONMENT, P.L.C., Dlhá 8, 949 01 Nitra

*Abstract.* The paper presents possibilities for using geochemical databases for solving problems of the influence of geological environment contamination on the health state of people. Using statistical methods it was confirmed that significant correlation exist between chemical elements in stream sediments of Slovakia (analysed for As, B, Be, Bi, Ca, Co, Cr, Cu, Hg, Mn, Sb and Se) and demographic and medical indicators of the health state of population of the Slovak Republic (e.g. PYLL – potentially lost years of life; POD-2500 – low birth weight expressed in percentage from all born children per 100 000 inhabitants, Ca-UMR – mortality rate due to all types of malignancy per 100 000 inhabitants; HUO – gross mortality of inhabitants; etc.).

*Key words:* medical geology, geochemistry and health, Slovakia

### Introduction

Along the life style (the way of life and work), genetic factors and the level of health care the environment is one of the critical factors influencing the health state of population and thereby also the quality of life and life expectancy of people. Its significance and influence rises especially in polluted regions where even a geographically important occurrence of increased sickness rate can appear.

Geographical factors of extension of some diseases are known virtually since the existence of medicine as a science. Already in the 4<sup>th</sup> century A.D. the Chinese were familiar with the influence of environmental factors on the human health, especially related to an endemic occurrence of struma. Despite the fact that the medical science knows long ago that the sickness rate of some diseases in some individual parts of the world is different, the medical geography or geographical medicine as a science originated virtually just in the first decades of the 20<sup>th</sup> century. Of course, during the study of spread of various diseases, in geographical terms, some connections have been sought particularly related to climatic or topographic factors. However, in most cases the connection of geography and medicine can not explain the causality between significant geographical differences and spread of some diseases. In order to resolve this causality responsibly it is absolutely necessary to use geochemical information. Than, in this manner, the space for independent scientific field – medical geochemistry has been opened.

### Chemical elements and their relationship to diseases

The relationship between the geochemical background and the human is far closer than generally supposed. A state of illness of a human occurs if the balance between the organism and factors of external environment is disturbed. This can happen due to the influence of endogenous factors (state of organism of an individual human) as well as due to the effect of exogenous factors (the influence of environment). Then, geomedical research can be applied here. Medical geochemistry deals with the application of geochemistry and geochemical mapping to the health state of plants, animals and humans.

Medical geochemistry, as a branch of geomedicine, is a scientific field that deals with the influence of chemical composition of geochemical environment of natural and anthropogenous origin, waters, soils, recent sediments and rocks to the human and animal health in the context of external environmental factors (Khun, 1992).

Nowadays, a great amount of examples exist in literature where the causal relation between an excess or a lack of chemical elements in geochemical environment and an increased occurrence of some diseases has been shown on various world and slovak localities. In the table 1 selected examples are presented, processed based on several literature sources (Zýka, 1975, Fergusson, 1990; Bencko at al, 1991; Khun, 1992; ATDSR, 1992; Thornton, 1993; Alloway-Ayres, 1993; Škárka – Ferenčík, 2000; WHO, 1996 and others). Apparently, the table shows that nowadays the influence of the excess of individual ele-

Table 1 The influence of deficiency or excess of chemical elements in geochemical environment on the occurrence of some diseases

	Deficiency	Excess
Al	–	– Alzheimer disease
As	– insufficient hair growth – enlargement of spleen	– skin, lungs cancer – terratogenic effects – skin diseases
B	–	– alimentary canal diseases
Ba	–	– mechanic damage of lungs – stomach cancer – nerves poison – influence on the central nerve system
Be	–	– „Urov disease,“ – berylliosis – professional or long-time exposures – carcinogenicity, elephantiasis
Ca	– bones deformations – cardiovascular diseases (water hardness)	– uric acid stones – atherosclerosis, hypertension – related to the water hardness (Ca+Mg) – inverse relation of mortality from these diseases to water hardness
Cd	– growth reduction	– prostate cancer – environmental carcinogen
Ce	–	– positive correlation with skin cancer and other malignant melanomas
Co	– anaemia – avitaminosis	– thyroid diseases (Co / I ratio)
Cr	– diabetes	– carcinogenicity, especially in a professional exposure – lungs cancer related to Cr content in asbestos
Cu	– anaemia	– Cu – toxicosis – relation of Cu content in water to atherosclerosis
F	– defects in bones and teeth evolution (caries)	– spottiness of teeth (fluorosis) – relation to hearth diseases in areas with high F content
Fe	– anaemia	–
Hg	– unknown	– relation between Hg and I contents in environs with spread of struma – disorders of central nerve system – acute toxic – effect on saddles, liver – environmental carcinogen
K	–	– virtually intoxic – possible influence on hypertension
Li	– relation between deficiency in drinking water and atherosclerosis	– assumed „protective,“ functions
Mg	– deficiency is related to phatogenesis of cancer – „anticarcinogenic,“ influence – cardiovascular diseases (water hardness)	– anaesthesia – relation to cardiovascular diseases (Ca+Mg)
Mn	– skeleton deformations	– shakiness of limbs – defective hearing
Mo	– teeth defectiveness – caries	– diseases of alimentary canal at livestock – reduction of growth
Na	–	– cardiovascular diseases
Ni	– skin diseases	– carcinogenicity (tetracarbonyl Ni, Ni in asbestos)
P	– rachitis	– minor relation between geochemical distribution of P and diseases
Pb	–	– sclerosis multiplex – carcinogenicity in relation to Pb content in soils – positive correlation between Pb content in drinking waters and mortality from cardiovascular diseases
Rn	–	– lungs and windpipe cancer – cardiovascular diseases
Sb	–	– professional exposure – poisonings, skin and eyes damage, respiratory problems – long-time exposures – respiratory problems, cardiovascular diseases, gastrointestinal defects
Se	– Keshan disease – endemic myocarditis, can cause progress of tumours in animal systems, sterility	– alimentary canal defects – skin hyperpigmentation, changes on nails
Sn	– reduced growth	– indirect influence (at professional exposure)
Sr	–	– diabetes – „Urov,“ disease – negative correlation between Sr content in environment and mortality from cardiovascular diseases – increased Sr content in cancerous tissues
Ti	–	–
V	– cardiovascular diseases	– negative influence at professional exposure only
W	–	– negative influence at professional exposure only
Zn	– strong reduction of growth – bad curability of wounds	– increased mortality from cancer (predominantly stomach)
Zr	– decrease in number of red corpuscles	– relation to elephantiasis
Ca+Mg (water hardness)	–	– negative effect of soft water on cardiovascular system – positive correlation between water hardness and some forms of cancer
NO <sub>3</sub> <sup>-</sup>	–	– alimentary methemoglobinemia – carcinogenic effect of nitrates metabolites – nitrites, nitrosamines

ments, especially toxic metals, on the occurrence of diseases is much more known, proved and evaluated than the influence of the deficiency of chemical elements. In industrially developed countries the cases of diseases resulting from primary and simple deficiency of trace elements are relatively rare, because the consummation of food from various parts of the state or even continents guarantees the minimum necessary reception of all elements. The influence of the deficiency is manifested especially locally in developing countries, where the majority of food is provided by the population itself from local sources.

### **Environmental geochemistry and medical geochemistry in Slovakia**

Based on the extensive geochemical mapping of the territory of the Slovak Republic, carried out in the 1990's by means of geochemical atlases and environmental-geochemical maps (Vrana et al., 1997; Rapant et al., 1999), several areas with extensive contamination of waters, soils, sediment, rocks, especially by toxic elements but also by major elements as well as organic pollutants, have been documented. These areas include mainly the regions with historical mining of mineral raw materials as well as regions with highly developed industry and agriculture. In several of these areas concentration of various harmful (including carcinogenic, mutagenic and toxic) elements and materials are known in such concentrations that a reasonable suspicion exists about the highly negative impact of the polluted environment on the human health. A representation of the global environmental load of the Slovak Republic by toxic elements is clear from the figure 1 – *Distribution of the degree of stream sediments contamination in Slovakia*. Spišsko-gemerské rudohorie Mts. region is one of the areas where the geochemical environment is characterised by high concentrations of toxic elements, but furthermore also for example by pollution from alkaline emissions from magnesite industry, contamination from agriculture and other anthropogeneous activities. Just this region was selected as a pilot area, where the Geological Survey of the Slovak Republic in collaboration with several other environmentally oriented organisations nowadays elaborates and tests the methodology of evaluation of the geochemical environment contamination in relation to the health state of population (Rapant et al., 1998). Within the framework of this project methodological procedures of connecting geochemical data with demographic and medical data are elaborated and evaluated. Apart from the total content of elements in individual environmental components, also the forms of their occurrence are monitored – speciations, their bioavailability and toxicity. Concentrations of major elements, toxic elements, but also selected organic macro- and micropollutants are evaluated and correlated. In collaboration with the State Health Institute, Košice the achieved results are processed and evaluated by direct medical monitoring on people living in the most contaminated areas.

Study of the health state of population is in focus of many scientific fields, among those geology and geochemistry has an important place. Geological structure determines the character and mode of exploitation of a country, while on the other hand it governs also its chemical composition. In Slovakia medical-geological research appears in a limited amount already for more than 50 years. The extensive study of an endemic struma occurrence in relationship to the geochemical environment, performed by Podoba in years 1949-1953 (Podoba, 1962) can be presented perhaps as the first work with implication of medical geochemistry in Slovakia. Deficient areas related to iodine content, which significantly correlated with the occurrence of endemic strum, have been determined. Among the more recent studies the medical-geochemical research in the Žiarska kotlina region has to be mentioned (Khun et al., 2000), where the health state of the monitored children population was related to the potential negative influence of the geochemical background (e.g. fluorine content in soil and sediments, concentration of nitrates in drinking water, etc.).

The problem of the negative impact of a polluted environment on the human health is complicated not only from the practical but also from the human and social point of view. Industrial evolution gives birth to an increase of social and economic standard of people, but on the other hand it usually determines the deterioration of the state of environmental contamination and consequently the increase of the negative impact of geochemical background of a country on the human health. Generally it is assumed that the environment of life (and work) participates approximately with 20 % on the health state of people. The life style (the way of life and work) is the most important with about 50 % of participation. Genetic factors represent 20 % and the level of the public health service has 10 % of influence. However, in heavily polluted areas the contribution of the environment to the health state of population can be markedly higher.

### **Demographic and medical indicators**

Health and diseases have a very broad scale of characteristics and features that can be used as indicators. Generally, health state indicators, as well as indicators related to some exposure, have to satisfy some requirements. They have to be relevant in term of the health policy and they have to be simple and understandable, well reflecting state changes, and also they have to have a goal and a threshold value. Moreover they must be able to merge into relational units in information systems. Due to scientific conditions of construction and application of health indicators, their theoretical justification and their validity are based on international standards. Characteristics of the human health are influenced besides the risk factor itself also by the duration of exposure. On the other hand, apart from the risk factors, duration of exposure and their intensity, the ability of an organism to compensate damages in organism, that could lead to an apparent (clinic) injury or a disease, work in the opposite way.

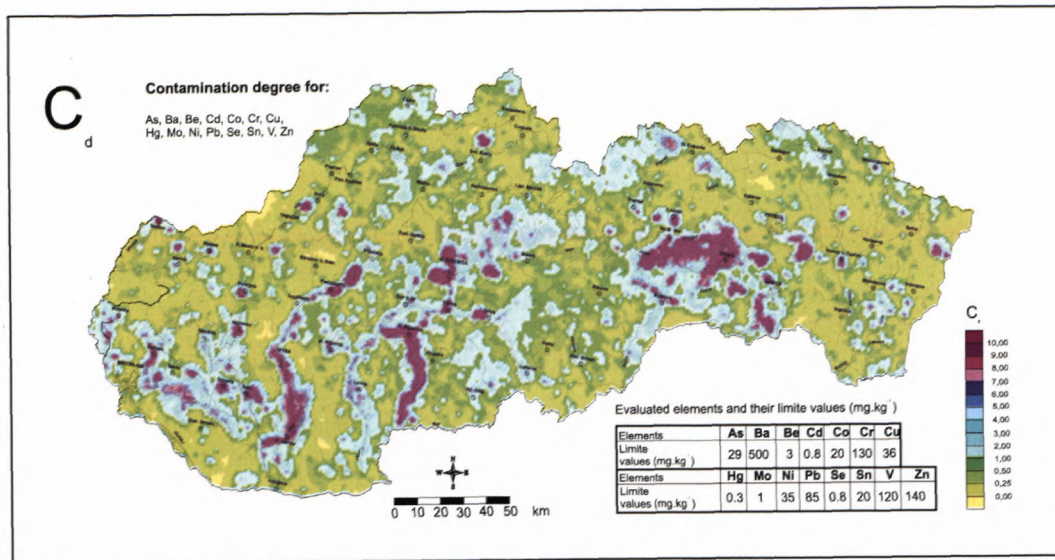


Fig. 1 Map of the degree stream sediments contamination in Slovakia.

Moreover, the level of the medical care has also a significant role. All these mutually combining and variably interfering components will be manifested in the health of population.

All medical and demographic data, used in the current medical-geochemical research in Slovakia, represent data validated by the National Institute of Health of the Slovak Republic. Data used in calculations represent average values from a five-year period, namely for the years 1993–1997. The distribution of selected health state indicators in 79 counties and in 2 873 health-regional units of Slovakia is shown in figure 2.

Health state of population indicators, used below, could be divided into following main groups:

- demographic data
- reproduction health of population data
- total mortality rate
- mortality rate due to malignancy
- chronic diseases of lungs
- cardiovascular diseases

In all of the above groups several individual groups are evaluated in terms of the age and sex and various separate diagnosis are followed. The health state of population of the Slovak Republic is evaluated in 2 873 medical-territorial units (MTU) that according to the character of settlement could be divided in the following way:

towns ( $\geq 10\ 000$ inhabitants)	72 MTU
country ( $< 10\ 000$ inhabitants)	2 801 MTU
country – villages with $< 500$ inhabitants	1 208 MTU
country – villages with 500 – 1 999 inhabitants	1 298 MTU
country – villages with 2 000 – 9 999 inhabitants	295 MTU

#### Linking of health state indicators and geochemical data

In evaluation of the potential influence of a geochemical environment we come out of an assumption that increased concentrations of contaminants in environment

are negatively manifested in the health state of population, i.e. they are manifested in an increase of values of unfavourable health indicators or in changes of links among them. Hence these changes have to be quantified at least by a few of the followed set of health state indicators and they have to show a statistical dependency among the evaluated variables.

Valid linking of databases is conditioned by the application of convenient statistical methods and correct databases. Correlation coefficients are used for the expression of tightness of a stochastic relation between two random variables, representing the characters being evaluated. Classic pair coefficient expresses the extent of the linear stochastic relation. However, the relation between studied characters naturally could have also a different character. The most classic correlation coefficient is sensitive towards possible extreme values. Due to the above reasons we have selected the Spearman serial correlation coefficient for the analysis of dependency of studied features – the element content in geochemical environment and the indicator of the health state:

$$\rho = 1 - \frac{6}{n(n^2 - 1)} \sum_{i=1}^n (d_i - s_i)^2,$$

where

$n$  is the range of the selected set,

$d_i$  ( $i = 1, 2, \dots, n$ ) are series of the first character,

$s_i$  ( $i = 1, 2, \dots, n$ ) are series of the second character.

For  $n \geq 8$  we use  $H_0$  for the verification of the validity of the zero hypothesis:  $\rho = 0$  test statistics

$$t = \frac{|\hat{\rho}| \sqrt{n-2}}{\sqrt{1-\hat{\rho}^2}},$$

that has asymptotically the division of Student with  $(n-2)$  degrees of freedom.

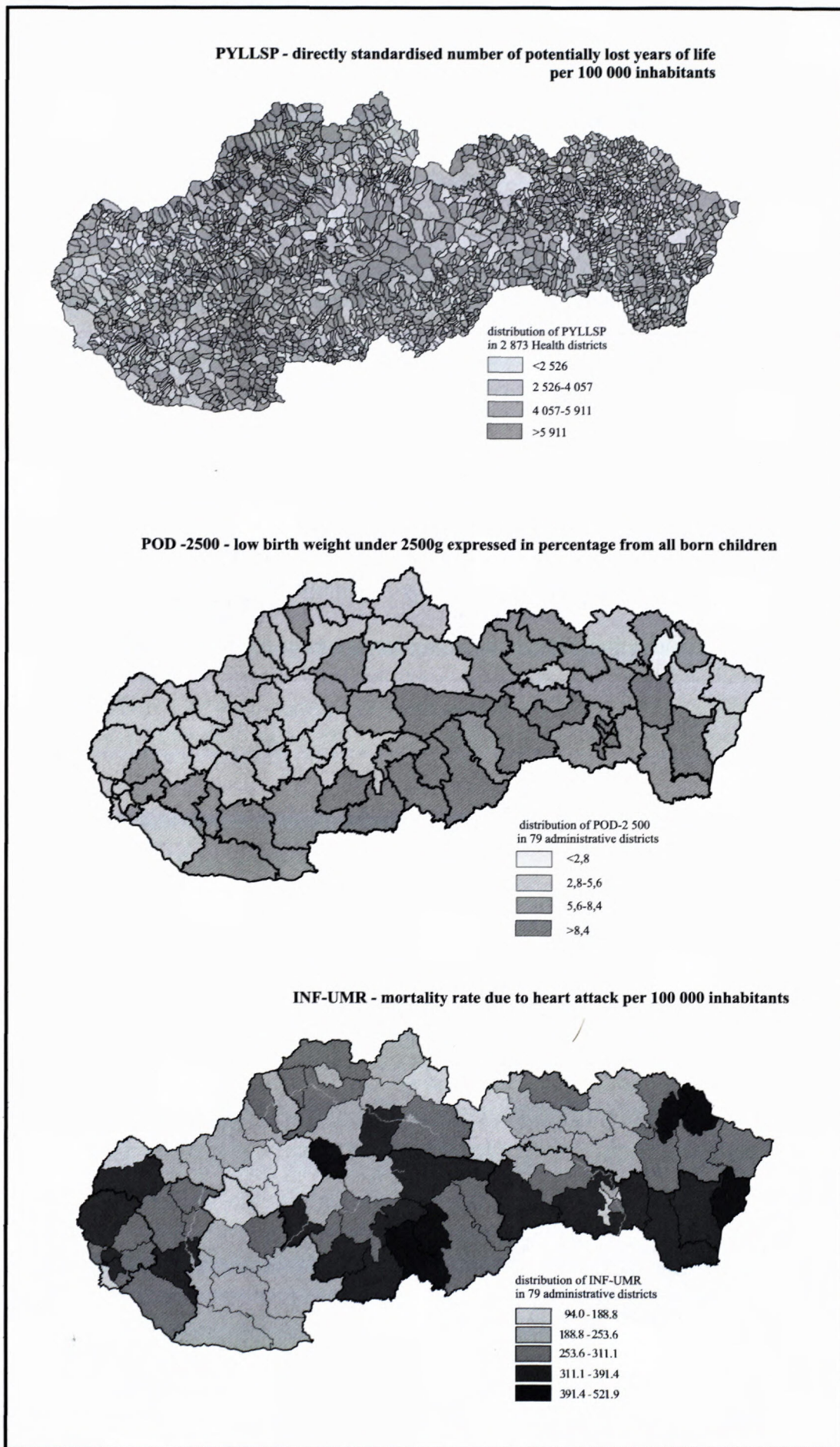


Fig. 2 Distribution of selected indicators of health state for 79 administrative counties and 2 873 health-regional units

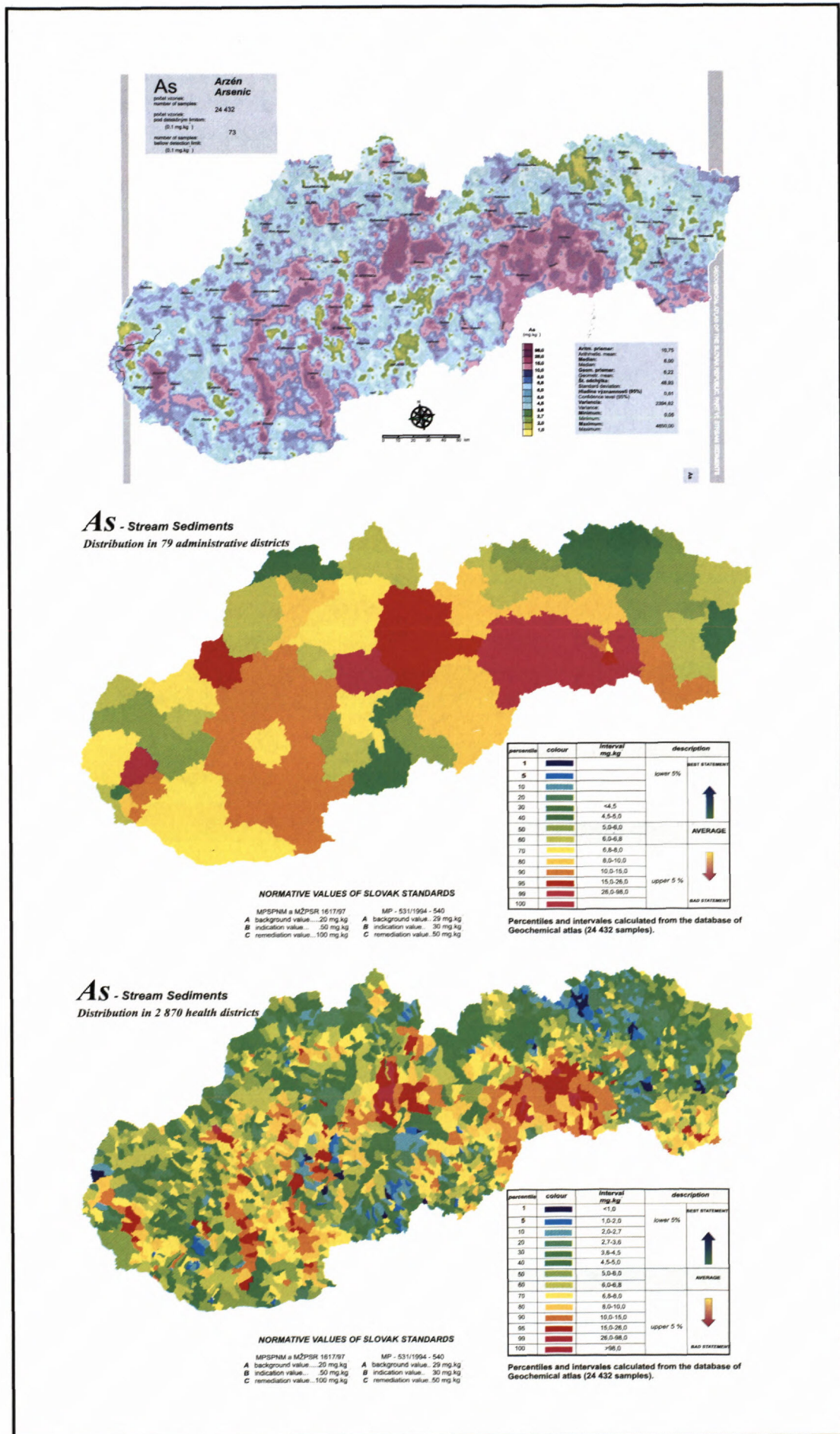


Fig. 3 Data transformation from Geochemical atlas of stream sediments into 79 administrative counties and 2 873 health-regional units

The zero hypothesis is rejected at the confidence level  $\alpha$  if the test statistics value  $t$  is bigger or equal at the most to value  $1-\alpha$  of the quantile  $\chi^2$  division with  $(n-2)$  degrees of freedom. Then we say that values of studied characters do not (significantly) correlate.

If the same series of the first character  $d_i$  ( $i = 1, 2, \dots, n$ ), or second character  $s_i$  ( $i = 1, 2, \dots, n$ ) occur, it is necessary to perform a correction during the calculation of the Spearman correlation coefficient as well as the test statistics.

Dependencies between indicators of the health state and concentrations of a chemical element are regarded as stochastically confirmed if the calculated values of confidence level  $\alpha$  reach less than 0.05. The following empirical evaluation is used to express a proof for the calculated relations:

$\alpha \leq 0.001$	very high dependence	+++
$\alpha \leq 0.01$	high dependence	++
$\alpha \leq 0.05$	proved dependence	+

### Achieved results and their discussion

The evaluation of the methodology of searching stochastic dependencies between geochemical data and indicators of the health state of population was performed on nine chemical elements *As, B, Be, Ca, Cr, Cu, Hg, Sb and Se* in stream sediments of Slovakia and on four health indicators – *PYLL* (directly standardised number of *potentially lost years of life*), *POD-2500* (low birth weight expressed in percentage from all born children), *Ca-UMR* (mortality rate due to all types of malignancy per 100 000 inhabitants) and *INF-UMR* (mortality rate due to heart attack per 100 000 inhabitants).

Geochemical databases and databases of demographic and health indicators were unified in equivalent forms according to administrative and health-regional units (fig. 3). Average concentrations of chemical elements from points falling within individual administrative units have been calculated. In this manner they have been processed for 79 administrative counties and 2 873 health-regional units in a graphic as well as in a database form. In first approach relations of nine chemical elements in stream sediments and four indicators of the health state of population have been statistically tested for the whole Slovak Republic (2 873 MTU) and all studied groups of town and country inhabitants.

Values of calculated Spearman correlation coefficients, confidence levels  $\alpha$  together with empirical evaluation of provableness of the studied features for 2 799 health-regional units of country inhabitants, are shown in table 2. The achieved results show that significant correlation has been confirmed statistically between the distribution of several chemical elements and the occurrence of individual indicators of the health state. In some cases, the high confidence level of correlation, together with literature knowledge of the influence of individual chemical elements on the human health, indicates that the presented stochastic relations could be regarded as causal in several cases, e.g. the distribution of *As* vs. *POD-2500* and *PYLL*, *Sb* vs. *POD-2500*, *Cu* vs. *PYLL* and others.

Considering the variability of features and reasons related to the health state of population (apart from the geochemical background) the correlation coefficient values are relatively low. If nation-wide data are recalculated (2 801 correlated variables) the values reach only about 0.1 or less (table 2). In addition to the correlation coefficients values the confidence value  $\alpha$  of calculated coefficients also represents the significance and dependence between correlated features and sets. Higher values of correlation coefficients have been recorded for calculations of 79 counties. (table 3). Directly in the pilot area of the Spišsko-Gemerské Rudohorie Mts., where regarding the relatively high degree of contamination of the geological component of the environment the influence of the geochemical environment on the the health state of population can be expected to be higher, correlation coefficients reach values 0.3–0.5 (table 3) beside values of  $\alpha$  less than 0.001. Within the area of the Spišsko-Gemerské Rudohorie Mts. the causality of negative influence of increased chemical elements concentrations in geochemical environment on the health state of population is confronted with common geochemical and medical studies in one of the most contaminated villages of the area – Zlatá Idka. In this village primarily the *Sb* and *As* contents are increased (geo-induced) in all parts of the geological environment – ground and surface waters, sediments, soils as well as in forest biomass. The State Health Institute, Košice (Dietzová, 2000) concurrently monitors *As* and *Sb* contents in biological materials of people (blood, urine, hair and nails) and moreover it traces concentrations of these elements in locally grown vegetables and fruits. In several cases an overrun of particular biological limits of the followed toxic metals was recorded in biological materials of people.

The performed calculations of geochemical and medical-demographic data for individual groups of inhabitants unequivocally show that the usage of parameters for country inhabitants is the most suitable for the evaluation of the characteristic of the potential influence of geochemical background on the health state of population.

Furthermore, it is probable that chemical elements, regarding their relations to individual health indicators, could be divided into:

„*Causal elements*„ (e.g. *Cd, Hg, As, Sb,...*) – with proved relationship between health indicators and excess or deficiency of a chemical element in the geochemical background and

„*Indicating elements*„ (e.g. *Bi, Be,...*) – with high stochastic dependence thanks to the geochemical relationship with causal elements.

### Conclusions

The solving of problems of the influence of geochemical background on the health state of population is currently just in the stage of verification of preliminary results and processing of methodical procedures. Proposed methodical principles of linking geochemical data with medical and demographic indicators of the health

Table 2 Spearman correlation coefficients, confidence levels  $\alpha$  and significance of relations dependencies of selected chemical elements in river sediments of Slovakia and indicators of the health state of population of the Slovak Republic – country inhabitants (2 801 MTU)

		N	Spearman S	t(N-2)	$\alpha$	significance
As	PYLL	2 801	0.04994	2.64465	0.00822	++
As	PODM_2500	2 801	0.06317	3.34734	0.00083	+++
As	CA_UMR	2 801	0.04062	2.15011	0.03163	+
As	INF_UMR	2 801	0.06326	3.35220	0.00081	+++
B	PYLL	2 801	0.01940	1.02594	0.30501	
B	PODM_2500	2 801	0.00560	0.29593	0.76731	
B	CA_UMR	2 801	0.02940	1.55569	0.11990	
B	INF_UMR	2 801	-0.03000	-1.58733	0.11255	
Be	PYLL	2 801	0.06899	3.65751	0.00026	+++
Be	PODM_2500	2 801	0.06196	3.28309	0.00104	++
Be	CA_UMR	2 801	-0.05499	-2.91272	0.00361	++
Be	INF_UMR	2 801	-0.01335	-0.70611	0.48018	
Ca	PYLL	2 801	-0.01496	-0.79128	0.42885	
Ca	PODM_2500	2 801	-0.01740	-0.92052	0.35738	
Ca	CA_UMR	2 801	0.06251	3.31256	0.00094	+++
Ca	INF_UMR	2 801	0.04396	2.32739	0.2002	+
Cr	PYLL	2 801	-0.02395	-1.26692	0.20529	
Cr	PODM_2500	2 801	0.00848	0.44871	0.65367	
Cr	CA_UMR	2 801	0.03710	1.96349	0.04969	+
Cr	INF_UMR	2 801	-0.04647	-2.46040	0.01394	+
Cu	PYLL	2 801	0.07227	3.83238	0.00013	+++
Cu	PODM_2500	2 801	-0.00652	-0.34477	0.73030	
Cu	CA_UMR	2 801	0.02094	1.10744	0.26820	
Cu	INF_UMR	2 801	0.03612	1.91156	0.05603	
Hg	PYLL	2 801	0.03577	1.89295	0.05847	
Hg	PODM_2500	2 801	0.05922	3.13737	0.00172	++
Hg	CA_UMR	2 801	0.01713	0.90587	0.36508	
Hg	INF_UMR	2 801	0.08620	4.57603	0.00000	+++
Sb	PYLL	2 801	0.01521	0.80426	0.42132	
Sb	PODM_2500	2 801	0.07654	4.05987	0.00005	+++
Sb	CA_UMR	2 801	0.00421	0.22277	0.82373	
Sb	INF_UMR	2 801	0.03594	1.90206	0.05727	
Se	PYLL	2 801	-0.00192	-0.10170	0.91900	
Se	PODM_2500	2 801	-0.04736	-2.50745	0.01222	+
Se	CA_UMR	2 801	0.05568	2.94949	0.00321	++
Se	INF_UMR	2 801	0.00687	0.36352	0.71624	

$\alpha \leq 0.001$     very high dependence    +++  
 $\alpha \leq 0.01$     high dependence    ++  
 $\alpha \leq 0.05$     proved dependence    +

state of population are currently being elaborated in all geochemical environments (soils, waters, sediments) and in much broader range of chemical elements and indicators of the health state of population. Thereafter, they will be a basis for working-out analyses of the environmental risk and in the most critical areas for analyses of the health risk. In addition, results of special laboratory work, mainly the assessment of the occurrence of evaluated toxic elements and toxicity tests (acute and chronic) on samples of waters, soils and sediments, will be used.

The proven significant relation between medical and environmental-geochemical parameters could provide a very important tool for the environmental analysis in decision processes. The outlined approach for the evaluation of the influence of geochemical background on the health state of population will provide a possibility to discover health risk in time. Even if the risk can not be entirely avoided, their consequences can be minimised at least.

Table 3 Statistic relation between chemical elements contents in river sediments and indicators of the health state of population

Element	Health indicator	R	$\alpha$	Significance
<b>79 counties of Slovakia</b>				
<b>Co</b>	PODM_2500	0.001	0.973	
	HÚO	0.391	0.000	+++
	PPÚO	0.351	0.002	++
	PYLL	0.376	0.001	+++
<b>Mn</b>	PODM_2500	0.325	0.004	++
	HÚO	0.314	0.006	+
	PPÚO	0.332	0.003	++
	PYLL	0.368	0.001	+++
<b>82 MTU of the Spišsko-gemerské rudohoria Mts.</b>				
<b>As</b>	PPÚO	0.472	0.000	+++
	UMR_ZNP	0.335	0.002	++
	PYLL	0.284	0.009	++
	PODM_2500	0.090	0.419	
<b>Bi</b>	PPÚO	0.454	0.000	+++
	UMR_ZNP	0.148	0.182	
	PYLL	0.198	0.074	
	PODM_2500	-0.02	0.799	

**Note:** R – Spearman order correlation coefficient;  $\alpha$  - confidence level; PYLL (directly standardised number of potentially lost years of life); PODM\_2500 (percentage of children with birth weight under 2500g); HÚO (gross mortality rate of population); PPÚO (percentage of untimely deaths of inhabitants over 65 y.); UMR\_ZNP (mortality rate due to lungs malignancy per 100 000 inhabitants)

## Literature

- Alloway, B. J. & Ayres, d. c. 1993: *Chemical Principles of Environmental Pollution*. Blackie Academic and Professional, 291 p.
- Augustin, J. & Zejda, R. 1991: *Cancer incidence and geochemical factors in the environment*. The Sci. Tot. Environment, 106, p. 155–163.
- ATSDR – Agency for Toxic Substance and Disease Registry, 1992: Toxicological Profile for Antimony. U.S. Public Health Service, U.S. Department of Health and Human Service. Atlanta. GA, 245 p.
- Bencko, V., Cikt, M. & Lener, J. 1995: *Toxické kovy v životním a pracovním prostředí člověka*. GRADA Publishing. Praha, 282 p.
- Bodiš, D. & Rapant, S. eds., 1999: *Geochemical Atlas of Slovak Republic-part VI.- Stream sediments*. Monography, Geol. Survey of Slovak Republic, Bratislava, 145 p.
- Bodiš, D. & Rapant, S. 2000: *Environmental Geochemistry and Environmental-Geochemical Mapping of the Slovak Republic*. Slovak Geol. Magazine. 1/2000. GS SR, Bratislava. p. 5–16.
- Dietzová, Z. 2000: *Odhad zdravotného rizika z arzenu a antimónu prítomného v životnom prostredí u obyvateľov obce Zlatá Idka*. Manuskript ŠZÚ Košice.
- Fergusson, J. E. 1990: *The Heavy Elements: Chemistry, Environmental Impact and Health Effects*. Pergamon Press. 614 p.
- Khun, M., 1992: Medical geochemistry. Temporary teaching texts. Manuscript. Department of Geochemistry, Faculty of Natural Sciences, Comenius University, Bratislava, 66 p (in Slovak).
- Khun, M., Jurkovič, E. & Urmínská, J. 2000: *Medical Geochemistry: A Brief Outline of the Problems and Practical Application in the Region of Žiarska kotlina Basin*. Slovak Geol. Magazine. 1/2000. GS SR, Bratislava, p. 17–26.
- Letkovičová, M., Stehlíková, B, Smatanová, K. & Ďurov, M. 2000: The evaluation of potential influence of geochemical environment on the health state of population in region SGR – Analysis of indicators of demographical development and health state of population in SGR. Partial report, Manuscript. ENVIRONMENT, a.s. Nitra (In Slovak).
- Podoba, J. 1962: *Endemická struma na Slovensku*. Vyd. SAV, Bratislava, 187 p.
- Rapant, S., Bodiš, D., Mackových, D. Mjartanová, H. Čížek, V. & Pramuka, S. 1998: The evaluation of potential influence of geochemical environment on the health state of population in region SGR. Project of geological works. Manuscript. GS SR, Bratislava (In Slovak).
- Rapant, S., Rapošová, M., Bodiš, D., Marsina, K. & Slaninka, I. 1999: *Environmental-geochemical mapping program in the Slovak Republic*. Journal of Geochemical Exploration. 66 (1999). p. 151–158.
- Škárka, B. & Ferenčík, 2000: *Biochémiá*. Slovak academic Pres, spol. s r. o., Bratislava.
- Thorton, I. 1993: *Environmental geochemistry and health in the 1990s: a global perspective*. Applied Geochemistry. Supp. Issue, No 2, p. 203–210.
- Vrana, K., Rapant, S., Bodiš, D., Marsina, K., Lexa, J., Pramuka, S., Maňkovská, B., Čurlík, J., Šefčík, P., Vojtaš, J., Daniel, J. & Lučivianský, L. 1997: *Geochemical Atlas of Slovak Republic at a scale 1 : 1 000 000*. Journal of Geochemical Exploration, 60, p. 7–37.
- Zýka, V. 1975: *Vliv anomálního geochemického prostředí na rozšíření zhubných novotvarů*. Sbor. Geol. Věd., Technol. Geochem. Praha. 201 p.
- WHO – World Health Organisation, 1996: Arsenic – Guidelines for drinking water quality. In: Health criteria and other supporting information. 2<sup>nd</sup> ed. Vol. 2., Geneva, p. 156–167.



## Monitoring and the FLONET/TRANS model as tools to characterize the nitrate distribution and transport in the Noor catchment (the Netherlands)

JOZEF KORDÍK<sup>1</sup>, HENNY A.J. VAN LANEN<sup>2</sup> and ROEL DIJKSMA<sup>2</sup>

<sup>1</sup>Geological Survey of Slovak Republic, Mlynská dolina 1, 817 04 Bratislava, Slovakia

<sup>2</sup>Wageningen University, De Nieuwlanden 11, Wageningen, the Netherlands

**Abstract.** Intensive human activities, such as agricultural practices, groundwater abstraction or land use changes, have had a negative impact on the state of the natural environment in The Netherlands. The increased inputs of fertilisers and animal manure after 1950 have boosted crop production to a high level, but have also contributed to increased nitrogen emissions from agriculture to groundwater, surface waters and atmosphere. Since 1991, a comprehensive hydrological and hydrogeological research project has been started in the Noor (chalk) catchment situated on the Dutch-Belgian boundary due to situation has become critical in this region. The investigation covers analysis of the hydrogeological system of the Noor catchment, including the relationship between recharge, groundwater heads, springflow, streamflow and chemical composition of water. The monitoring shows that groundwater under the plateau is heavily polluted (often  $\text{NO}_3^-$  concentrations  $> 100 \text{ mg.l}^{-1}$ ). Springs also have high  $\text{NO}_3^-$  contents (mean:  $64 \text{ mg.l}^{-1}$ ) because they are fed by this groundwater. Groundwater under the wet valley is less polluted (mean:  $27 \text{ mg.l}^{-1}$ ) due to denitrification and being old, unpolluted water. Water in the Noor brook and its tributaries is coming from the polluted springs and from seepage areas in the wet valley that drain the less polluted groundwater there. The nitrate concentrations of the Noor brook and its tributaries (mean:  $42\text{-}46 \text{ mg.l}^{-1}$ ) reflects the characteristics of diluted spring water. The modelling with FLONET/TRANS confirms that the  $\text{NO}_3^-$  contents in the Noor catchment in the late 1990's can be explained with the historical  $\text{NO}_3^-$  input and the groundwater flow pattern. Scenario studies indicate that a reduction of 75 % of the  $\text{NO}_3^-$  input is required to start a decline  $\text{NO}_3^-$  concentrations in the water system.

**Key words:** Nitrate, Water Quality, Monitoring, Modelling, FLONET/TRANS, the Netherlands

### Introduction

The study area is situated in the southeastern part of the Netherlands (Limburg province) and the Northeast of Belgium, in the centre of the triangle Maastricht - Aachen - Liege (Fig. 1). Because of the hydrogeological properties of the Noor chalk catchment area, the surface water in the Noor brook is predominantly controlled by the groundwater system (Van Lanen & Dijkmsa, 1999). The land use, mainly agriculture, causes several problems (especially deterioration of the water quality by nitrates). The physical properties of nitrates and hydrogeological characteristics of the study area dictate the groundwater pollution according to the spatial patterns of the groundwater flow. Because the surface water flow is predominantly fed by groundwater flow, the increased  $\text{NO}_3^-$  concentrations in the groundwater system affect also the surface water quality subsequently. Generally, the contamination affects the natural conditions (environment, nature reserve) as well as human health (deterioration of drinking water of some remote farms with own water supply) and well being.

The Sub-department of Water Resources of the Wageningen University started a research study in 1991, also called the „Zuid-Limburg project“. The investiga-



Fig. 1 Situation Map

tions cover analysis of the hydrogeological system of the Noor catchment, including the relationship between recharge, groundwater heads, springflow and streamflow and chemical composition of water. In the context of this project, the database with monitoring data has been used to investigate water flow and nitrate transport through the

groundwater system towards the groundwater-fed Noor stream. Subsequently, these data and hydrogeological information were used to develop a model using FLONET/TRANS. With the model the groundwater flow pattern, the current  $\text{NO}_3^-$  distribution and possible  $\text{NO}_3^-$  developments in the coming decades were explored.

The main objectives of the paper are twofold:

- characterisation of the nitrate distribution in the Noor catchment using basic statistical procedure;
- analysis of the current situation and prediction of future nitrate patterns with application of three nitrate load reduction scenarios of 25, 50 and 75 % using the FLONET/TRANS simulation modelling package.

### Natural conditions of the study area

The Noor brook catchment covers an area of 1056 ha. According to the Koppen's classification, the study area is classified as moderately rainy and humid throughout all seasons. The average rainfall equals about  $750 \text{ mm.yr}^{-1}$ , whereas the average potential evapotranspiration is  $575 \text{ mm.yr}^{-1}$ . The region is situated on the Chalk (Margraten) Plateau. Most of the valleys are dry and only the downstream parts of the deeply incised valleys carry water (van Lanen et al., 1995). Over the last ten years the discharge varied at the outlet between 0,25 and  $0,90 \text{ mm.d}^{-1}$ .

The investigation area together with the surrounding plateaus belongs to the marginal part of the Ardennes and strongly coincides to this geological setting (Nota - van de Weerd, 1978; Demoulin, 1995). The oldest geological unit consists of consolidated Palaeozoic rocks, which form the impermeable base of the investigated hydrogeological domain. It is overlain by Upper Cretaceous and Quaternary sediments, which constitute a multi-aquifer system. Except in the north, topographic and groundwater divides of the Noor catchment are assumed to coincide.

The Upper Carboniferous unit is generally characterised by consolidated sandstones and shales. Due to both, extensive erosion and hiatuses, the Permian, Triassic, Jurassic and Lower Cretaceous sediments are missing (van Lanen et al., 1995). Upper Cretaceous sediments discordantly overlie the Palaeozoic rocks. The Aachen and Vaals Formations represent the lower part. The Aachen Formation mostly consists of sandy sediments. The Vaals Formation is represented by clayey and silty sediments interbedded with sandstone layers. The upper part of the Cretaceous sedimentation cycle is characterised by deposition of carbonates and is divided into two units: the Gulpen and Maastricht Formations. In the Tertiary the sedimentation changed from carbonates, via marine clays and sands into fluvial deposits due to a regression of the sea. The deposition of sands and gravel by the Maas River took place in the Early Pleistocene. In the Late Pleistocene, a loess (eolic sediment) layer covered the area. During the Middle and Late Tertiary and Pleistocene strong weathering and erosion removed all sediments in this area up to the Gulpen Formation. This chalk deposit is covered by unconsolidated regolith (Eindhoven Formation). During the Pleistocene and Holocene the

drainage pattern developed and the deposition of the valley fillings (Singraven Formation) occurred on the top of the Cretaceous sediments (van Lanen et al., 1995). In a cross-section through the catchment perpendicular to the Noor brook, the following typical physio-geographic units can be distinguished: plateau, foothill, transition area and wet valley. The first two units do not have surface water.

The hydrogeological parameters of the main studied geological units are shown in Tab. 1. Overall permeability of the Vaals formation is rather low ( $10^{-3} \text{ m.d}^{-1}$ ). Nevertheless, water transmissivity of the Vaals formation become higher due to the presence of several 0,1-0,2 m thick fractured sandstone layers with permeability of  $20-50 \text{ m.d}^{-1}$ . Due to the low effective porosity of the Gulpen Formation, reaching up to 5-10% only, the primary (intergranular) permeability of the chalk is low ( $0,5 \text{ m.d}^{-1}$ ). Overall permeability can be increased in the areas with well-developed karstic phenomena and can reach  $10 \text{ m.d}^{-1}$ . Regolith is a mixture of clay, flints and Maas deposits derived from denudation and erosion of Cretaceous, Tertiary and Quaternary sediments. The vertical permeability of regolith (Eindhoven Formation) reaches from 0,5 to  $5 \text{ m.d}^{-1}$ . The Singraven Formation comprises of valley fillings consisting of the fine-grained sediments interbedded with gravel and peat layers. Its permeability differs strongly from place to place and varies between  $10^{-3}$  to  $10^{-1} \text{ m.d}^{-1}$  (van Lanen et al., 1995; Schunselaar – van der Hoeven, 1993; Nota – van de Weerd, 1978).

### Methods of data processing and modeling

Since 1991 the Sub-department of Water Resources of the Wageningen Agricultural University has started a research in the Noor catchment by establishing a monitoring network. Data has been collated on recharge, groundwater heads, springflow, streamflow and chemical composition of water. The hydrogeological and hydrochemical database consists of data from 63 piezometers (located in 5 cross-sections), 4 springs, 3 dug wells and 12 surface water monitoring locations (Noor brook and its tributaries). The chemical analyses have taken place in the *conventional laboratory* of the Sub-department of Soil Science and Geology of the Wageningen University. Since 1994 a special device, a set of integrated, *selective ions (Hydrion-10, HYDRION B.V., Wageningen)* has also been used to analyse chemical components. The water sampling is carried out regularly during the year. The frequency of the sampling varies for different locations. It depends on the temporal variability and the demand for detailed hydrochemical research and interpretation.

The calculation of the basic statistical moments (mean, median, standard deviation, minimum, maximum) has been used to describe the current distribution of nitrate in the Noor catchment. The data was also clustered according to several criteria, and statistical moments are described separately for the springs, piezometers, wells, Noor brook and its tributaries. The statistical analysis was developed separately for the samples analysed in the con-

Tab. 1 Hydrogeological parameters of the investigated formations

Formation	Total thickness	Overall permeability
Singraven Formation	1 to 5 m	$10^{-3}$ to $10^{-1}$ m.d <sup>-1</sup>
Eindhoven Formation	regolith - 1 to 5 m	regolith - 0,5 to 5 m.d <sup>-1</sup> , loess - 10 and $10^{-2}$ m.d <sup>-1</sup>
Gulpen Formation	30-35 m	0,5 and 10 m.d <sup>-1</sup>
Vaals Formation	40 and 50 m	low - $10^{-3}$ m.d <sup>-1</sup> sandstone layers 20 and 50 m.d <sup>-1</sup>
Upper Carboniferous; Namurien	>50 m	very low - $< 10^{-6}$ m.d <sup>-1</sup> consolidated sandstones and shales

ventional laboratory and samples analysed with the Hydrion-10. For selected monitored locations a trend analysis was performed using regression techniques.

The FLONET/TRANS model has been used as a tool to simulate groundwater flow and nitrate transport. FLONET/TRANS has been designed to approximate natural, three dimensional (3D) groundwater systems in either the two-dimensional (2D) horizontal plane or vertical cross-section. It suits especially all hydrogeological domains with significant vertical variation in physical properties or with significant vertical flow gradients. This software package is a combination of two numerical finite element models: a steady state saturated groundwater flow model and a transient advective-dispersive contaminant transport model. The model solves flow equations using the dual formulation (Frind & Matanga, 1985), which formulates the flow equations in terms of hydraulic potential and stream function:

$$\frac{\delta}{\delta x} \left( K_{xx} \frac{\delta \phi}{\delta x} \right) + \frac{\delta}{\delta y} \left( K_{yy} \frac{\delta \phi}{\delta y} \right) = 0$$

$$\frac{\delta}{\delta x} \left( \frac{1}{K_{yy}} \frac{\delta \psi}{\delta x} \right) + \frac{\delta}{\delta y} \left( \frac{1}{K_{xx}} \frac{\delta \psi}{\delta y} \right) = 0$$

where:

- $x$  horizontal co-ordinate [m]
- $y$  vertical co-ordinate [m]
- $K_{xx}$  hydraulic conductivity in the x direction [ $m \cdot s^{-1}$ ]
- $K_{yy}$  hydraulic conductivity in the y direction [ $m \cdot s^{-1}$ ]
- $\phi$  hydraulic head [m]
- $\psi$  stream function [ $m^2 \cdot s^{-1}$ ].

In advective-dispersive contaminant transport FLONET/TRANS solves the 2D equation with linear retardation and first-order decay:

$$\frac{\delta}{\delta x_i} \left[ \frac{D_{ij}}{R} \frac{\delta c}{\delta x_j} \right] - \frac{\delta}{\delta x_i} \left( \frac{v_i}{R} c \right) - \lambda c = \frac{\delta c}{\delta t}$$

where:

- $x, y$  spatial co-ordinates [m]
- $v_i$  average linear flow velocity [ $m \cdot s^{-1}$ ]
- $D_{ij}$  hydrodynamic dispersion coefficient [ $m^2 \cdot s^{-1}$ ]
- $R$  retardation [-]
- $\lambda$  linear decay rate [ $s^{-1}$ ]
- $t$  time [s]
- $c$  concentration [ $mg \cdot dm^{-3}$ ].

Groundwater flow velocities are derived from the stream function solution of the flow equation (Guiger et al., 1996):

$$v_x = \frac{q}{\theta}; \quad v_y = \frac{q_y}{\theta}$$

where:

- $\theta$  effective porosity [-]
- $q$  groundwater flux [ $m \cdot s^{-1}$ ]

The program assumes several conditions: a) steady 2D groundwater flow; b) fully saturated conditions; c) constant density pore water; d) contaminant in the dissolved phase; e) contaminant dilution with a temperature equal to that of the pore water. The program supports the following boundary conditions (Tab. 2).

The model was applied for different values of the recharge (dry, normal and wet period) and results of this sensitivity analysis are given.

## Results and discussion

### Statistical analysis

The general characteristics of all samples analysed both in the conventional laboratory and with Hydrion-10 are given in Tab. 3, Graph 1 and 2. The nitrate concentration in the Noor catchment is characterised by a very high variation from 0,5 to 147,6  $mg \cdot l^{-1}$  of  $NO_3^-$ . The observed mean value 41,1 (42,0 Hydrion-10)  $mg \cdot l^{-1}$  is very closed to the drinking water standard of 50  $mg \cdot l^{-1}$   $NO_3^-$  in the European Union.

The measured  $NO_3^-$  concentrations in the conventional laboratory and with the Hydrion-10 reasonably agree. The median value measured with the Hydrion-10 is little bit higher than the one derived from the conventional laboratory analysis (45,3 versus 42,1  $mg \cdot l^{-1}$ ). With the Hydrion-10 more low concentrations (23%  $< 7$   $mg \cdot l^{-1}$ ) are measured than with the conventional laboratory methods (17%  $< 7$   $mg \cdot l^{-1}$ ). According to the Hydrion-10, 56% of the samples is below the drinking water standard, whereas the conventional method results in 68%. Both methods have 4% of the samples above 98  $mg \cdot l^{-1}$ .

The nitrate concentrations of the *Noor brook* show a different pattern (Tab. 4). The mean nitrate content is 45,7  $mg \cdot l^{-1}$  (52,6  $mg \cdot l^{-1}$  Hydrion-10) which is a little bit more than the catchment mean concentration. The variation is very high with a minimum value of 26,3  $mg \cdot l^{-1}$  and a maximum concentration of 60,6  $mg \cdot l^{-1}$ . The statistical

Tab. 2 Flow and transport boundary conditions available in FLONET/TRANS (Guiger et al., 1996)

Boundary type	Groundwater flow	Contaminant transport
First Dirichlet	$\phi = \phi_0$ Fixed head boundary (e.g. river or lake, or at a distant exit boundary)	$c = c_0$ Fixed concentration boundary (e.g. a large, well-mixed source)
Second Neumann	$q_n = q_0 = K \frac{\delta\phi}{\delta n}$ Specified flux boundary (e.g. recharge across water table, inflow or outflow boundary or no-flow boundary $q = 0$ )	$\frac{\delta c}{\delta n} = 0$ Zero-concentration gradient (e.g. no outflow or impermeable boundary)
Third Cauchy	not available	$\frac{q_0 c_0}{\theta} = vc - D \frac{\delta c}{\delta x_i}$ Dispersive flux boundary (e.g. source with known influx $q_0$ and concentration $c_0$ )

Tab. 3 Basic statistical parameters of nitrate concentration (mg.l<sup>-1</sup>) in the Noor valley

Measure technique	Mean	Median	Standard Deviation	Minimum	Maximum	Number of samples
Conv. laboratory	41,1	42,1	27,0	0,5	147,6	479
Hydrion-10	42,0	45,3	30,2	1	140,8	917

Tab. 4 Statistical moments of the nitrate concentrations (mg.l<sup>-1</sup>) in selected groups of water samples

	Mean	Median	Standard Deviation	Minimum	Maximum	Number of samples
<b>Conventional laboratory</b>						
all groundwater	41,2	36,9	37,6	0,5	152,5	252
all surface water	43,9	43,5	8,4	24,5	70,7	227
Noor brook	45,7	45,5	7,7	26,3	60,6	102
Piezometers	26,5	12,6	33,5	0,5	138,3	173
Springs	64,0	65,7	10,3	45,2	82,5	51
Tributaries	42,4	40,9	8,7	24,5	70,7	125
Wells	90,4	95,2	30,9	0,5	152,5	28
<b>Hydrion-10</b>						
All groundwater	38,5	34,8	36,1	1	140,8	604
All surface water	48,7	48,5	9,8	23,3	80,4	313
Noor brook	52,6	52,9	8,6	23,3	80,4	137
Piezometers	27,0	11,7	31,2	1	140,6	461
Springs	66,2	68,6	10,9	38,4	89,7	93
Tributaries	45,6	43,8	9,7	26,0	76,6	176
Wells	92,9	96,6	30,8	1	140,8	50

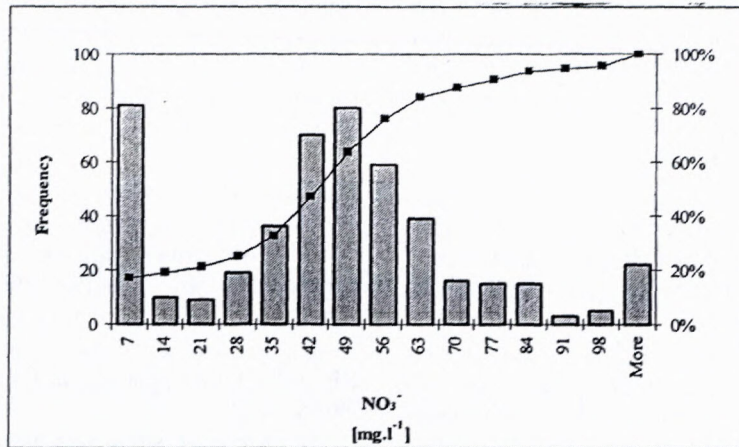
moments of the *Noor tributaries* are very similar to those of the main stream with mean values of 42,4 mg.l<sup>-1</sup> (45,6 mg.l<sup>-1</sup> Hydrion-10). The variation is slightly higher from 24,5 mg.l<sup>-1</sup> to 70,7 mg.l<sup>-1</sup> (Tab. 4).

The sampled *springs* occur on the foothill, where the chemical composition of the groundwater is determined by mixing of groundwater following shallow and deep flowpaths. This results in quite high variation of nitrate concentrations, from 45,2 to 82,5 mg.l<sup>-1</sup> (38,4 to 89,8 mg.l<sup>-1</sup> measured by Hydrion-10) - Tab. 4. Moreover, it is

very characteristic for the objects situated on the foothill and on the plateau, that the population of low concentrations is missing due to the intensive agricultural activities in this part of the valley, from which the groundwater flows to the spring outlets and because of denitrification.

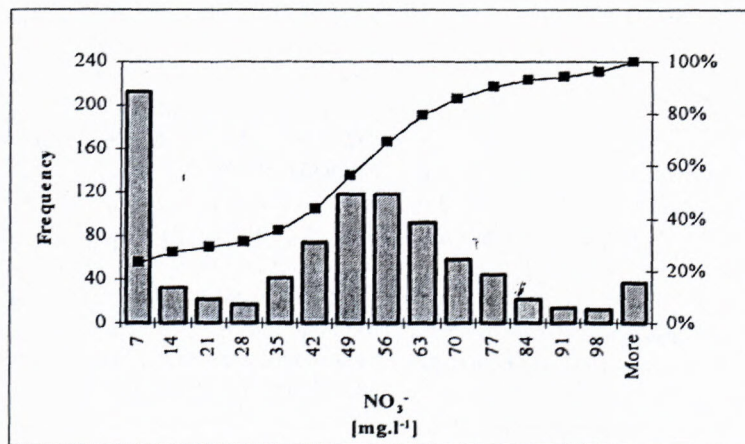
The nitrate concentrations of groundwater sampled from the *piezometers* that mainly occur in the wet valley are the lowest from the selected groups. The mean nitrate contents reach values of 26,5 mg.l<sup>-1</sup> (27,0 mg.l<sup>-1</sup> Hydrion-10). The long groundwater travel time from the plateau

$NO_3^-$ class	Frequency	Cumulative %	$NO_3^-$ class	Frequency	Cumulative %
0-7	81	17%	49-56	49	79%
7-14	10	19%	56-63	28	85%
14-21	9	21%	63-70	23	89%
21-28	19	25%	70-77	13	92%
28-35	45	34%	77-84	11	94%
35-42	75	50%	84-91	2	95%
42-49	89	68%	91-98	5	96%
			>98	20	100%



Graph 1 Statistical characteristics of the nitrates ( $mg.l^{-1}$ ) for all samples in the Noor catchment (analysed in the conventional laboratory)

$NO_3^-$ class	Frequency	Cumulative %	$NO_3^-$ class	Frequency	Cumulative %
0-7	213	23%	49-56	118	69%
7-14	33	27%	56-63	92	79%
14-21	21	29%	63-70	59	86%
21-28	17	31%	70-77	45	91%
28-35	41	35%	77-84	22	93%
35-42	74	44%	84-91	14	95%
42-49	118	56%	91-98	13	96%
			>98	37	100%



Graph 2 Statistical characteristics of the nitrates for all samples in the Noor catchment (analysed with Hydriion-10)

towards the riparian area is a possible reason for the lower  $\text{NO}_3^-$  concentrations. It means that the water has been infiltrated before the  $\text{NO}_3^-$  input became high (before 1950's). Moreover denitrification processes are assumed to take place in the aquifer. The very low nitrate load in the middle of the valley (nature reserve area is not being used for agricultural purposes) probably contributes also this fact (van Lanen et al., 1995).

The number of the analysed samples from the monitored *dug wells* is too small to give a reliable description and interpretation of the current situation on nitrate pollution (Tab. 4). However, the mean concentration of nitrates is very high, i.e.  $90,4 \text{ mg.l}^{-1}$  ( $92,2 \text{ mg.l}^{-1}$  Hydrion-10) of  $\text{NO}_3^-$ . This confirms the fact the nitrate pollution in the Noor catchment is caused by human activities, because the wells are very close to the dwellings or agricultural fields situated on the plateau and foothill, which are characterised by high loads of nutrients.

In the northern part of the valley generally higher mean concentrations of nitrates were observed than in the southern one (Kordík, 1998) probably due to higher loads of nutrients in the northern valley (e.g. different land use, agriculture practices).

The evolution of nitrate concentration in time is controlled by the long-term variation in groundwater recharge. Another important factor is the nitrate input, which is controlled by the intensity of agricultural activities and type of farming. Linear trend analysis shows generally an increasing trend in nitrate concentration for most of the monitored locations (Kordík, 1998).

Figure 2 presents the trend analyses for the *Sint Brigida spring* (Br1), the *dug well* (OW5) with extremely high nitrate contents since 1996, the *Noor brook* (profile NE) and the *piezometers* (B3a and WP96). In many piezometers the nitrate content has increased rapidly during the last decade up to values of  $100 \text{ mg.l}^{-1}$ . The *deep piezometer* (WP 96), which is situated on the northern plateau, is characterised by a negative trend. This trend might be caused by implementation of the nitrate policy into the practice. However, in most monitoring locations the nitrate concentrations exceed the drinking water standard of  $50 \text{ mg.l}^{-1}$  in the European Union.

### Simulation modelling

#### Simulation of nitrate transport

Nitrate as a stable form of dissolved nitrogen, is very mobile in groundwater (e.g. Freeze and Cherry, 1979). Generally, the nitrate migration in groundwater systems depends mostly on groundwater flow, its direction and velocity (under aerobic conditions). Groundwater flow direction and velocity depend on the geological framework and recharge conditions. Therefore a model was proposed for different recharge conditions based on hydrological characteristics such as precipitation, reference evapotranspiration, soil moisture characteristics and crop factors (for different types of land use structure and vegetation). Groundwater recharge has been calculated by the soil water

balance model NUT\_NEE for the period 1960-1995. According to the simulated annual groundwater recharge values, three types of steady-state groundwater system conditions have been defined (Kessels, 1997): dry, average and wet. They reflect the different recharge conditions from practically zero in the wet valley to  $0,001123 \text{ m.d}^{-1}$  on grassland during wet conditions. In this study the hydrodynamic model developed by Kessels (1997) was used. He used the FLONET/TRANS software package to develop the model. The basic hydrogeological properties (hydraulic conductivity in the x, y-direction; effective porosity) have been derived from field research and some were further calibrated by the MODFLOW model (van Lanen et al., 1995).

In principle, the results of the groundwater flow simulation are the following. The groundwater flow velocities are highest in the chalk sediments (Gulpen Formation) and regolith formation, mainly in the transition area (Fig. 3). Generally, the groundwater flow velocities are increasing towards the valley. Low velocities are observed towards the water divides. In the less permeable clayey silts of the Vaals Formation a decrease of groundwater velocities occurs. The groundwater flow path starts at the plateau or in the transition area and terminates usually in the valley centre (van Lanen et al., 1995; Kessels, 1997).

The transport parameters have been defined according to published physical properties of nitrate (Domenico - Schwartz, 1997; Freeze - Cherry, 1979): namely contaminant and source decay rate  $\lambda$ ,  $\beta = 0 \text{ d}^{-1}$  because of stability and low retardation of nitrates; diffusion coefficient  $D = 0,00001 \text{ m}^2.\text{d}^{-1}$ ; longitudinal dispersivity  $\alpha_L = 10 \text{ m}$  and transverse dispersivity  $\alpha_T = 0,1 \text{ m}$ . Zero-flux boundaries of the flow model (impermeable base and hydrologic water divides) have been interpreted in the transport model as zero-concentration gradient ones. The upper boundary coinciding with the groundwater table has been approached as a dispersive flux one. So, this is the only boundary, where nitrates are entering the multi-aquifer system. The average value of the  $\text{NO}_3^-$  input at the groundwater table is higher in the northern part of the catchment ( $115,7 \text{ mg.l}^{-1}$ ) than in the southern one ( $83,4 \text{ mg.l}^{-1}$ ). The nitrate-input concentrations are lowest within the valley centre ( $55,0 \text{ mg.l}^{-1}$ ). The initial input nitrate concentration for all recharge situations was assumed to be  $20 \text{ mg.l}^{-1} \text{ NO}_3^-$ . The recharge values depend on the different earlier-defined three hydrological situations (model under the average conditions has developed Klonowski, 1997).

The nitrate migration has been simulated for the last about 50 years (Kordík, 1998). The simulated nitrate distribution for the three recharge conditions is given in Fig. 4 for the early 1950's (600 days) and the late 1990's (18000 days). Nitrates, after migration through the unsaturated zone (long travel time – up to 10 years), are reaching the groundwater table and start moving according the groundwater flow pattern. In the early stage (600 days), the higher concentration (about  $25 \text{ mg.l}^{-1}$ ) occurs at the foothill and in the transition area (especially in the regolith formation, in which the groundwater velocities

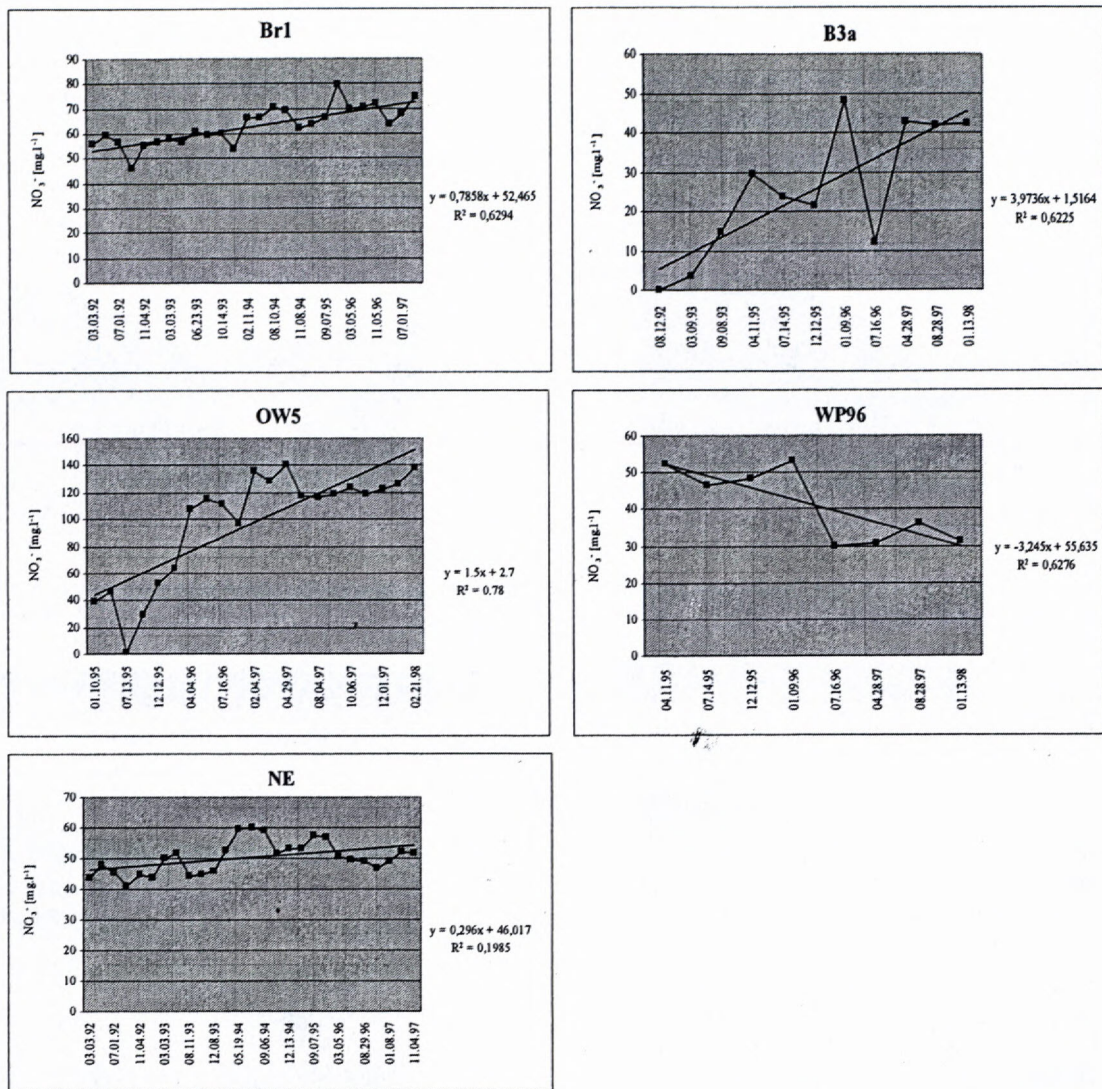


Fig. 2 Trend analysis of nitrates for some selected monitoring locations (Br1-spring Sint Brigida; OW5-dug well; NE-Noor brook; B3a-piezometer; WP96-deep piezometer)

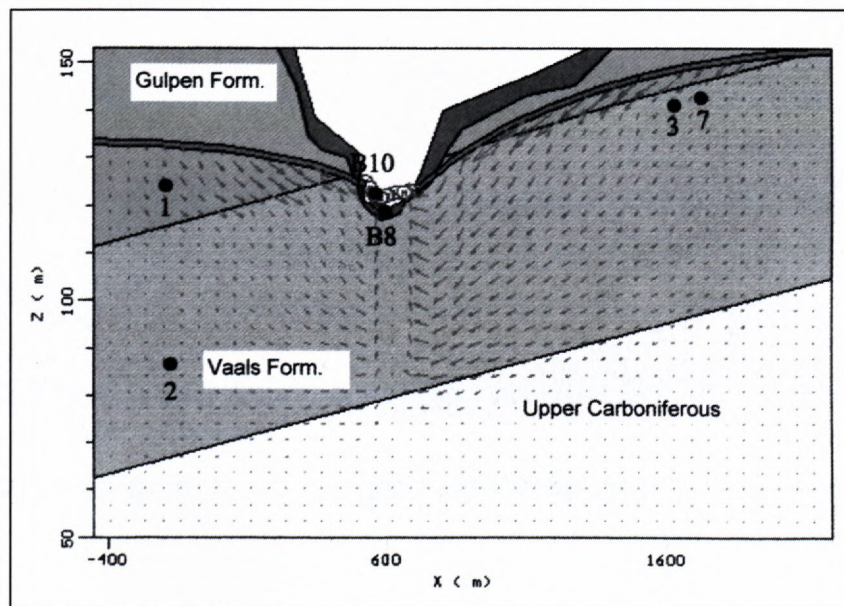
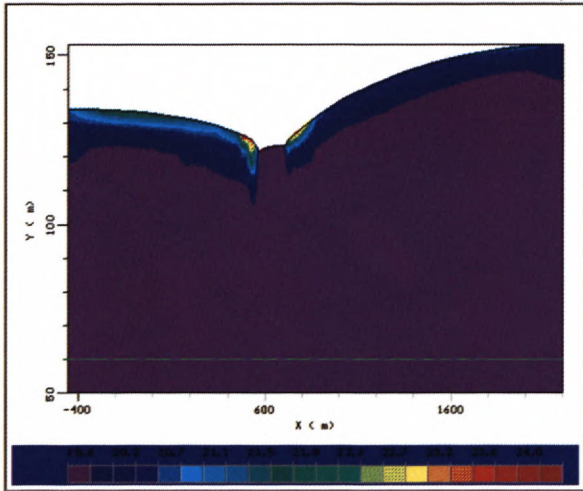


Fig. 3 Simulated groundwater velocities using FLONET/TRANS (Kessels, 1997)

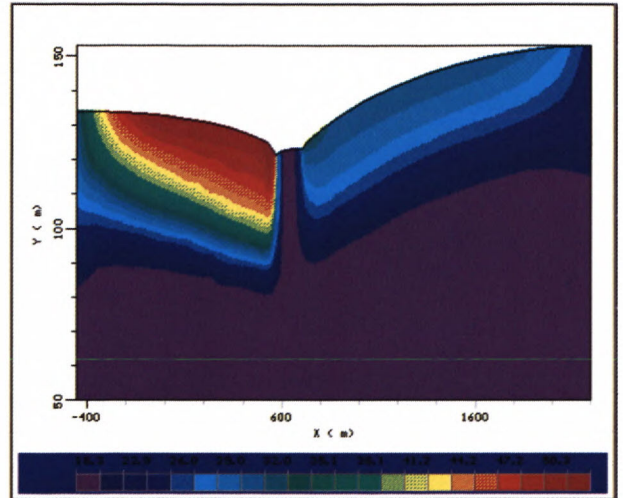
are the highest and the fastest contamination of groundwater by nitrates is expected). On the plateau, the migration of the nitrate plume is going more slowly. After 600 days, the nitrates do still not affect the deeper parts of the aquifer.

dry conditions – 600 days

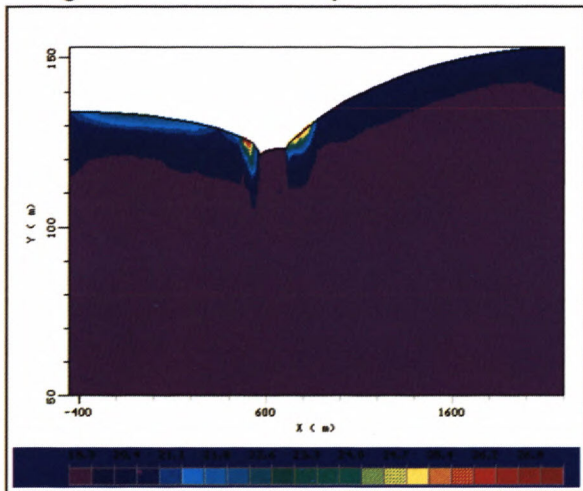


Almost the same migration patterns prevail in the following years (e.g. late 1990's), although the polluted zone expands. The nitrate concentration in the transition area would have reached the drinking water standard of  $50 \text{ mg.l}^{-1}$  after about 25 years under wet conditions, after 33

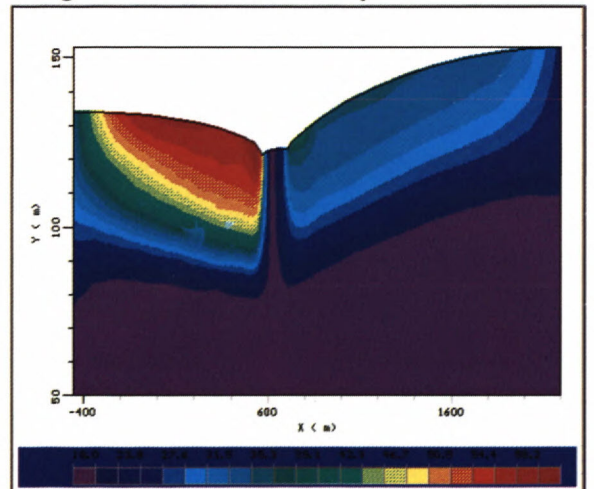
dry conditions – 18000 days



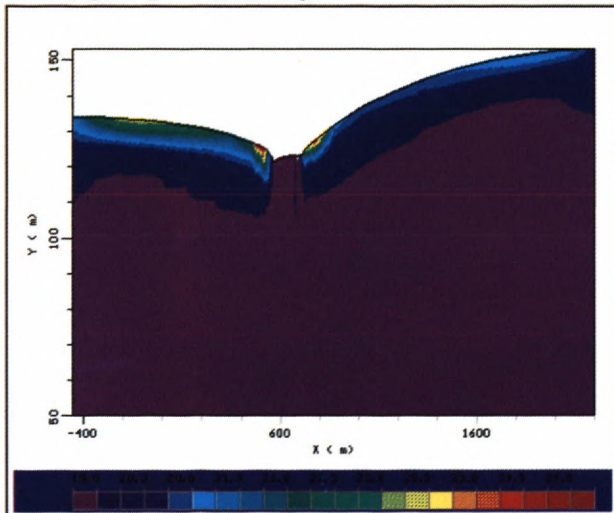
average conditions – 600 days



average conditions – 18000 days



wet conditions – 600 days



wet conditions - 18000 days

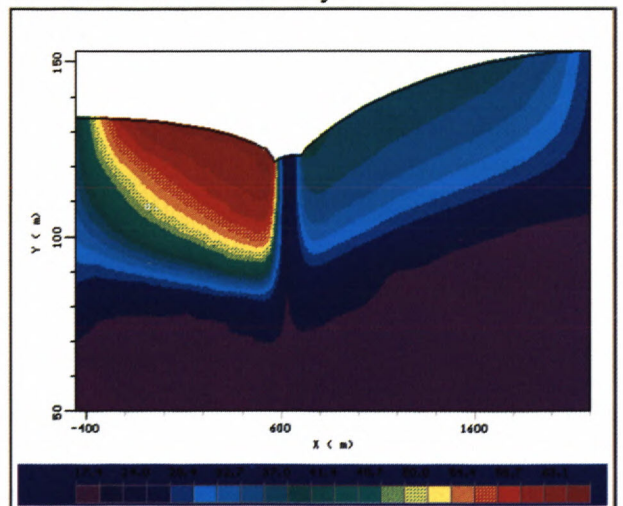


Fig. 4 Distribution of nitrates simulated by FLONET/TRANS after 600 and 18000 days for three different recharge conditions

years under average conditions and after 50 years under dry conditions. It means that in the Noor catchment the nitrate contamination is two times faster under wet conditions than under dry circumstances. After about half a century, almost the whole multi-aquifer system is affected by nitrate pollution, which corresponds with current observations in the Noor catchment. The contamination appears even at the end of the longest flowpaths in the valley filling sediments. The nitrate migration, according to the spatial groundwater flow patterns, shows a zone of stagnant groundwater at the bottom of the aquifer (Fig. 4). It does not take an active role in groundwater flow and is characterised by low nitrate concentrations.

The breakthrough curves of selected points (piezometers B8, B10 and hypothetical points 1, 2, 7; Fig. 3) confirm the migration patterns (Fig. 5). The points 1 and 7 are located under the northern and southern plateau about 10 m below the simulated groundwater table. The point 2 is situated deeper in the Vaals Formation, where lower concentrations of  $\text{NO}_3^-$  were expected. The quickest response to the contamination is shown in *piezometer B8*. It is situated in the transition area, in which groundwater follows short and shallow flow paths. Relatively high values of nitrates are already observed in the first year of simulation. The concentrations reach very high values at the end of the simulation period (late 1990's), i.e. about 50–65  $\text{mg.l}^{-1}$  depending on the hydrological conditions. Initially, *location 1* shows a relatively slow response to the contamination. After about 3 years of simulation the values start increasing and running almost parallel to the curve of B8. It reaches also high concentrations of nitrates at the end of the simulation (about 47–60  $\text{mg.l}^{-1}$ ). The response on *location 7* is similar to location 1, but the final value is the lowest (about 30  $\text{mg.l}^{-1}$ ). A very slow response to the contamination was simulated in the piezometer B10 and location 2. The *piezometer B10* is situated within the valley centre, at the end of the longest groundwater flowpath. Not earlier than about 20–25 years, the concentration is suddenly increasing and reaches a final concentration of 30–40  $\text{mg.l}^{-1}$  for B10 and 22–40  $\text{mg.l}^{-1}$  for *location 2*. The breakthrough curve of location 2 confirms the fact, that the nitrate pollution can reach even deeper zone of the hydrogeological structure.

#### Exploration of future nitrate pollution

Based on the previous simulation, a model to explore future nitrate concentration and distribution has been defined. The model describes three different scenarios of nitrate input reduction, i.e. reduction by 25%, 50% and 75%. No significant differences in precipitation and evapotranspiration are assumed to occur in the near future. Therefore the groundwater recharge has not been adapted. The simulations were carried out for dry, average and wet recharge conditions. The calibrated transport parameters, the hydrogeological properties and the flow boundary conditions of the multi-aquifer system have remained unchanged as well. The initial nitrate concentrations have been derived from the previous model by means of six

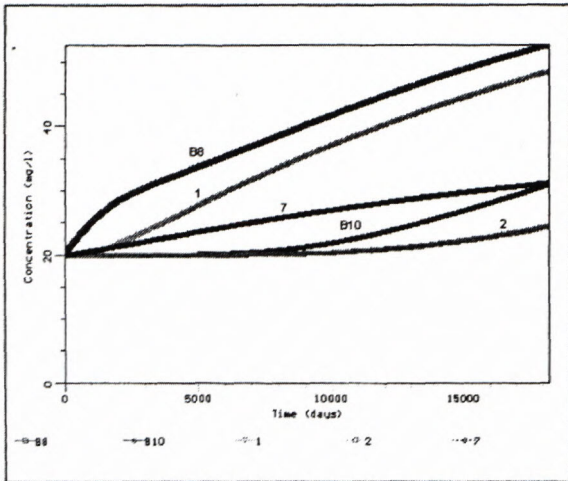
polygons with a characteristic average concentration of  $\text{NO}_3^-$  inside the polygons following the groundwater table, the water divides and some nitrate iso-concentration lines, i.e. 20, 30, 40 and 50  $\text{mg.l}^{-1}$ . The lowest initial concentration of 20  $\text{mg.l}^{-1}$  of  $\text{NO}_3^-$  remains the same and is assigned to the Upper Carboniferous impermeable base or stagnant zone of the aquifer, respectively. All simulations have been carried out for a time period of 36000 days (about 98,5 years; Kordik, 1998).

The results of the **25% nitrate reduction scenario** show high, steadily growing nitrate concentrations. The nitrate concentrations for the different locations (Fig. 3) are shown in the Fig. 5. Already after a very short time the concentration in *piezometer B8* reaches a very high value of more than 50  $\text{mg.l}^{-1}$  for all simulated conditions, which is a response to the already existing nitrate contamination under the plateau. Afterwards, the nitrate concentration is slightly increasing with concentrations of 57–70  $\text{mg.l}^{-1}$  at the end of the simulation (late 2090's). The curve of the *location 1* is almost parallel with the curve of piezometer B8 and the final concentrations reach values of 60–70  $\text{mg.l}^{-1}$  depending on the recharge conditions. The curve of *piezometer B10* starts with the lowest concentrations of 35–47  $\text{mg.l}^{-1}$ . After reaching a local maximum and a local minimum, the concentration is increasing steadily to final values of 52–60  $\text{mg.l}^{-1}$ . The curve of *location 3* has a stable or slightly decreasing character with the final concentration of 31  $\text{mg.l}^{-1}$ . Generally, a reduction of  $\text{NO}_3^-$  by 25% is not sufficient to reduce future  $\text{NO}_3^-$  concentration in the Noor catchment. The nitrate input after 25% reduction (i.e. 62,5  $\text{mg.l}^{-1}$ ) is still higher in most places than the concentration by the end of the 1990's. The decreasing concentration at location 3 is not clear. Incorrect simulation of the nitrate concentrations might occur because of not precise and limited assignment of polygons to define the initial concentration or because the Peclet and Courant accuracy criteria has not been met.

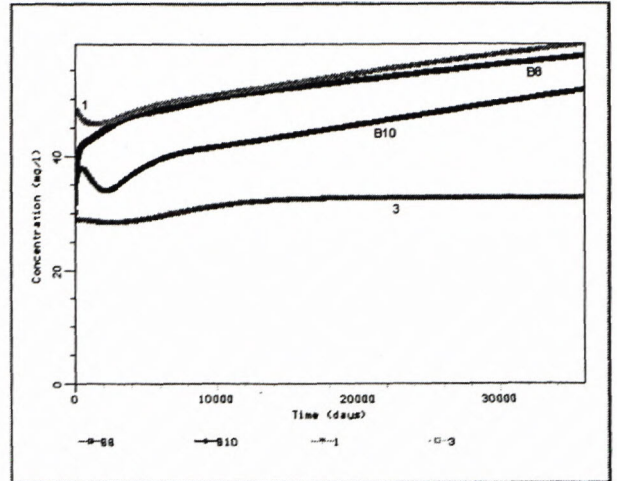
**50% reduction scenario** (Fig. 6): under the northern plateau the concentration does not undergo significant changes in time and under the southern part of the valley the concentrations slightly decline. The curves of the *locations 1, B10 and B8* show no significant changes in concentrations after passing either a local maximum or minimum and they are characterised by values of 43–51  $\text{mg.l}^{-1}$  at the end of the simulation depending on the recharge conditions. The simulation shows that even a reduction of the nitrate load by 50% will not significantly reduce the nitrate concentration in the groundwater system of the Noor catchment for all simulated recharge conditions. A completely different situation occurs at *location 3*, where the concentration of nitrates significantly declines in time with a final concentration of about 25  $\text{mg.l}^{-1}$ . The earlier-mentioned problems of modelling with the FLONET/TRANS software package are the reason for this.

The **reduction scenario of 75%** (Fig. 6) shows a gradual decrease of the nitrate concentration in time for all recharge conditions and for all locations. The final concentrations of nitrates at the end of simulation (late 2090's) are very similar in the *locations 1, B8 and B10*

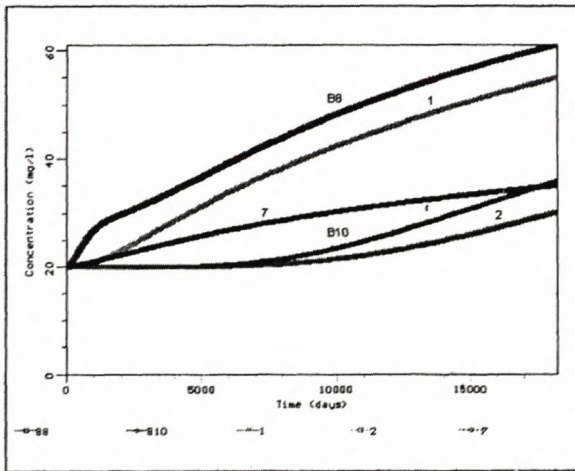
**Last 50 years  
dry conditions**



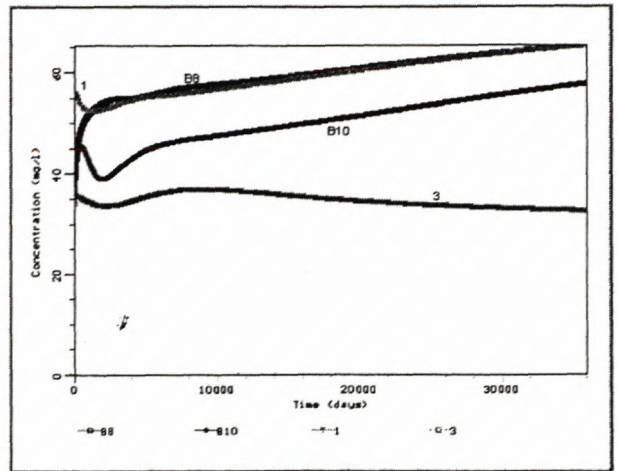
**25% reduction scenario  
dry conditions**



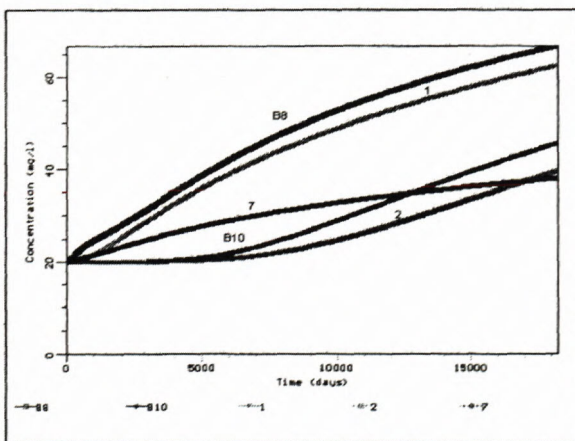
**average conditions**



**average conditions**



**wet conditions**



**wet conditions**

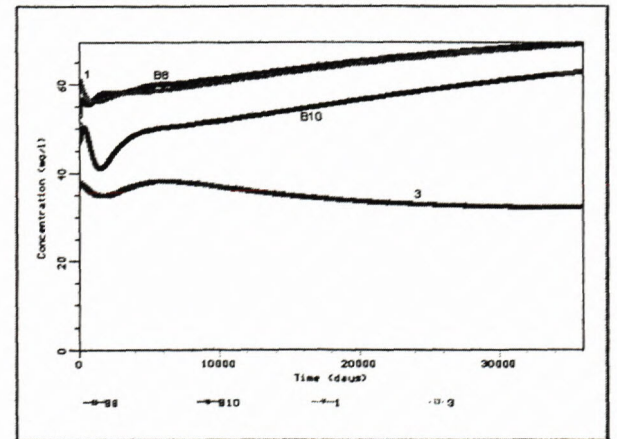
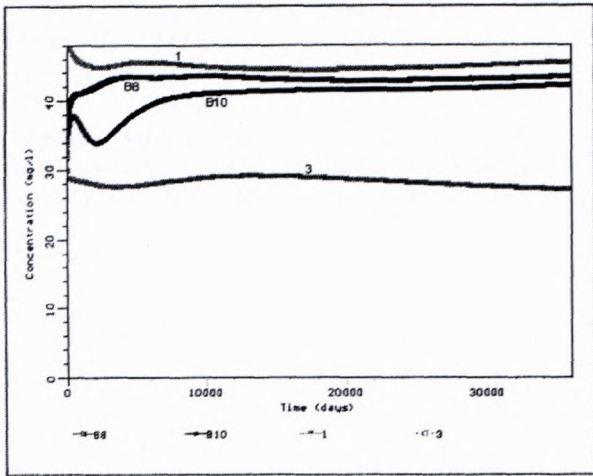
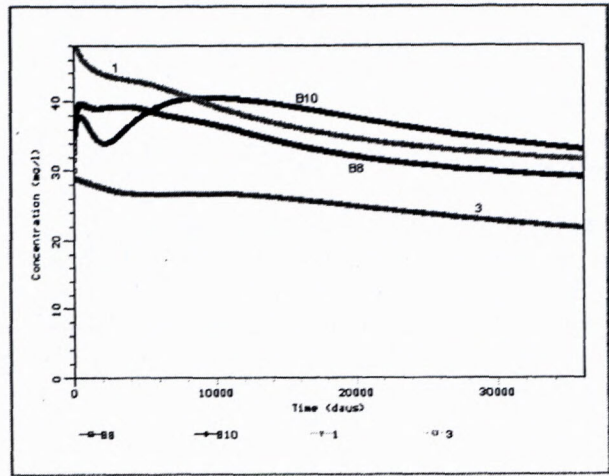


Fig. 5 Simulated breakthrough curves of  $\text{NO}_3^-$  for some points (simulated for the last 50 years and for a reduction scenario of 25%)

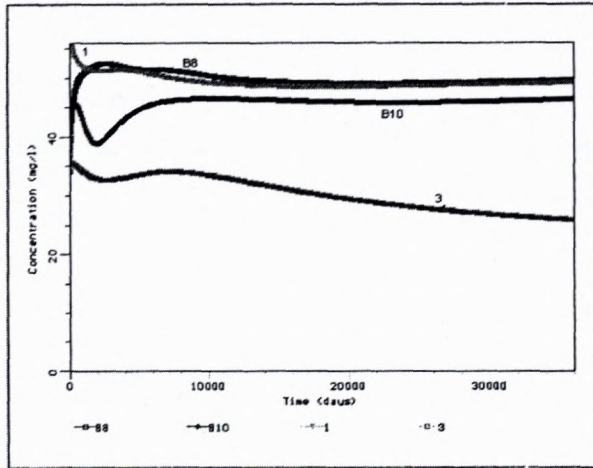
**50% reduction scenario**  
dry conditions



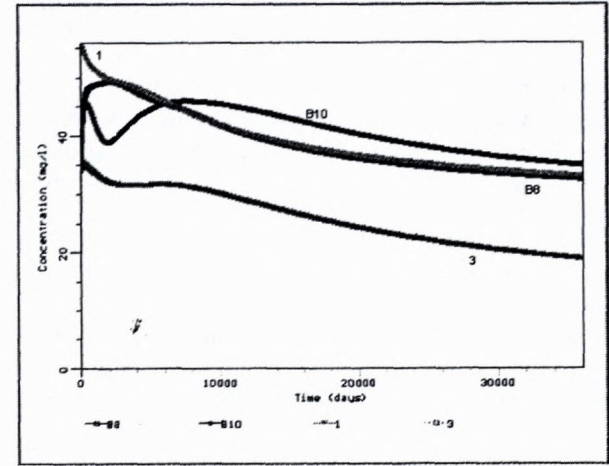
**75% reduction scenario**  
dry conditions



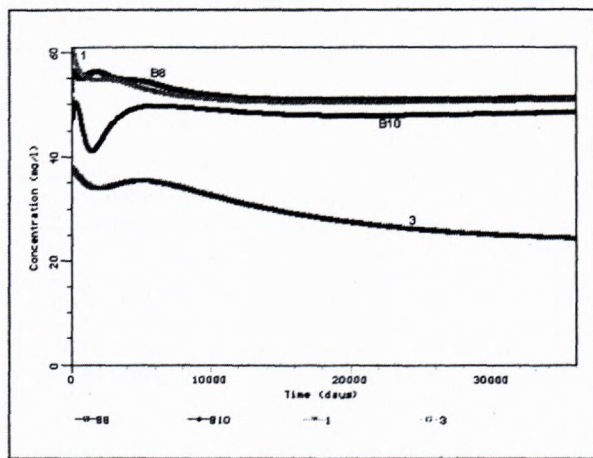
average conditions



average conditions



wet conditions



wet conditions

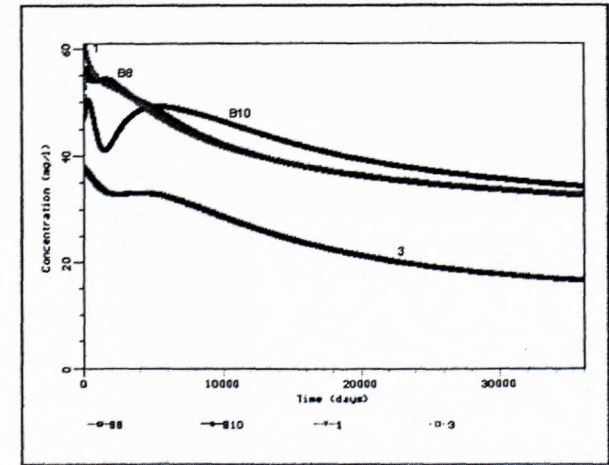


Fig. 6 Simulated breakthrough curves of NO<sub>3</sub> for some points (reduction scenarios of 50 and 75 %)

(about 29-38 mg.l<sup>-1</sup>). The final concentrations at location 1 are lower (19-24 mg.l<sup>-1</sup>). The breakthrough curves show, that a reduction of the nitrate input by 75% is required to decrease the NO<sub>3</sub><sup>-</sup> concentration below the drinking water standard (50 mg.l<sup>-1</sup>) and to improve the overall environmental situation in the Noor catchment.

## Conclusions

The investigated region belongs to the most fertile part of the Netherlands and about 97 % of the Noor catchment is used for agricultural purposes. The deterioration of the environment (especially decreasing of water quality) by nitrates is a very urgent problem. The nitrate concentration in the Noor valley is characterised by a very high variation from 0,5 to 147,6 mg.l<sup>-1</sup>. The mean values of about 42 mg.l<sup>-1</sup> are very close to the drinking water standard of 50 mg.l<sup>-1</sup>. The *dug wells* under the plateau have the highest NO<sub>3</sub><sup>-</sup> concentration (often > 100 mg.l<sup>-1</sup>). The *piezometers* that mostly occur in the centre of the valley have substantially lower concentrations (mean 26,5 mg.l<sup>-1</sup>) due to old, unpolluted groundwater, denitrification, and low NO<sub>3</sub><sup>-</sup> input in the wet valley. The *springs* (64,0 mg.l<sup>-1</sup>), which are predominantly fed by polluted groundwater from the plateaus have clearly higher values than the *Noor brook and its tributaries* (42,4-45,7 mg.l<sup>-1</sup>). Inflow from groundwater low in nitrate (denitrification, old groundwater) dilute spring water, so that water in the Noor and its tributaries is lower in nitrate than the springs. The trend analysis shows generally an increasing trend in the nitrate concentration for almost all monitored locations.

The *FLONET/TRANS* model has been used as a tool for the simulation of groundwater flow and nitrate transport. The model was applied to different recharge conditions (dry, normal and wet period) to analyse the current situation and to explore the future nitrate distribution in the valley for three nitrate load reduction scenarios of 25, 50 and 75 %.

Nitrates, after migration through the unsaturated zone, reach the groundwater table and start moving according to the groundwater flow pattern. In the early stage of simulation (early 1950's) high concentration of about 25 mg.l<sup>-1</sup> occurs in the regolith formation, in which the groundwater velocities are highest. Under the plateau, the migration of the nitrate plume is going more slowly. The concentration in the transition area would reach 50 mg.l<sup>-1</sup> (drinking water standard) after 25 years under wet conditions, after 33 years under average conditions and after 50 years under dry recharge conditions. It means that the groundwater system exceeds the pollution limit two times faster under wet conditions than under dry circumstances. At the end of simulation (late 1990's) almost the whole multi-aquifer system is affected by nitrate pollution.

The results of the **25 % nitrate reduction scenario** show high, steadily growing nitrate concentrations due

to still higher nitrate inputs than the concentration in the late 1990's. The results of the **50 % reduction scenario** indicate that under the northern plateau the concentration would not undergo significant changes in time and under the southern part of the valley the nitrate content would slightly decline. The breakthrough curves show that a **reduction of the nitrate input by 75 %** is needed to decrease the NO<sub>3</sub><sup>-</sup> concentration below the drinking water standard (50 mg.l<sup>-1</sup>) and to improve the overall situation of the environment in the Noor catchment.

## Acknowledgements

The first author carried out the study in the context of European Postgraduate Course in Environmental Management (EPCEM) and with financial support of the TEMPUS program. He thanks the Director of the Geological Survey of Slovak Republic for giving permission to study in the Netherlands. This study was done in the framework of the Wageningen Institute for Environment and Climate Research (WIMEK) as a part of the Research School SENSE.

## References

- Demoulin (Ed.), 1995. Physical Geography of the Ardennes. Department of Geography and Quaternary, University of Liege (Belgium) (in French).
- Domenico, P.A. & Schwartz, F.W., 1997: Physical and Chemical Hydrogeology. 2<sup>nd</sup> Edition, New York, Chichester, Brisbane, Toronto, Singapore: John Wiley & Sons, Inc.
- Freeze, R.A. & Cherry, J.A., 1979: Hydrogeology. Englewood Cliffs, New Jersey: Prentice-Hall.
- Frind, E.O. & Matanga, G.B., 1985: The dual formulation of flow for contaminant transport modelling. Review of theory and accuracy aspects. Water Resources Res., 21-2, 159-169.
- Guiger, N. – Molson, J. – Franz, T. & Frind, E., 1996: FLONET/TRANS User Guide Version 2.2. Ontario: Waterloo Hydrogeologic Software, Waterloo Centre for Groundwater Research.
- Kessels, J.C.H.M., 1997: Groundwater heads in some cross-sections in the Noor catchment. Modelling with the FLONET/TRANS software package. MSc. thesis, Department of Water Resources, Wageningen University (in Dutch).
- Klonowski, M., 1997: Waterflow and migration of nitrate in the chalk catchment of the Noor brook and impact on the Noorbeemden Nature Reserve. Internship Report of European Course in Environmental Management. Wageningen University.
- Kordik, J., 1998: Waterflow and nitrate transport in the Belgian-Dutch chalk region. Exploration of consequences to the environment for the Noor brook catchment. Internship Report of European Course in Environmental Management. Wageningen University. 81 p.
- Lanen, H.A.J. van – Weerd, B. van de – Dijkma, R., van Dam, H.J. & Bier, G., 1995: Hydrogeology of the Noor catchment and the impact of groundwater abstraction from the western boundary of the Margraten Plateau. Department of Water Resources, Wageningen University.
- Lanen, H.A.J. van & Dijkma, R., 1999: Water flow and nitrate transport to a groundwater-fed stream in the Belgian-Dutch chalk region. Wageningen: Hydrological Processes 13: 295-307.
- Nota, D.J.G. & Weerd, B. van de, 1978: A hydrogeological study in the basin of the Gulp creek - 1. Groundwater characteristics. Department of Water Resources, Wageningen University.
- Schunselaar, S.S. & Hoeven, K.M.L.J. van der, 1993: Valley fillings a source for hydrogeology. The 3D distribution of the valley fillings and the hydraulic properties in the upstream part of the Noorbeemden Nature Reserve and its impact on groundwater flow. Department of Water Resources, Wageningen University (in Dutch).

## Origin and evolution of ore-forming fluids at Pezinok-Kolársky Vrch Sb deposit (Western Carpathians, Slovakia)

PETER ANDRÁŠ<sup>1</sup>, JÚLIA KOTULOVÁ<sup>1,2</sup>, ANNA HAŠKOVÁ<sup>2</sup>, JARMILA LUPTÁKOVÁ<sup>1</sup>

<sup>1</sup>Geological Institute, Slovak Academy of Sciences, Severná 5, 974 01 Banská Bystrica, SR  
andras@savbb.sk; kotulova@gssr.sk; luptakova@savbb.sk,

<sup>2</sup>Geological Survey of Slovak Republic, Mlynská dolina 1, 817 04 Bratislava, SR

**Abstract.** The article presents the main results of the Pb- isotope study of stibnites, S- isotope study of sulphide minerals, as well as the O- and C- isotopes study of carbonates and quartz from Pezinok – Kolársky Vrch deposit. Pb-isotope study in galenas from epigenetic deposits of Malé Karpaty Mts. shows the magmatic origin of lead in ore-forming fluids. Pb-isotope distribution in stibnites indicates upper crustal origin of lead. Model ages in stibnite are influenced by „J-effect.“ They vary from 220 to 230 Ma and from 110 to 130 Ma. In ores, the heavy sulphur <sup>34</sup>S was contaminated by light sulphur isotope <sup>32</sup>S. Distribution of carbon and oxygen isotopes in carbonates shows an increasing role of meteoric water in ore forming fluids during the hydrothermal process.

In quartz of the 1<sup>st</sup> stage of the epigenetic Sb-Au mineralization only data from secondary fluid inclusions were available. In the 2<sup>nd</sup> to 4<sup>th</sup> stages salinities of the ore-forming fluids are relatively higher: 2 – 25 wt % NaCl equiv. In the 4<sup>th</sup> stage the presence of Ca<sup>2+</sup> cations was detected in the solutions.

Thermal maturation of organic matter from ore-bearing black schists from Pezinok deposit indicates temperatures close to 400°C.

**Key words:** fluid inclusion, S-, O- and C- isotopes, organic matter reflectance

### Introduction

The Pezinok - Kolársky Vrch deposit is situated in the Malé Karpaty Mts. crystalline complex (Fig. 1, 2). It belongs to small Sb deposits. During the 1790 to 1811 period and later from 1914 to 1995 (with exception of years 1948/1949) 1 million tons of Sb-ores were exploited with average content 1.3 % Sb, 9-11 ppm Au and 20-40 ppm Ag. The stibnite-concentrate was very poor, it contained about 25 % Sb in average. Identified geological resources of antimony and gold are of the order of 5000 t and 5.5 t respectively.

Based on the C- and O- isotope study of carbonates, Andráš (1983) assumed an increasing role of the meteoric waters during the development of hydrothermal fluids (originally the fluids were nearly endogenous). The first temperature study of the 1<sup>st</sup> and 2<sup>nd</sup> stage was published by Andráš et al. (1998). Using fluid inclusion study and the arsenopyrite geothermometer he calculated the crystallization temperature of the 1<sup>st</sup> and 2<sup>nd</sup> stage: 425-450°C and 350-450°C respectively.

### Ore mineralization

According to Ilavský (1979), Pezinok-Kolársky Vrch deposit belongs to the group of Sb-FeS<sub>2</sub> ores of eugeo-synklinal formation in association with basic volcanism (Fig. 3).

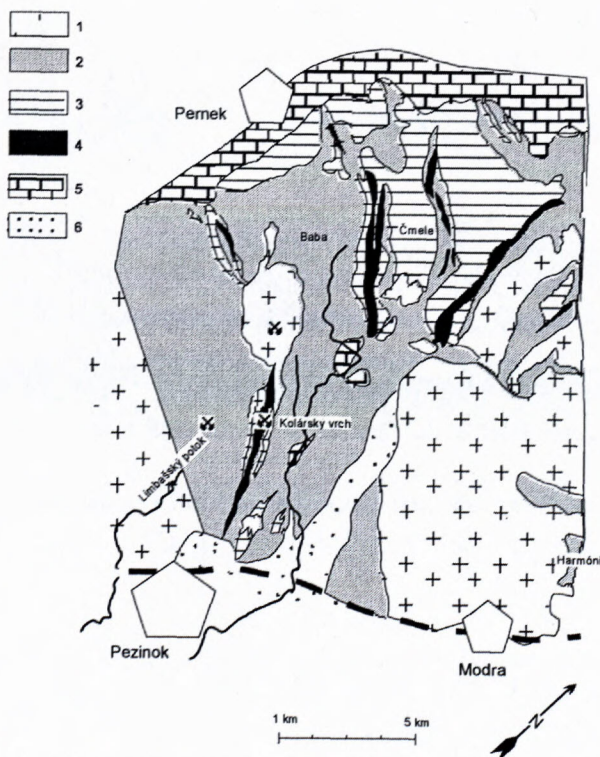


Fig. 1: Geological map showing the location of the Pezinok-Kolársky Vrch deposit (according to Cambel 1959 and Polák & Rak 1980 – modified) 1 – granitoid rocks, 2 – metamorphic rocks (phyllites, paragneisses), 3 – metabasalts, 4 – mineralized zones, 5 – carbonates, 6 – Tertiary and Quaternary sediments

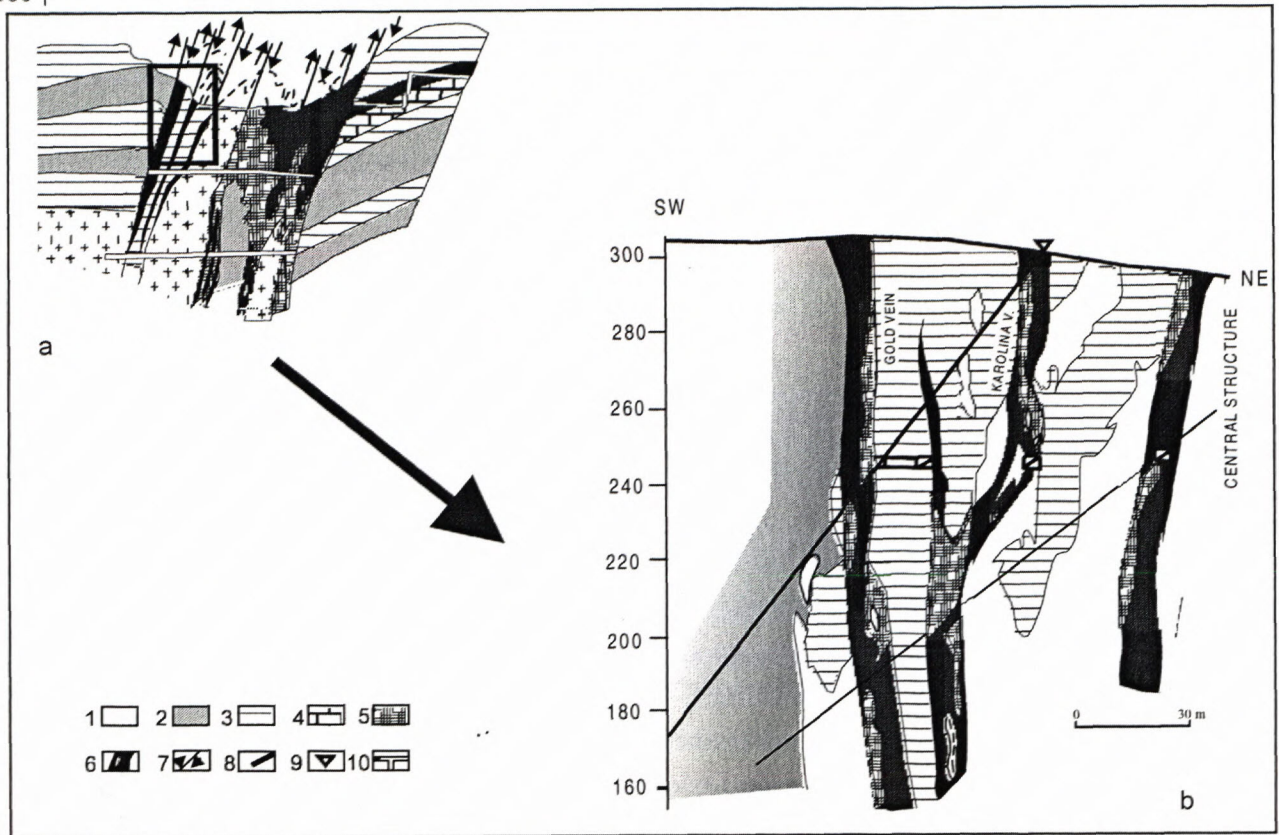


Fig. 2: Geological cross section of the central zone of the Pezinok-Kolársky Vrch Sb deposit (according to Ilavský 1979 and Mikula 1994). 1 – granitoid rocks, 2 – amphibolites, 3 – metamorphic rocks (phyllites, paragneisses), 4 – carbonates, 5 – black schists with syngenetic pyrite-pyrhotite mineralization, 6 – epithermal mineralization with quartz lenses, 7 – fault zones, 8 – bores, 10 – adits

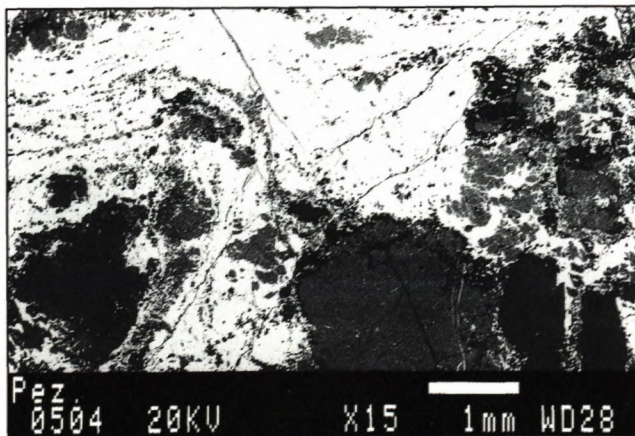


Fig. 3: Fine-grained metamorphosed, primarily exhalation-sedimentary pyrite (white) -pyrrothite (grey) ore in black schist.

MINERALS	STAGES AND ASSEMBLAGES			
	QUARTZ ARSENOPYRITE I	QUARTZ PYRITE ARSENOPYRITE II	STIBNITE CARBONATE QUARTZ III	STIBNITE KERMESITE IV
QUARTZ	■	■	■	■
PYRITE	■	■		
ARSENOPYRITE	■	■		
ANKERITE		■	■	
SIDERITE		■	■	
TETRAHEDRITE		■		
CHALKOPYRITE		■		
LÖLLINGITE		■		
GUDMUNDITE			■	
PYRRHORITE			■	
SPHALERITE			■	
GLAUKODOTE			■	
JAMESONITE			■	
BOULANGERITE			■	
BERTHIERITE			■	
DOLOMITE			■	
STIBNITE			■	■
CALCITE				■
GARAVELLITE				■
BISMUTH				■
HOROBETSUITE				■
ANTIMONY				■
KERMESITE				■
VALENTINITE				■

Fig. 4: Succession scheme of Sb mineralization at the Pezinok-Kolársky Vrch deposit (according to Cambel 1959 and András 1983 – modified).

The Pezinok – Kolársky Vrch deposit is situated in about 3500 m long tectonic fault of NW-SE direction. At the surface the mineralized structure is 25-70 m thick and about 430 m long (Mrákava, 1987). Two types of ore mineralization can be distinguished: 1 – metamorphosed, primarily exhalation-sedimentary pyrite mineralization genetically related to Devonian basic volcano-sedimentary cycle which was subsequently metamorphosed (Cambel 1956; Polák 1956) and 2 – hydrothermal Sb (Au-As) mineralization of epigenetic character which is located mostly in beds of tectonically deformed black shales. Metals could have been mobilised from the black shales by the circulation of fluids released during regional and periplutonic metamorphism, caused by granitoid rock intrusion (Cambel & Khun 1983; Chovan et al. 1992).

The main ore mineral is stibnite. There is a higher amount of berthierite and gudmundite in some zones. About 20 000 t of antimony was exploited by a 50x300 m open pit and several underground galleries (Uher et al. 2000). Identified resources of antimony are 5000 t of ores and 5.5 t of gold. According to various authors, the average gold content in ore varies from 3.04 to 4.20 ppm, silver content from 3.20 to 9.10 ppm and stibnite content is 0.10 %. Sb-flotation concentrate (data from 1990) contained 9-11 ppm of gold, 20-40 ppm of silver. 0.40 ppm of gold was lost in the waste (Mikula 1992).

Cambel (1959) described three mineralization stages of Sb epigenetic mineralization. and Andráš (1983) described the oldest gold-bearing arsenopyrite-pyrite stage and completed the succession scheme (Fig. 4):

- 1 – gold-bearing quartz-arsenopyrite-pyrite (Fig. 5),
- 2 – quartz-pyrite-arsenopyrite  $\pm$  löllingite, tetrahedrite, chalcopyrite (Figs. 6, 7),
- 3 – quartz-carbonate-stibnite  $\pm$  gudmundite, pyrrhotite, pyrite, sphalerite, Pb-Sb sulphosalts, berthierite (Figs. 8 – 10)
- 4 – stibnite-kermesite  $\pm$  antimony, valentinite, bismuth, Bi-Sb sulphosalts (Figs. 11 – 13).

Sb mineralization is spatially associated with exhalation-sedimentary metamorphosed pyrite and pyrrhotite mineralization. Patterns of its remobilization are observed in the form of stibnite films on surfaces of alpine faults in granitoids and gneisses (Chovan et al. 1990).

## Methods

Pb isotope analyses in stibnite were performed in laboratories of Vereinigung der kooperativen Forschungsinstitute der Österreichischen Wirtschaft, Arsenal in Vienna (analysed by M. Kralik). Distribution of sulphur isotopes in gold-bearing sulphides of the 1<sup>st</sup> stage of epigenetic mineralization was analysed in BRGM Orléans, France (analysed by A. M. Fouillac). Isotope analyses of oxygen and carbon in carbonates were performed in laboratories of the Czech Geological Survey in Prague (analysed by V. Šmejkal) and isotope analyses of oxygen in quartz in laboratory of the Geological Survey of Slovak Republic in Bratislava (analysed by A. Hašková).

Pyrolytic analyses of black shales were performed at the Czech Geological Survey in Brno using device Rock-Eval (analysed by Juraj Franců).

The reflectance of organic matter was measured in standard condition on rock polished sections using Leitz Orthoplan microscope with microphotometer MPV 2. Conditions: as a standard a glass-prism  $R_o=7.39\%$  was used, measuring field  $2 \times 2 \mu\text{m}$ , 50x lens, immersion oil, wavelength of light 545 nm, analysator in position of  $45^\circ$ . Maximum ( $R_{\text{max}}$ ) and minimum ( $R_{\text{min}}$ ) values of reflectance were measured on phytoclasts in 4 positions of microscope table.

Fluid inclusion studies were performed with THM 600 Linkam (Geological Institute, Slovak Academy of Sciences) and THMSG 600 Linkam (Faculty of Natural Sciences, Comenius University) freezing-heating stages calibrated using natural fluid inclusions with pure  $\text{CO}_2$  and inorganic compounds with known temperatures of phase transitions. Uncertainty of the final melting and homogenization temperatures is within  $\pm 0.2^\circ\text{C}$ .

## Isotope study

Distribution of Pb-isotopes in galena indicates magmatic origin of fluids (Černýšev et al. 1984) in postorogenic phase of the Variscan cycle. The present study shows the relatively inhomogenous Pb-isotope distribution in stibnites (Tab. 1), which corresponds with average values of upper crustal Pb origin (Fig. 14). Application of Stacey-Kramer classification (1975) enables to distinguish two fields of model ages: the first one ranges from 220 to 230 Ma and the second one, probably corresponding with ore remobilization, about 110-130 Ma. Low model ages are consequence of the „J-effect“, caused by contamination by radiogenic lead during the ore remobilization in metamorphic process.

Tab. 1 Pb-isotope distribution in stibnites from Pezinok-Kolársky Vrch deposit

Sample	$^{206}\text{Pb}/^{204}\text{Pb}$	$^{207}\text{Pb}/^{204}\text{Pb}$	$^{208}\text{Pb}/^{204}\text{Pb}$
1	18.638	15.702	38.542
2	18.553	15.677	38.442
3	18.626	15.698	38.534
4	18.747	15.702	38.533

Analysed in Vereinigung der kooperativen Forschungsinstitute der Österreichischen Wirtschaft laboratories, Arsenal, Vienna (analysed by Dr. M. Kralik)

According to Kantor (1974) and Andráš et al. (1998) (tab. 2), the  $\delta^{34}\text{S}_{\text{(CDT)}}$  isotope distribution varies in the range from 2.0 to  $-21.5\%$  (Fig. 15). The increase of light  $^{32}\text{S}$  isotope content in syndepositional pyrite-pyrrhotite ores is a consequence of the influence of bacterias. Sb-Ferminerals (gudmundite and berthierite) crystallized from solutions, which penetrated through these ores. They show the same high content of  $^{32}\text{S}$ . The  $^{32}\text{S}/^{34}\text{S}$  ratio in stibnite is close to that of the troilite standard, resp. to the hypogene plutogenic sulphur (Kantor 1974). Existence of more sulphur sources and intensive contamination of hypogenous sulphur by light  $^{32}\text{S}$  isotope was proved.

Carbon and oxygen isotope distribution in carbonates associated with Sb (Au) mineralization of four hydro-

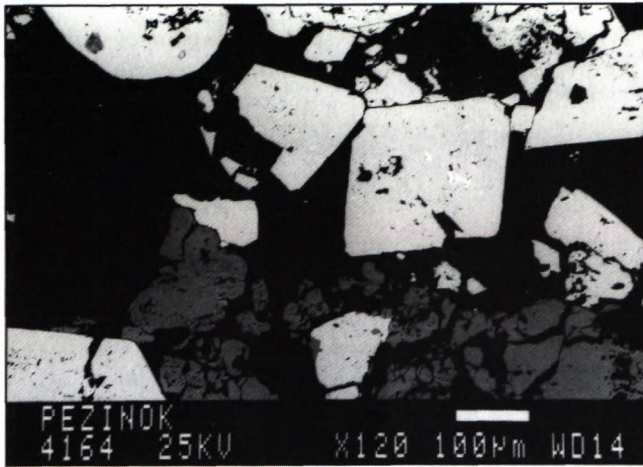


Fig. 5: Euhedral gold-bearing arsenopyrite (white) and pyrite (grey) in quartz (black) of the 1<sup>st</sup> stage

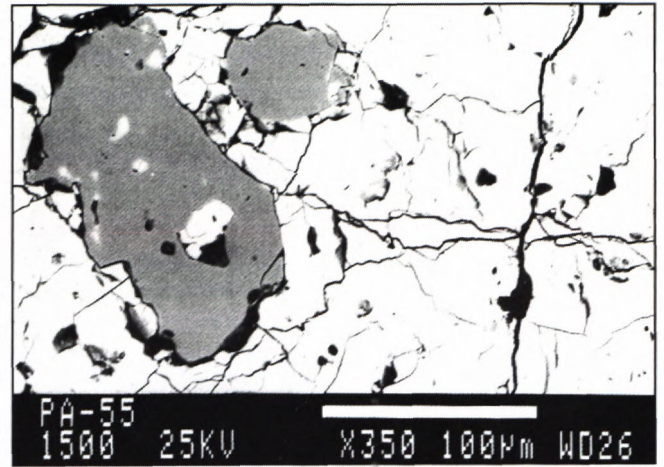


Fig. 6: Brecciated massive arsenopyrite (white) and pyrite (grey) mineralization of the 2<sup>nd</sup> stage.

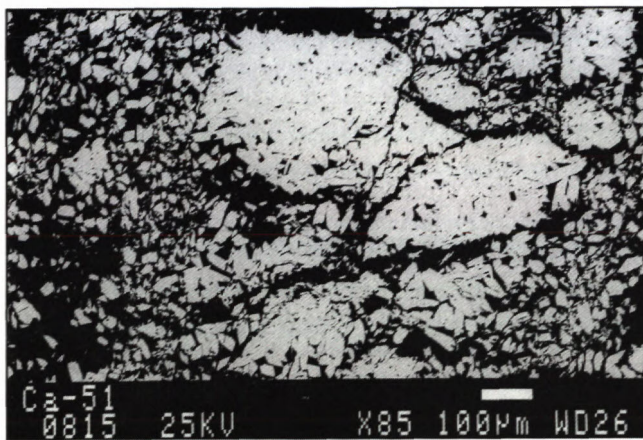


Fig. 7: Relic texture of original pyrite aggregate replaced by euhedral löllingite crystals – 2<sup>nd</sup> stage.

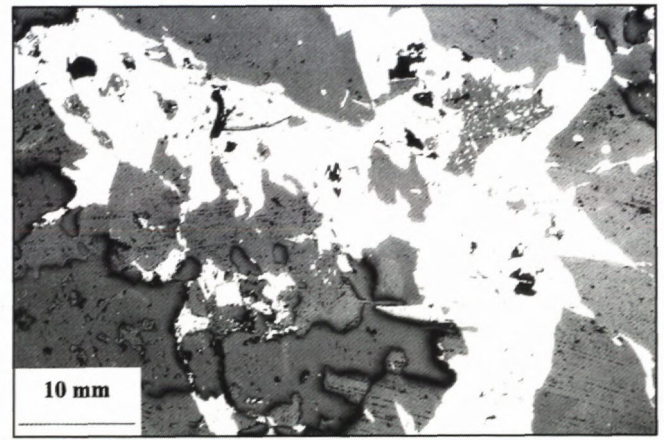


Fig. 8: Aggregate of stibnite (white) in quartz (grey), // nicols – 3<sup>rd</sup> mineralization stage.



Fig. 9: Morphology of rare stibnite needles (3<sup>rd</sup> stage).

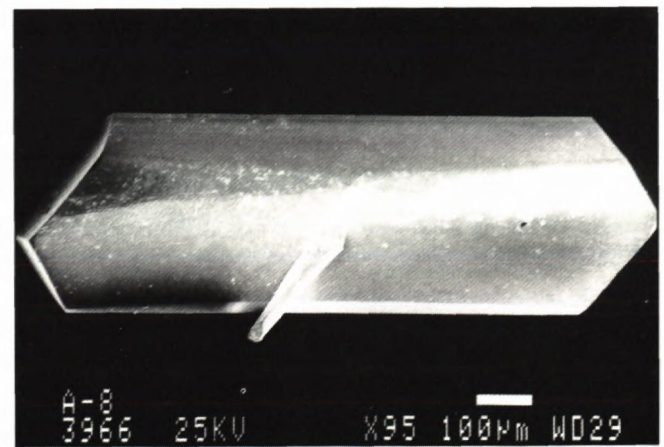


Fig. 10: Morphology of euhedral gudmundite crystal from the 3<sup>rd</sup> mineralization stage.

thermal stages is considerable inhomogeneous (Tab. 3, Fig. 16) and vary in the following ranges:  $\delta^{13}\text{C}_{\text{PDB}}$  = from -13.2 to 9.1 ‰ and  $\delta^{18}\text{O}_{\text{PDB}}$  = from -17.5 to -13.6 ‰ ( $\delta^{18}\text{O}_{\text{SMOW}}$  = -13.89 up to -20.54 ‰).  $\delta^{18}\text{O}_{\text{PDB}}$  isotope distribution in quartz (from -10.01 to -16.46) indicates meteoric origin of fluids. In carbonates it is possible to observe a moderate shift of  $^{18}\text{O}$  values to the field of metamorphogenous and endogenous origin of oxygen in direction: calcite-dolomite-ankerite/siderite. Comparison of O-isotope data with those of  $^{12}\text{C}/^{13}\text{C}$  ratio gives an evidence about the increasing role of meteoric fluids predominantly in the final stages of crystallization.

Tab.2  $\delta^{34}\text{S}_{(\text{CDT})}$  isotope data in gold-bearing arsenopyrites and pyrites of the 1<sup>st</sup> mineralization stage from the Pezinok-Kolársky Vrch deposit

Sample	Mineral	$\delta^{34}\text{S}_{(\text{CDT})}$
RB-201	arsenopyrite	-0.5
RB-201	pyrite	-14.4
RB-206	arsenopyrite	+1.3
RB-214	pyrite	-11.9
RB-214	arsenopyrite	-1.6
RB-217	pyrite	-3.0
RB-217	arsenopyrite	0.0
RB-223	pyrite	-14.0

Analysed in BRGM, Orléans, France (Dr. A. M. Fouillac)

Tab. 3 Distribution of  $\delta^{13}\text{C}$  and  $\delta^{18}\text{O}$  (‰ PDB) isotopes in vein carbonates and in quartz from Sb mineralization from the Pezinok-Kolársky Vrch deposit

a) carbonates

Sample	Mineralization		‰ PDB $\delta^{13}\text{C}$	‰ PDB $\delta^{18}\text{O}$
	Mineral	stage		
RB - 77	ankerite	2	-13.10	-17.54
RB - 12	ankerite	2	-10.83	-16.11
RB - 13	ankerite	2	-10.75	-16.22
RB - 47	ankerite	2	-10.20	-13.60
PA - 14	siderite/dolomite	3	-10.50	-16.34
RB - 48	siderite/dolomite	3	-9.80	-15.10
RB - 47	calcite	4	-9.00	-14.97
RB - 79	calcite	4	-10.10	-14.55

b) quartz

Sample	Mineralization		‰ PDB $\delta^{18}\text{O}$
	Mineral	stage	
RB-204	black quartz	1	-13.52
P-20	black quartz	2	-15.36
RB-109	grey quartz	2	-16.05
RB-205	grey quartz	2	-12.98
RB- 10	black quartz	3	-14.12
RB-108	grey quartz	3	-13.80
RB-216	milky quartz	4	-16.46

Department of Isotopic Geology of the Geological Survey of Slovak Republic, Bratislava (A. Hašková)

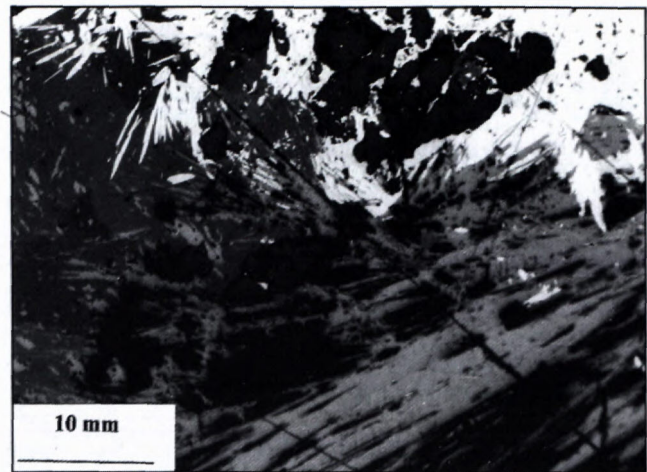


Fig. 11: Typical mineral assemblage of the 4<sup>th</sup> stage: euhedral crystals of stibnite (white), long needles of valentinite (light grey) and kermesite (dark grey) in quartz (black).

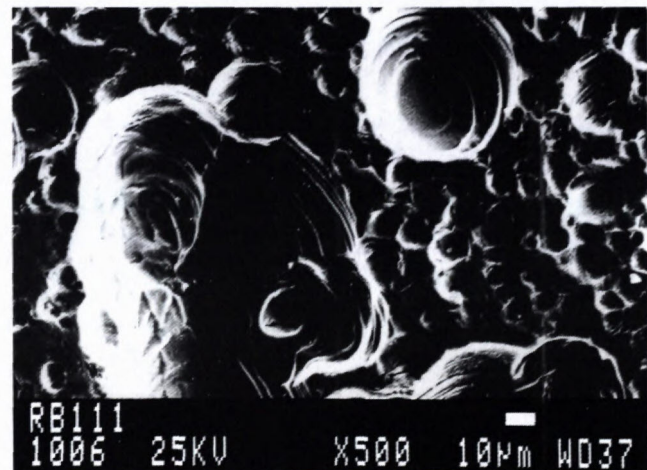


Fig. 12: Sulphuric acid-etched surface of native antimony aggregate (4<sup>th</sup> stage).

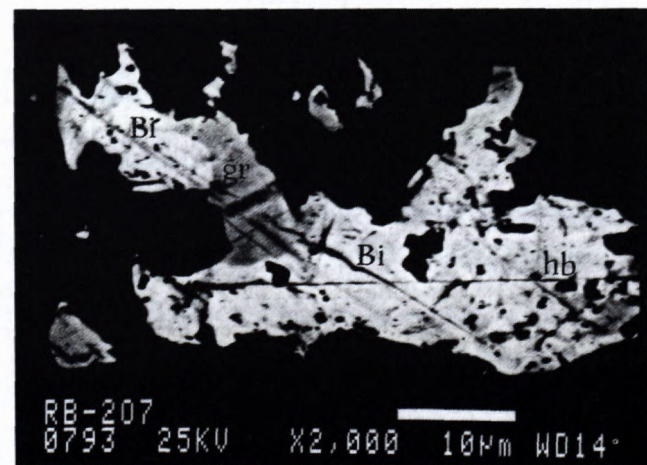


Fig. 13: Intimate intergrowths of Bi-minerals (4<sup>th</sup> stage): native bismuth (Bi), horobetsuite (hb) and garavellite (gr).

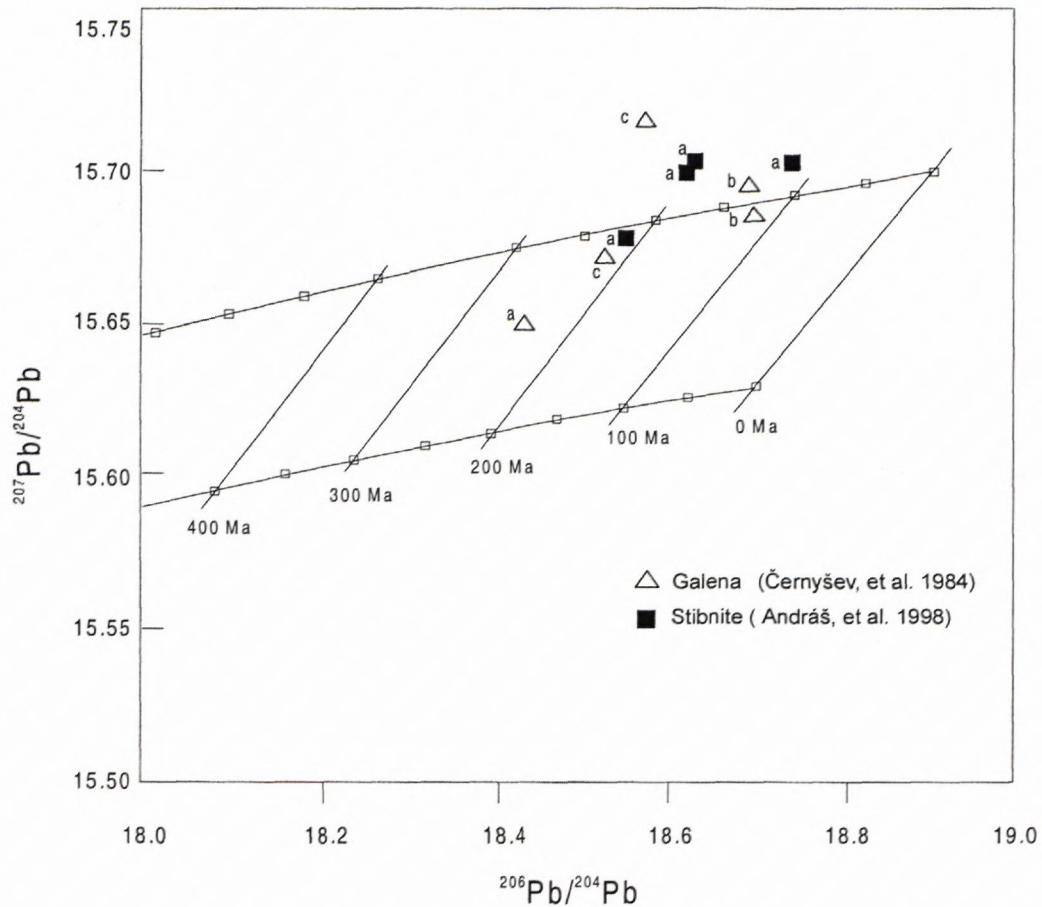


Fig. 14: Evolution diagram of Pb-isotopes in galenas and stibnites from the Pezinok-Kolársky Vrch deposit (according to Stacey-Kramer 1975). 1 – 4: analyse numbers in tab. 1; galena is from the following occurrences: a – Pezinok, – Pod Babou, c – Častá

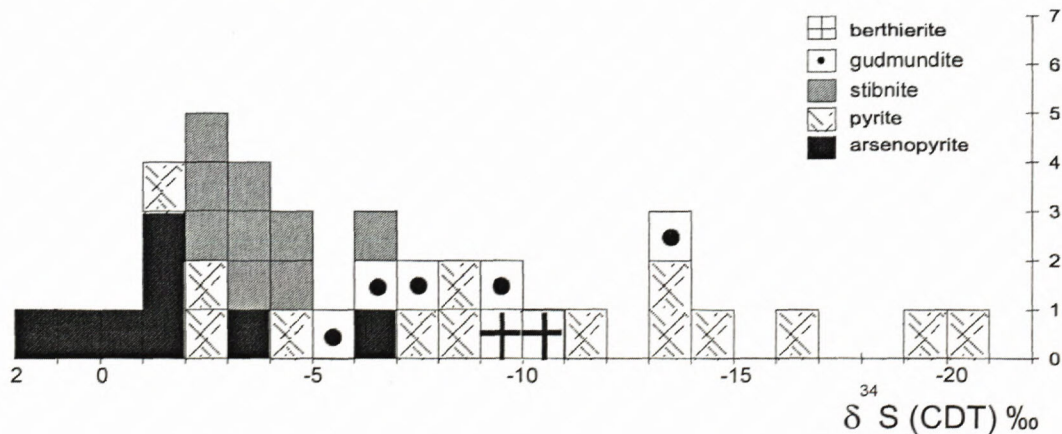


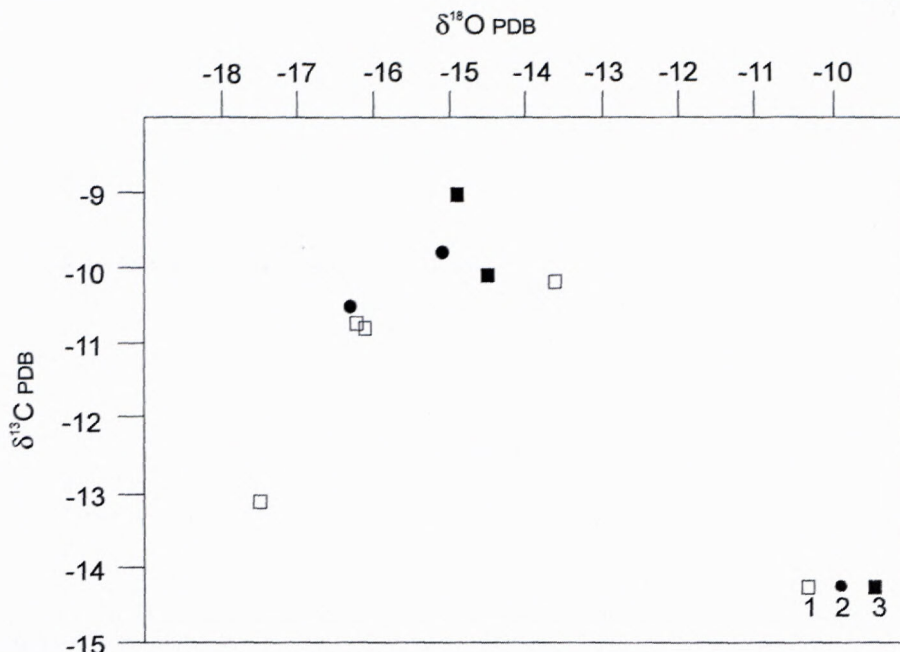
Fig. 15:  $\delta^{34}\text{S}$  isotope data in sulphides from hydrothermal mineralization (Kantor 1974 and Andráš et al. 1998)

### Thermometric study

Syndepositional exhalation-volcanogenic ores were recrystallized during the regional-periplutonic metamorphism in greenschist and amphibolite facies. According to Cambel et al. (1990) the temperature of this metamorphism varies in the range 350 – 600 °C and the

pressure is about 3.5 – 5.5 kbar. Graphite geothermometer gives the temperature about 450 °C and pressure 3 (up 3.5) kbar (Andráš & Horváth 1985). Such temperature and pressure enable mobilization of metallic elements. Different character of fluids, varying temperature and changes of pressure caused the final variability of the mineralization.

Fig. 16:  $\delta^{13}\text{C} / \delta^{18}\text{O}_{\text{PDB}} \text{‰}$  plot of isotope distribution in carbonates in association with Sb mineralization: 1 - ankerite, 2 - siderite/dolomite, 3 - calcite.



Contents of organic carbon ( $C_{\text{org}}$  in tab. 4) show that the black shales are, sensu Hunt (1972) classification, „rich“ (RB-102 and 24/482-3), and „very rich“ (RB-101, RB-104, 43/329) in organic carbon. The contents of the distillable and pyrolytic hydrocarbons are low. This fact indicates a high degree of graphitization (maturation) of the organic matter. Parameter  $S_3$  - pyrolytic  $\text{CO}_2$  (mg/g of sample) indicates oxidation of the organic matter.

Tab. 4 Pyrolytic analyses of mineralized black schists

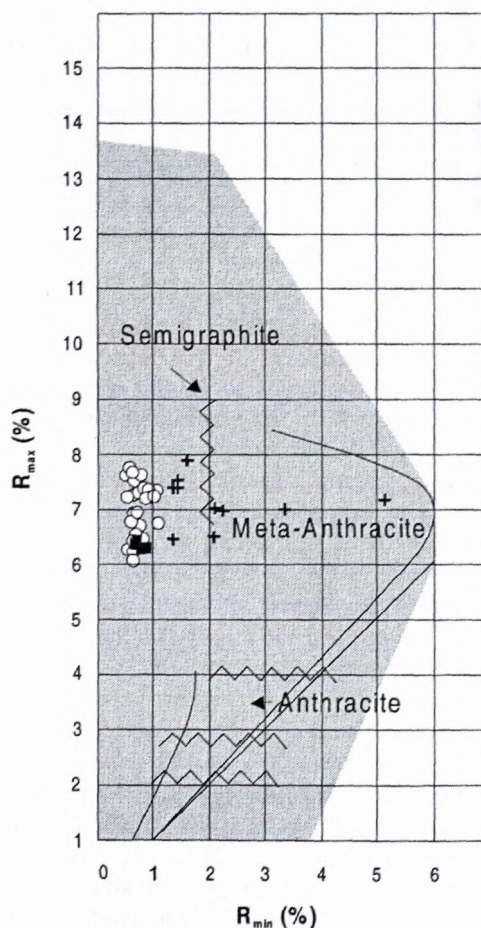
Sample	$S_3$	TC	$C_{\text{org}}$
RB-101	0.36	4.62	3.5
RB-102	0.56	0.71	0.5
RB-104	0.12	2.60	1.5
24/482-3	0.38	0.50	
43/329		3.98	2.0

$S_3$  =  $\text{CO}_2$ -pyrolytic  
 TC - total-carbon  
 $C_{\text{org}}$  - organic carbon

Two main types of organic matter were distinguished in samples of ore-bearing black schists from Pezínok deposit:

1. Flocky organic matter of the size 2 – 5  $\mu\text{m}$ , parallel with the rock foliation. Thermal overwork of the organic substance destroyed original textures. Small size and strong thermal reworking of particles do not permit distinguish original textures of organic particles and to state terrestrial or marine origin of the organic matter.

2. Organic matter of high level of maturation in stylolithes and in calcite and quartz veinlets. Individual particles have predominantly size about 2 – 5  $\mu\text{m}$ , rarely 7  $\mu\text{m}$ . This second type of organic substance represents pyrobitumen. The bitumen was probably generated in the past - during the diagenetic stage from organic matter stored in sediments and later temperature-overworked during the metamorphosis of the rock complex.



- Pezínok - Kolársky vrch - Budúcnosť mine, organic particles reflectance
- Pezínok Augustín mine, organic particles reflectance
- + Pezínok - Trojárová mine, solid bitumen reflectance

Fig. 17 Reflectances of organoclasts from ore-bearing black schists from Pezínok deposit

Tab. 5 Characteristics of ore forming fluids

Stage	Salinity (wt. % NaCl equiv.)	Chemical composition of fluids	Homogenization temperature (°C)	Crystallization temperature(°C)	Eutectic temperature (°C)	Density of fluids g/cm <sup>3</sup>
1	6-11	secondary inclusions	180-275	425-450*	-45 to -55	
2-3	7-20	NaCl-KCl-H <sub>2</sub> O	145-200	350-450**	< -45	0.98-0.93
4	8-25	CaCl <sub>2</sub> -H <sub>2</sub> O (±NaCl)	82-198		-57 to -48	0.99-1.16

\* sensu Dubaj (in Andráš et al. 1998)

\*\* only for the 2. stage sensu Dubaj (in Andráš et al. 1998)

Increasing temperature caused irreversible changes in molecular structure of the organic matter which correspond to the increasing light reflectance of the organic matter. The maximum reflectance ( $R_{max}$ ) of organic particles, as well as of solid bitumen, varies in the range 6.0 – 7.8 %. Organic matter in black shales from Pezinok deposit has reached the meta-anthracite up to semigraphite stages (Fig. 17).

By using average  $R_{max}$  values of organic particles ( $R_{max} = 6.95\%$ ) and solid bitumen ( $R_{max} = 7.14\%$ ) in Barker & Pawlewicz (1986) and Baker & Bone (1995) equations for calculation of maximum temperature of metamorphism, we have obtained temperature close 400 °C.

#### Fluid inclusion study

Fluid inclusions were studied in relation to mineral assemblages in doubly polished wafers (thickness of 0.2 – 0.5 mm) of quartz and carbonates. Fluid inclusions had almost regular shape and occurred in small clusters or planes and trails. Studied fluid inclusions were of a very small size <10  $\mu$ m, which made measurements more difficult, particularly at low temperatures. Another frequently encountered problem was non-transparency of the host mineral. The following phase changes have been recorded: eutectic or first melting temperature ( $T_e$ ), to determine salt-water system; final melting temperature of ice ( $T_{mi}$ ), to calculate salinity; total homogenization temperature ( $T_h$ ), to calculate the density of fluids and estimate the formation temperature.

Phase changes at low temperatures were studied before those upon heating because of the risk of decrepitation.

After heating of completely frozen inclusions (to –100°C) the first appearance of liquid phase was observed in the temperature range from –56.7 to –42.7 °C. This indicates the presence of chlorides of bivalent cations such as Ca<sup>2+</sup> or Mg<sup>2+</sup> in the fluids (Borisenko 1977).

In some cases it was not possible to observe melting of ice, however, as an indirect evidence of ice melting the last sudden movement of vapour bubble was considered (Roedder 1984).

All inclusions homogenised to liquid. Some of them decrepitated before homogenisation ( $T_h = 80 - 402^\circ\text{C}$ ), nevertheless massive decrepitation (if measured) occurred at temperatures around 400°C. In a few cases some solid phases have been observed.

#### 1<sup>st</sup> stage

In quartz of the 1<sup>st</sup> stage of the epigenetic Sb-Au mineralization only data from secondary fluid inclusions were available. Homogenization temperatures of inclusions varied from 180 to 275 °C (Fig. 18a).

Salinity of the solutions is 6-11 wt. % NaCl equiv., eutectic temperature ranges from –45 to –55 °C (Tab. 5).

Using the data obtained by independent geobarometer and the tables of Hurai (1988) it is possible to ascertain the real temperature of the quartz crystallization. According to Andráš et al. (1998), the crystallization temperatures in the gold-bearing arsenopyrite-pyrite 1. stage are equal with range from 425 to 450 °C.

#### 2<sup>nd</sup> and 3<sup>rd</sup> stage

Quartz of 2<sup>nd</sup> and 3<sup>rd</sup> stage contained two-phase (liquid-vapour) aqueous inclusions, with occasionally observed solid phases (daughter crystals), represented by halite and ore minerals. Eutectic (first melting) temperatures below –45 °C suggest the presence of CaCl<sub>2</sub> in H<sub>2</sub>O-NaCl solution. Homogenization temperatures range from 145 to 200 °C (Fig. 18b). Decrepitation temperature peak is around 400°C. Salinities are in the range of 7 – 25 wt.% NaCl equiv.

The temperature calculation corresponding with the highest possible ore forming pressure of 3 kbar (Andráš & Horváth 1985), using the pressure-temperature curves (Hurai 1988), gives the quartz crystallization temperature 350 – 390 °C.

The arsenopyrite thermometers of Kretschmar & Scott (1976) and Sundblad et al. (1984), used on massive arsenopyrite of 2<sup>nd</sup> stage, give temperatures 350 – 410 °C and 350 – 450 °C, respectively (Andráš et al. 1998).

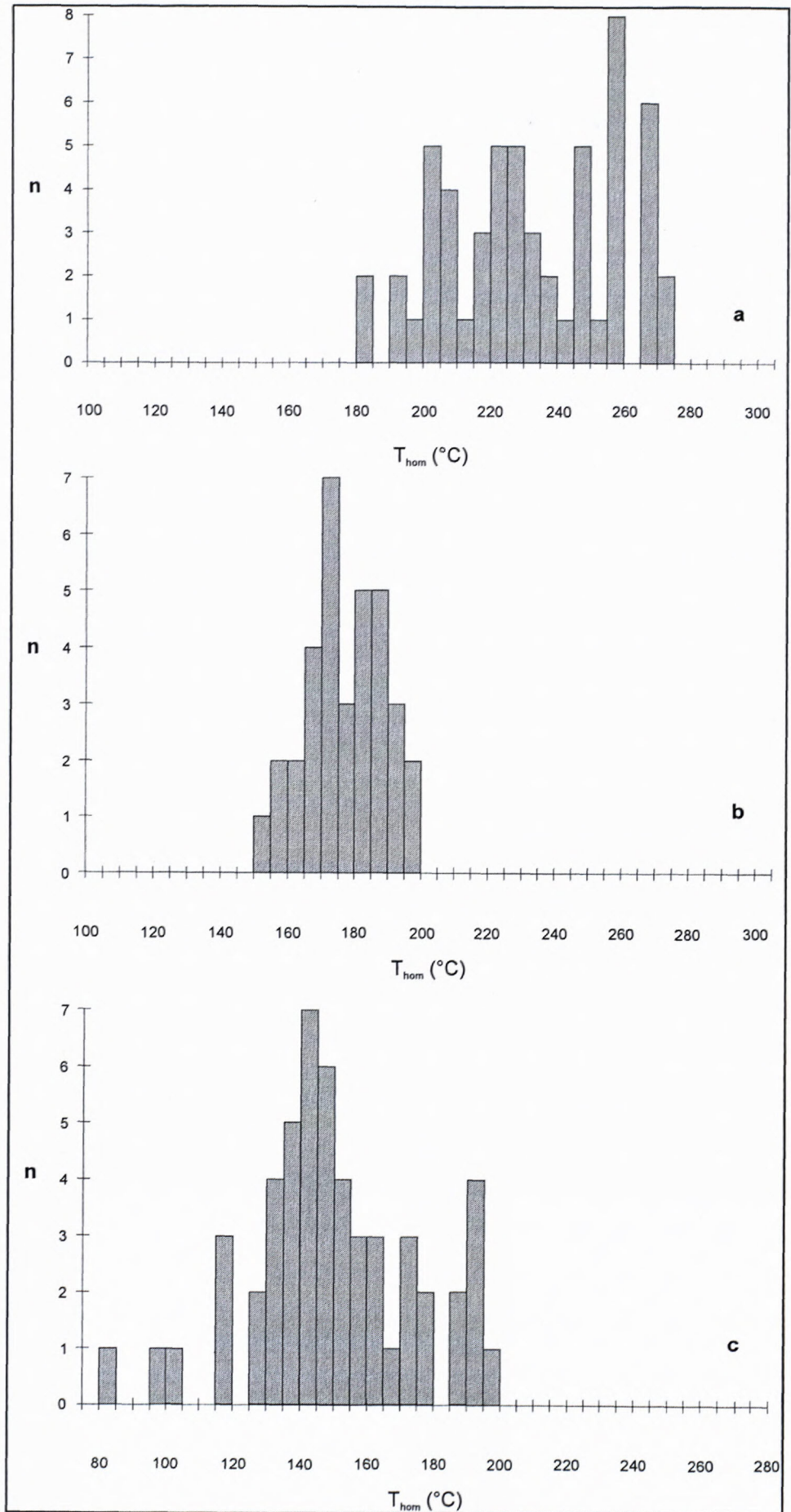
#### 4<sup>th</sup> stage

Milky quartz of 4<sup>th</sup> stage contained two-phase (L + V) aqueous inclusions, with the average size of about 6  $\mu$ m. The vapour bubble occupies less than 10 vol. % of the total volume.

Eutectic temperature varies between –56.7 and –42.7 °C, corresponding to the CaCl<sub>2</sub>+NaCl+H<sub>2</sub>O system. Final melting of ice was observed in a wide temperature range, from –30.4 up to –5.1 °C. Homogenisation to liquid occurred in the range of +82 to +199 °C (Fig. 18c) with the

Fig. 18: Histogram of homogenization temperatures in fluid inclusions from quartz from Sb epigenetic mineralization:

a) 1<sup>st</sup> stage, b) 2<sup>nd</sup> and 3<sup>rd</sup> stage, c) 4<sup>th</sup> stage.



main interval between 130 and 160 °C. Salinities were calculated from ice melting temperatures using equation of state (EOS) of Oakes et al. (1990) and vary between 8 – 25 wt. % CaCl<sub>2</sub> equiv. Densities were calculated from the homogenisation temperatures using EOS of Zhang and Frantz (1987) and range from 0.99 to 1.66 g/cm<sup>3</sup>.

## Conclusions

Lead in stibnites is of upper crustal origin. The young model ages (220-230 and 110-130 Ma) are the consequence of the „J-effect“, caused by the younger metamorphogenous processes and rejuvenation of Sb (-Au) ores. Isotope distribution shows at least two sources of sulphur. Biogenic sulphur had an important role predominantly in metamorphosed, primarily exhalation-sedimentary pyrite mineralization and in Sb hydrothermal minerals with Fe content (gudmundite, berthierite). Sulphur isotopes in gold-bearing sulphide mineralization are differentiated: the light biogenic sulphur is incorporated into pyrite while the sulphur from deep lying source is incorporated into arsenopyrite. Ore fluids mainly of 3<sup>rd</sup> and 4<sup>th</sup> stage are probably meteoric in origin but they incorporated predominantly magmatic sulphur, which could have been juvenile or derived from older plutonic rocks.

Distribution of carbon and oxygen isotopes in carbonates and oxygen isotopes in quartz from Sb mineralization is inhomogeneous. The values show a relatively wide range and indicate predominantly meteoric origin of fluids.

It is possible to distinguish two types of fluid inclusions. In direction from the oldest 1<sup>st</sup> gold-bearing sulphide stage to pyrite-arsenopyrite, carbonate-stibnite and stibnite-kermesite mineralizations of 2<sup>nd</sup> – 4<sup>th</sup> stages, the evolution of fluids is as follows:

Generally, the first type of inclusions is typical for secondary inclusions in the oldest quartz coexisting with gold-bearing arsenopyrite-pyrite. The salinity of these fluids is low: 6-11 wt % NaCl equiv. Temperatures of the eutectic point vary from -45 to -55°C and the fluid density is 0.88 g/cm<sup>3</sup>. The estimated pressure is about 3 kbar. These fluids were of endogenous-metamorphogenous (or magmatic) origin.

The second type is represented by aqueous, moderately saline, NaCl ± CaCl<sub>2</sub> bearing inclusions. They are typical for stibnite-sulphosalts mineralization of 2<sup>nd</sup> and 3<sup>rd</sup> stages. Homogenization temperatures range between 145-200 °C (Tab. 5). The salinity of the fluids is ranging from 7 to 25 mol % NaCl equiv. The temperature of crystallization changes according to way of calculations used. An increasing role of meteoric water and their intensive mixing with endogenous fluids during its penetration into the wall rock and during metamorphic process is suggested.

The salinity of CaCl<sub>2</sub>-NaCl-H<sub>2</sub>O solutions of the 4<sup>th</sup> stage ranges from 8 to 25 wt. % CaCl<sub>2</sub> equiv. The homogenization temperatures are low: 82-199°C (Tab. 5). The importance of meteoric water is equal or more significant as in the case of the fluids of the 2<sup>nd</sup> and 3<sup>rd</sup> stage.

Thermal maturation of organic matter from ore-bearing black schists from Pezinok deposit is in meta-anthracite and semigraphite stages and indicates temperatures close to 400°C.

## Acknowledgements

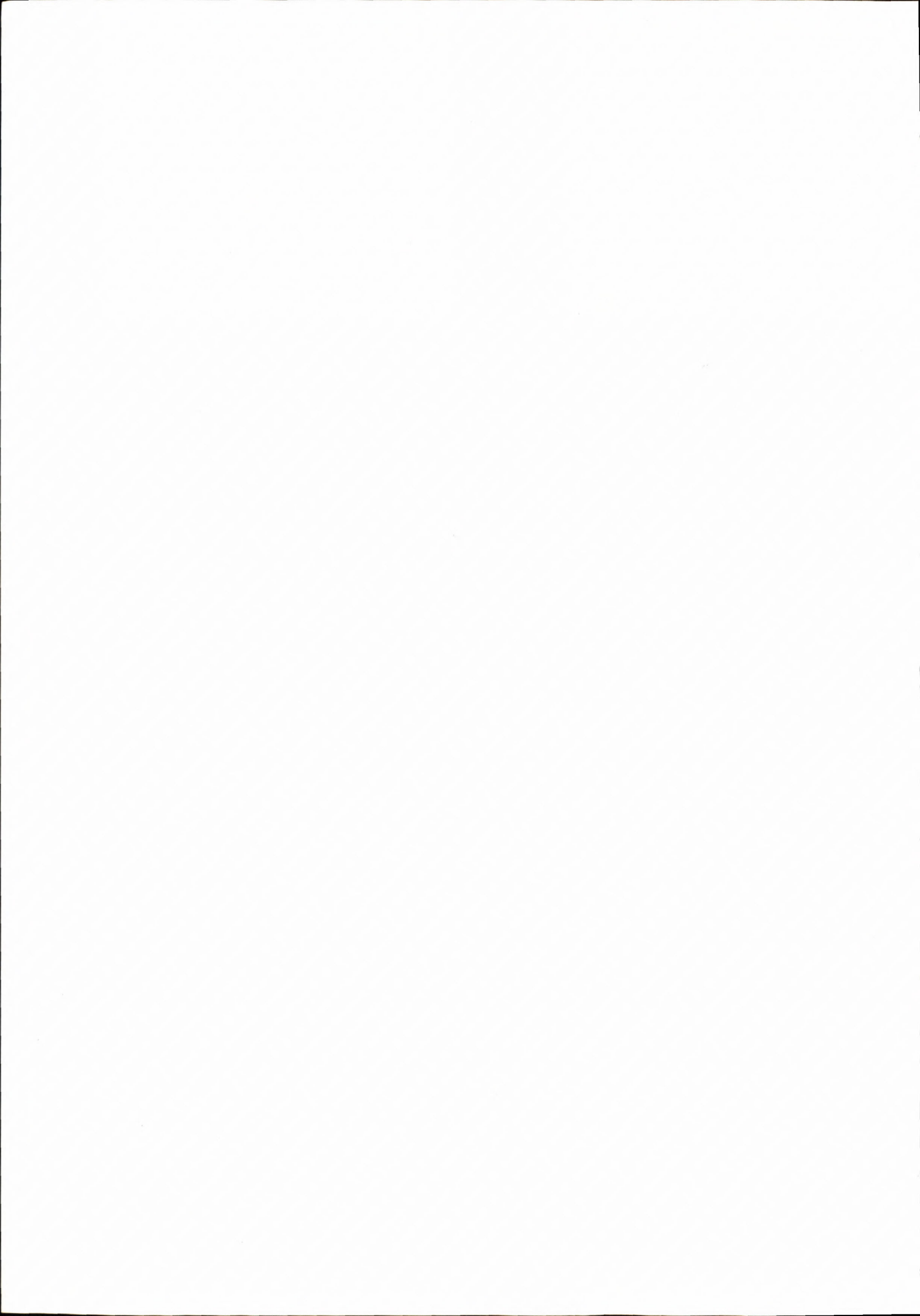
This study has been financially supported by grant 2/1138/21 of agency VEGA of Ministry of Education of the Slovak Republic and of Slovak Academy of Sciences.

The authors wish to thank to Dr. I. Repčok, CSc. from Geological Survey of Slovak Republic, Bratislava and to Assoc. Prof. M. Chovan, PhD. from the Comenius University, Bratislava for invaluable comments. They are also thankful to Dr. D. Dubaj for thermometric measurements, to Dr. A. M. Fouillac from BRGM, Orléans, France for ICP/MS - laser ablation analyses and to Dr. M. Králík (Vereinigung der kooperativen Forschungsinstitute der österreichischen Wirtschaft) for Pb-isotope analyses of stibnite and to Mrs. Nataša Halašiová for the technical works.

## References

- Andráš, P., 1983: Problems of the genesis of stibnite and gold mineralization at the deposit Pezinok. PhD Thesis, Manuscript, Geofond (Bratislava), 1-159
- Andráš, P. & Horváth, I., 1985: Thermoanalytical study of the metamorphism grade in Malé Karpaty Mts. region. *Geologický Zborník - Geologica Carpathica* (Bratislava), 36, 1, 75-84.
- Andráš, P., Dubaj, D. & Kotulová, J., 1998: Application of arsenopyrite geothermometer from Pezinok deposit (Western Carpathians, Slovakia). *Mineralia Slovaca* (Bratislava), 30, 2, 147-156
- Barker, C.E. & Pawlewitz, M.J. (1986): The correlation of vitrinite reflectance with maximum temperature in humic organic matter. - In: Buntebarth, G. Stegena L. (Eds): *Paleogeothermics*, Lecture Notes in Earth Sciences, 5, Springer, Berlin, 79-93
- Barker, C.E. & Bone, Y. (1995): The minimal response to contact metamorphism by the Devonian Buchan Caves Limestone, Buchan Rift, Victoria, Org. *Geochem.*, Vol. 22, No. 1, pp. 151-164
- Borisenko, A., S., 1977: Izučenie solevogo sostava rastvorov gazo-voždikich vklučeníj v mineralach metodom kriometrii. *Geol. i Geofiz.* 8, 16-27
- Cambel, B., 1956: Genetical problems of ore mineralization in Malé Karpaty Mts. *Geologické práce, Zprávy* (Bratislava), 9, 5-27
- Cambel, B., 1959: Hydrotermálne ložiská v Malých Karpatoch, mineralógia a geochémia ich rúd. *Acta geol. geogr. Univ. Comen.*, Geogr. 3, 338 p.
- Cambel, B. & Khun, M., 1983: Geochemical characteristic of black shales from the ore-bearing complex of strata of the Malé Karpaty Mts. *Geol. Zborník - Geologica Carpathica* 34, 3 (Bratislava), 255 - 382.
- Cambel, B., Miklós, J., Khun, M. & Veselský, J., 1990: Geochemistry and petrology of clay-metamorphic rocks of the Malé Karpaty Mts. Crystalline complex. *Geol. Inst. Slovak. Acad. Sci., Bratislava*, 1-267
- Černyšev, I., Cambel, B. & Koděra, M., 1984: Lead isotopes in galena of the Western Carpathians. *Geologický Zborník - Geologica Carpathica* (Bratislava), 35, 3, 307-327
- Chovan, M., Oružinský, V., Viliňovič, V. & Ženiš, P., 1990: Mineralogical, geochemical and petrographic study of the drill-core from Pezinok-Trojárová. Manuscript, Geofond (Bratislava), 119
- Chovan, M., Rojkovič, I., Andráš, P. & Hanas, P., 1992: Ore mineralization of the Malé Karpaty Mts. (Western Carpathians). *Geologica Carpathica* 43, 5, 275-286
- Hunt, J., M., 1972: Distribution of carbon in crust of Earth. *Bull. Amer. Assoc. Petrol. Geologists*, 56 (Tulsa) 2273-2277
- Hurai, V., 1988: P-V-T-X tables of water and x-25 weight percent NaCl-H<sub>2</sub>O solutions to 500 °C and 5000 x 10<sup>5</sup> Pa., *Acta geol. Geogr. Univ. Comen.*, 44

- Ilavský, J., 1979: Metallogenese de l'Europe alpine centrale et du sud-est. Geol. Inst. of D. Štúr, Bratislava, 414 p.
- Kantor, J., 1974: Sulphur isotopes of the stratiform pyrite deposit Turecký vrch and stibnite deposit Pezinok in the Malé Karpaty Mts. crystalline. Geol. Zborn. Geol. Carpath. (Bratislava), 25, 3, 311-334
- Kretschmar U & Scott S. D., 1976: Phase relations involving arsenopyrite in the system Fe-As-S and their application. *Canad. Mineralogist* 14, 364-368
- Míkula, P., 1992 b: Najnovšie výsledky geologického prieskumu na Zlatej žile v Malých Karpatoch. 8. Banícka vedecko-technická konferencia s medzinárodnou účasťou. Košice, 24-31
- Mrákava, F., 1987: Sprievodné zlato v antimónovej rúde ložiska Pezinok. In: Zlato na Slovensku, Jarkovská, J. & Beňka, J. Edit., (GÚDŠ, Bratislava) 41-44
- Oakes Ch. S., Bodnar R. J., Simonson J. M. (1990): The system NaCl-CaCl<sub>2</sub>-H<sub>2</sub>O: I. The ice liquidus at 1 atm total pressure. *Geochim. Cosmochim. Acta*, 54, 603-610.
- Polák, S., 1956: Relikty intrastratifikačných korugácií v metamorfovaných pezinských pyritových zrudneniach. *Geol. Práce - Zpr.* (Bratislava), 8, 78-87
- Potter, R. W., 1977: Pressure corrections for fluid-inclusion homogenization temperatures based on the volumetric properties of the system NaCl-H<sub>2</sub>O. *J. Res. USGS*, 5, 603-607
- Roedder, E., 1984: Fluid inclusions. *Mineral. Soc. Amer. Rev. Min.* 12, 644
- Sachan, H., K. & Chovan, M., 1991: Thermometry of arsenopyrite-pyrite mineralization in the Dúbrava antimony deposit (Western Carpathians *Geologica Carpathica*) 42, 5, 265-269
- Stacey, J. S. & Kramers, J. D., 1975: Approximation of terrestrial lead isotope evolution by a two-stage model. *Earth Planet. Sci. Lett.* 26, 207
- Sundblad, K., Zachrisson, E., Smers, S. H., Berglund, S. & Alinder, C., 1984: Sphalerite geobarometry and arsenopyrite geothermometry applied to metamorphosed sulfide ores in the Swedish Caledonides. *Econ. Geol.* 79, 1660-1668
- Uher, P., Michal, S. & Vítaloš, J., 2000: The Pezinok antimony mine, Malé Karpaty Mts., Slovakia. *The Mineralogical Record*, 31, 153-162
- Zhang-Frantz (1987): Determination of the homogenization temperatures and densities of supercritical fluids in the system NaCl-KCl-CaCl<sub>2</sub>-H<sub>2</sub>O using synthetic fluid inclusions. *Chemical Geology*, 64, 335-350.



## Distribution of Si in Stream Sediments of Slovakia – an Amendment to the Geochemical Atlas of the Slovak Republic

STANISLAV RAPANT<sup>1</sup>, DUŠAN BODIŠ<sup>1</sup>, DANIELA MACKOVÝCH<sup>2</sup>, & SILVESTER PRAMUKA<sup>2</sup>

<sup>1</sup>Geological Survey of the Slovak Republic, Mlynská dolina 1, 817 04 Bratislava

<sup>2</sup>Geological Survey of the Slovak Republic, Regional Centre Spišská Nová Ves

*Abstract.* Distribution and geochemical characteristics of silicon in stream sediments of Slovakia are presented in this paper. Si contents have been evaluated additionally from laboratory records, archived from the samples from the Geochemical Atlas of the Slovak Republic, part VI. – Stream Sediments. It was possible to credibly additionally evaluate and determine Si contents in 22 920 samples from the original 24 432 samples of stream sediments. Si contents in stream sediments range from 0.37 % to 46.13 %. Average content is 29.02 % (arithmetic mean), or 29.95 % (median), respectively. Si content in stream sediments is controlled mainly by its concentration in rock substrate of their source areas and by geochemical processes during weathering and migration. Si is the most abundant element in rock environments as well as in stream sediments. Particularly thanks to the high resistance of Si minerals during weathering and migration the average Si contents in stream sediments in source areas of various rock types differ between each other significantly less than in primary rocks of the source areas. The lowest average values of Si contents have been documented in the source areas of Mesozoic limestones and dolomites (23.48 %) and the highest in the rock environment of sandstones and siltstones of the Outer Carpathians (32.07 %).

*Key words:* silicon, stream sediment, Geochemical Atlas, Slovak Republic

### Introduction

During geochemical mapping of stream sediments in the framework of Geochemical Atlases of Slovakia programs (Vrana et al., 1997) 24 432 samples have been collected, that were analysed for total contents of 35 elements. Possibly due to conventional reasons, one of the most important main elements – silicon has not been determined, similarly to nearly all other national geochemical atlases (apart from Finland– Koljonen, T. (ed.) 1992), published at the end of 20<sup>th</sup> century. By the laboratory processing of the Geochemical Atlas of River Sediments of Slovakia (Bodiš – Rapant, eds. 1999) a fraction of each sample has been archived, so as it would be able to use it for consecutive laboratory works (e.g. to apply an analytical technique with more sensitive detection limits or to analyse elements not originally determined). In the same way, all laboratory analytical records, which contain also element records that were not originally evaluated, are archived.

As Si represents a very significant major element, important especially for interpretation of genesis of river sediments and rock weathering, its concentrations have been evaluated additionally from archived laboratory records. It was possible to additionally evaluate and determine Si contents in 22 920 samples from the original 24 432 samples of stream sediments, representing nearly 94 % of the total number of sample materials of the Geo-

chemical Atlas of Slovakia. Below, a concise geochemical characteristics and distribution of Si in stream sediments of Slovakia is reported, as it was presented at other elements in the framework of the Geochemical Atlas (Bodiš – Rapant, eds. 1999).

### Sampling, processing of samples and chemical analyses

Stream sediments have been sampled in the statistical density 1 sample per 2 km<sup>2</sup> and after drying they have been sieved to the fraction below 0.125 mm. For the quantitative analyses of silicon in stream sediments, atomic emission spectrometry with inductively coupled plasma (AES-ICP) method has been used after preliminary decomposition of samples by sintering with hydrogen peroxide.

Stream sediment samples were decomposed by sintering with Na<sub>2</sub>O<sub>2</sub> in a Pt crucible at the temperature 490 °C for the duration of 30 minutes. After termination of sintering and cooling, the content of the Pt crucible has been dissolved in HCl (1+1) and a deposit solution has been prepared. Chemicals with pure p.a. have been used. Simultaneously, with every sample series a blank experiment has been prepared for the used chemicals. Silicon was analysed on the simultaneous spectrometer of the firm ARL 34 000. In order to remove physical influences, related to the atomisation of samples with high content of dissolved components, to the transport of samples, etc.,

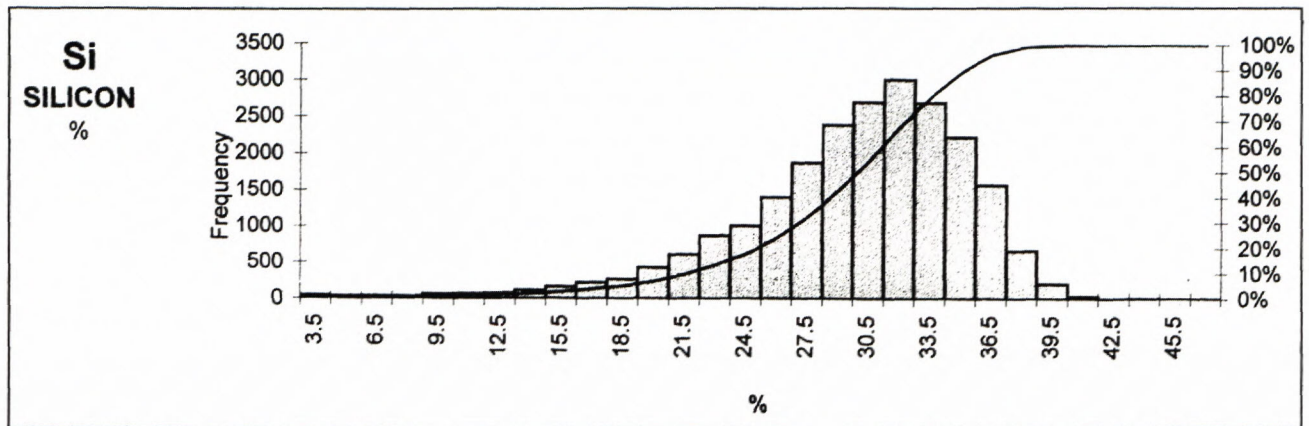


Table 1 Basis statistical characteristics of Si in stream sediments of Slovakia

Statistical Parameters		Classes	Frequency	Cumulative %	Classes	Frequency	Cumulative %
Arithmetic mean	29.022	3.5	45	0.20 %	26.0	1 407	23.87 %
Standard deviation	5.656	5.0	31	0.33 %	27.5	1 881	32.08 %
Geometr. mean	28.246	6.5	34	0.48 %	29.0	2 394	42.53 %
Median	29.950	8.0	35	0.63 %	30.5	2 704	54.32 %
Minimum	0.370	9.5	63	0.91 %	32.0	3 014	67.47 %
Maximum	46.130	11.0	67	1.20 %	33.5	2 696	79.24 %
25 %-il	26.250	12.5	78	1.54 %	35.0	2 236	88.99 %
75 %-il	32.940	14.0	120	2.06 %	36.5	1 577	95.87 %
99 %-il	38.220	15.5	168	2.80 %	38.0	670	98.80 %
Confidence level (95 %)	0.073	17.0	221	3.76 %	39.5	212	99.72 %
Detection limit	0.005	18.5	269	4.93 %	41.0	40	99.90 %
		20.0	432	6.82 %	42.5	8	99.93 %
Number of samples below Detection limit	0	21.5	616	9.51 %	44.0	10	99.97 %
		23.0	874	13.32 %	45.5	3	99.99 %
		24.5	1 012	17.74 %	<45.5	3	100.00 %

Table 2 Si contents in stream sediments of Slovakia sorted according to main rock types of source areas

Rock environment	Mean	Median	St. deviation	n
Neogene sediments	29.37	30.39	5.26	7 508
Neogene volcanics	28.10	28.35	4.04	2 614
Inner Carpathian Paleogene	30.24	31.24	5.32	2 535
Cretaceous and Paleogene of Outer Carpathians	32.07	32.80	4.23	4 296
Mesozoic carbonates	23.48	24.96	7.76	2 188
Mesozoic sediments other than carbonates	26.67	27.66	6.26	632
Inner Carpathian Late Paleogene	28.14	28.82	4.47	594
Inner Carpathian Early Paleogene	29.49	29.95	3.60	491
Tatricum and Veporicum basement	27.52	27.92	4.13	734
Inner Carpathian plutonites	27.70	28.21	3.95	1 247

Note: Contents are expressed in %, n = number of samples, rock types correspond to types according to Marsina et al, (1999).

the internal reference element Cd has been used. Thereby, improved, short-time and long-time, reproducibility has been achieved. Analytical signal has been evaluated using the calibration curve technique. Detection limit was 0.005 % Si. The accuracy and correctness has been tested on certified reference materials of river sediments GBW 07309, 07310.

#### Properties and distribution of silicon

After oxygen, silicon is the second most wide-spread element in earth's crust from the point of view of mass. In the nature it occurs almost exclusively in the oxidation level +4. It has a sharp affinity to oxygen and its bonds with oxygen in quartz or in silicates in the form of  $[\text{SiO}_4]^{4-}$  tetrahe-

drons have characteristic high strength in all geochemical conditions. During weathering processes the most widespread Si mineral – quartz is liable mainly to mechanical abrasion. Subject to normal PT conditions it is virtually insoluble in water (the solubility reaches 6–10 mg.kg<sup>-1</sup>) and chemical decomposition virtually does not occur. During weathering, other main and rock-forming minerals of silicon, silicates as well as aluminosilicates – e.g. feldspars, micas, olivines etc., are liable to partial or total hydrolysis, accompanied by the origin of hydrosilicates and hydroaluminosilicates in the form of hydromicas and clay minerals. At the same time the release and removal of a part of the silicon always occur, namely in the form of soluble silicates (especially Na and K), or in a colloid form. In term of Si content in stream sediments, the high weathering resistance of silicate rocks is essential. In stream sediments, similarly to sedimentary rocks, relative enrichment in silicon occurs thanks to the high resistance of Si minerals during weathering, while the SiO<sub>2</sub> concentrations often reach up to 90 % (more than 40 % Si).

Average silicon content in the continental crust is 263 580 mg.kg<sup>-1</sup> (Taylor, McLennan, 1985). Sandstones reach the highest concentrations (403 000 mg.kg<sup>-1</sup>) and in granites and granodiorites their contents are 337 000 mg.kg<sup>-1</sup>. Silicon has the lowest concentration in limestones (31 000 mg.kg<sup>-1</sup>). Average silicon content in fine fraction of glacial sediments (till) in Finland is 28.8±2.3 % (Koljonen, 1992). For instance, average Si contents in river sediments are 27.34 % for Czech Republic (fraction below 0.063 mm, median of 150 samples from main rivers, Veselý, 1995) and 298 388 mg.kg<sup>-1</sup> for the region of Harz, Germany – (fraction below 0.063 mm, median, in Reimann – Caritat, 1998). In natural ground and surface waters Si contents range from milligrams up to first tenths of milligrams per liter. Estimated average Si content in world ocean is 2.2 mg.l<sup>-1</sup> (Reimann – Caritat, 1998).

Silicon is an essential element for many organisms. It influences the growth, as it affects the building-up of the skeleton. As a nutrient, it is important just for a few organisms (e.g. diatomites). Some sorts of grasses are able to accumulate silicon. Silicon itself is not toxic, however, some of its compounds, e.g. asbestos, are carcinogenic. Silicon oxide is a fibroid causing silicosis.

Generally, natural sources of silicon prevail over its antropogenic sources, to which production of cement, quartz, building materials, etc., belong.

In natural conditions the environmental mobility of quartz is very low, namely in acid to neutral up to alkaline, as well as in oxidizable and reductive conditions.

The average Si content in stream sediments of Slovakia is 29.02±5.5 % and the median is 29.95 %, suggesting relatively uniform distribution of values. The maximum determined concentration is 46.13 %, while the minimum concentration is 0.37 % (table 1). In table 2 average Si contents in stream sediments, sorted according to basic types and rock substrate composition of source areas, are presented.

The distribution of silicon in stream sediments of Slovakia (fig. 1) has several typical features. The highest

concentrations (over 35 %) are focused into the region of Outer Flysh Belt, crystalline core of core mountains and Neogene volcanics of Slánske Vrchy Mts. and Vihorlat-ské vrchy Mts. This also indicates their source areas. The lowest silicon contents are present in source areas formed by Mesozoic limestones and dolomites (3–15 %) and in aluvial Quaternary sediments of the river Danube in Podunajská Nížina lowland (10–25 %).

In the rock environments, from the point of view of source areas, sandstones (37 %) granitoids (35 %), rhyolites and ryodacites (34 %), andesites (28 %) have the highest average contents of silicon and, on the contrary, limestones (0.6 %) and dolomites (0.4 %) have the lowest concentrations of silicon (Marsina et al., 1999). While Si contents in stream sediments in source areas, formed by silicite rocks (sandstones, shales, granitoids, andesites), roughly correspond to their contents in source rocks, in areas with low Si contents in primary rocks (especially limestones and dolomites) an apparent enrichment in silicon occurs in stream sediments, mainly at the expense of calcium and magnesium contents. This implies that the distribution of silicon, calcium and magnesium in stream sediments has its regularity and it is controlled not just by contents of the above elements in rock substrate but also by the character and intensity of geochemical processes during weathering, transport and sedimentation. The complicated and, from the lithological point of view, very variable geological structure of the Slovak Republic is also very significant. In stream sediments these relations have been also tested using the correlation analyse with the following correlation coefficients: Si-Ca = -0.758; Si-Mg = -0.689 and Ca-Mg = 0.642. By other words, the distribution of silicon is indirectly proportional to the distribution of calcium and magnesium, while the concentration of both of these elements decreases with increasing silicon content. The distribution of Si/Ca (fig. 2) and Si/Mg (fig. 3) ratios also document this regularity. The source areas, formed by clastic sediments of the Outer Flysh Belt, have the maximum influence on the high concentrations of silicon in the Východoslovenská Nížina lowland that, unlike the Podunajská Nížina lowland, has much higher silicon contents. The sediments of the Podunajská Nížina lowland have different source areas, which is also mirrored in Si/Ca and Si/Mg ratio values that are below 1.84 and 6.78, respectively. This is also reflected by the high content of carbonates in soil profile of the Podunajská Nížina lowland (Čurlík – Šefčík, 1999). Lower Si content is probably also influenced by the decomposition of more soluble Si minerals (feldspars) during long transport in Danube, and furthermore in the Danube sandy gravels a relative enrichment in insoluble quartz occurred. The prevailing lower silicon content in the area of Central Slovakia Neogene Volcanic Field, compared to the Eastern Slovakian Volcanic Field, is also interesting. Here probably the influence of Flysh Belt source areas has also occurred, that is best observable in the Ondava river basin.

The radius of the silicon migration from the source areas is relatively large. Silicon migrates most often in the

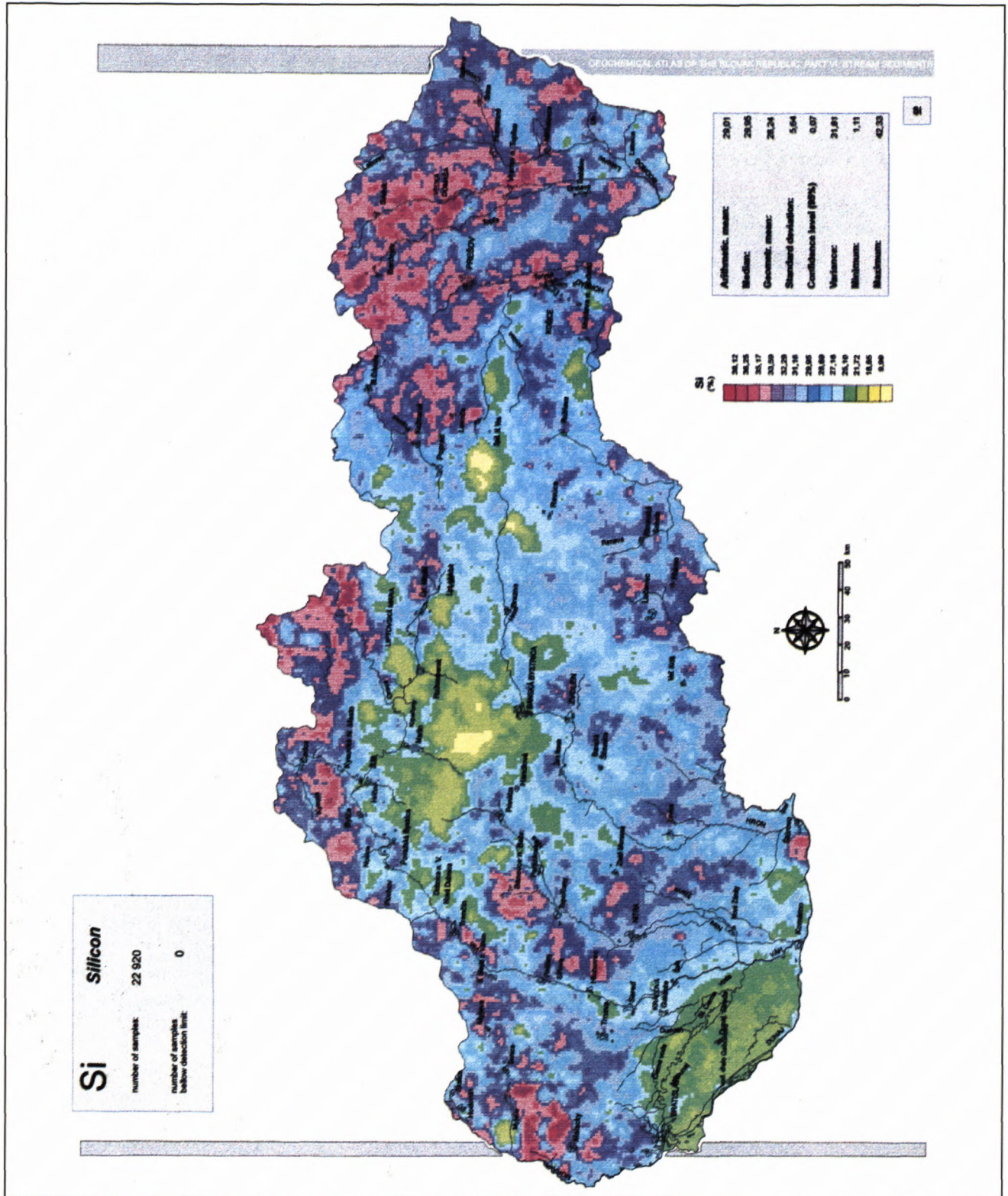


Fig. 1 Distribution of Si in stream sediments

form of quartz, that virtually does not have a geochemical barrier, and the migration is realised especially in a mechanical way. The distribution of silicon in stream sediments is proportional mainly to the distribution of calcium and magnesium. Due to different migration forms of these elements a mutual overlapping of their anomalies and thereby local, or eventually regional, variations can occur.

### Conclusions

In the paper, the distribution of silicon in stream sediments of Slovakia is presented, those analyses have been evaluated additionally from samples from the Geochemical Atlas of the Slovak Republic, part VI. – River Sediments (Bodiš – Rapant, eds. 1999). From the achieved

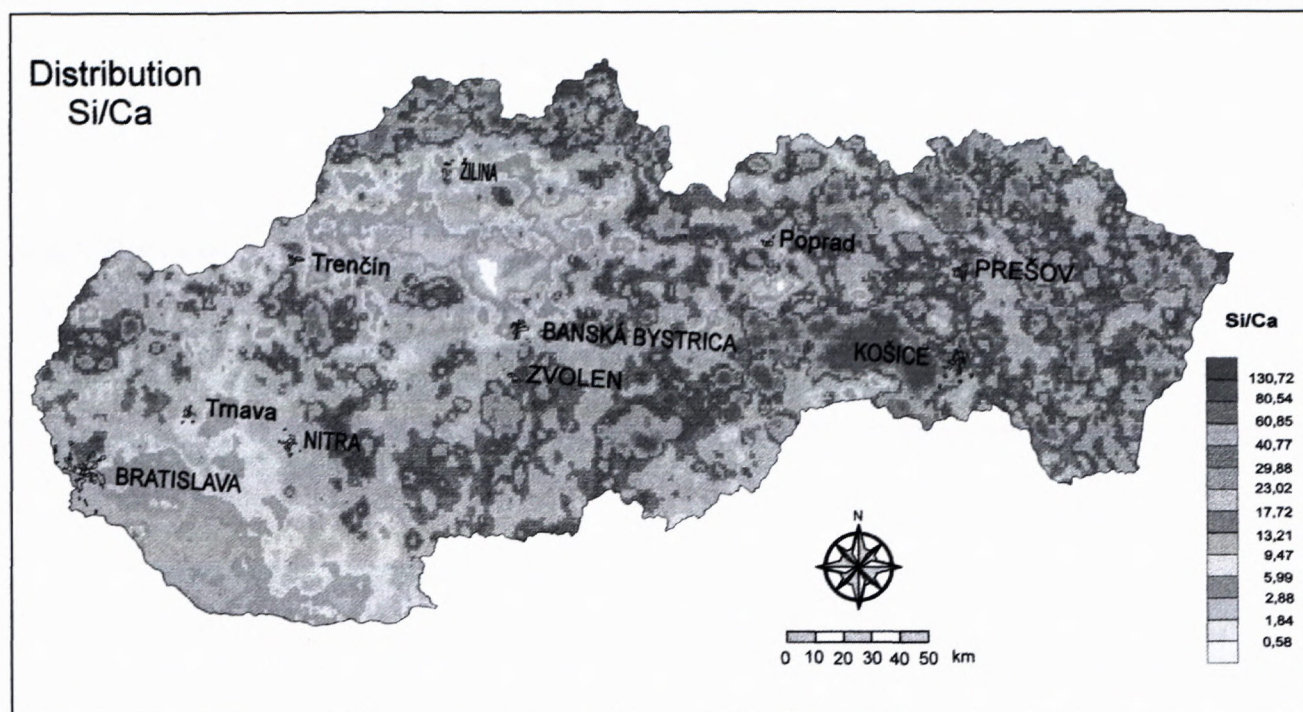


Fig. 2 Distribution of Si/Ca in stream sediments

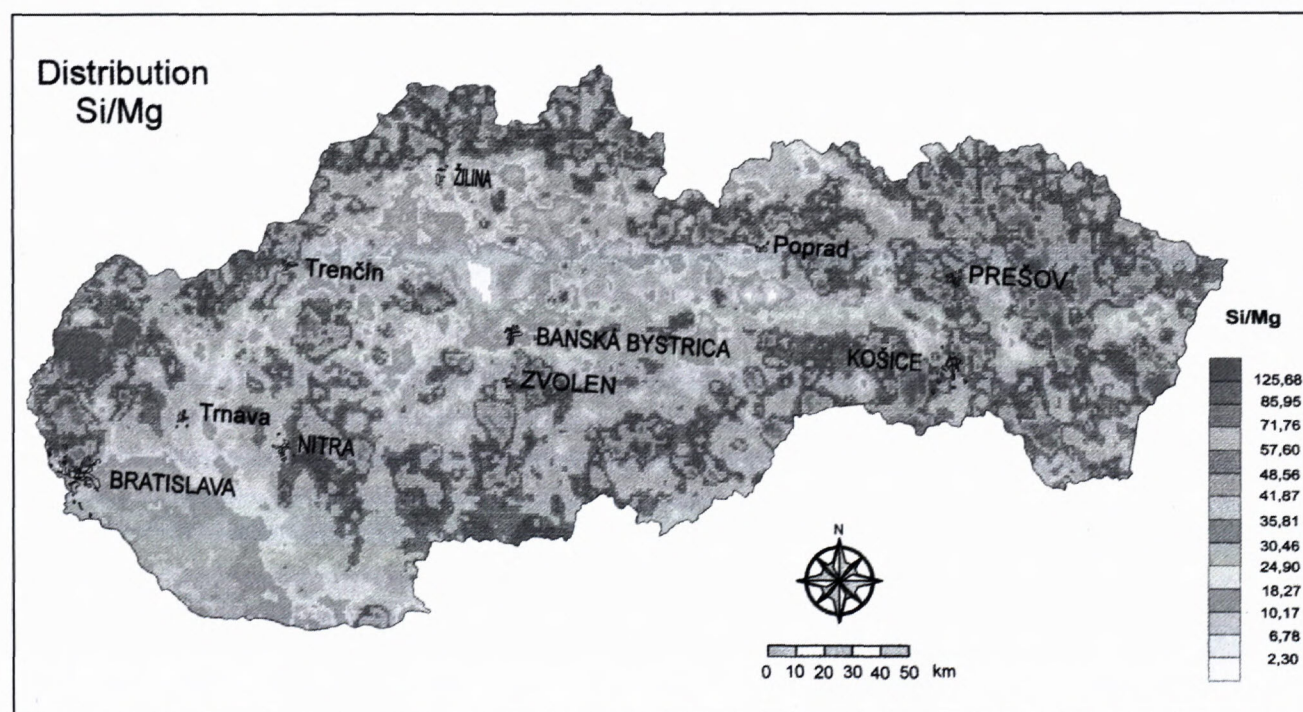


Fig. 3 Distribution of Si/Mg in stream sediments

results it is clear that Si content in stream sediments is mainly controlled by its content in rock substrate and by geochemical processes during weathering and migration. Si is the most abundant element in the rock substrate as well as in stream sediments. In stream sediments of Slovakia the radius of silicon migration from source areas is relatively large. In the conditions of the Slovak Republic it represents the order of up to tenths of kilometres.

Especially due to the high resistance of Si minerals during weathering and migration the average Si contents in stream sediments in areas of various rock types differ between each other apparently less than in primary rocks, forming source areas.

Si content is known and published for various natural environs. From the regional point of view mean Si concentrations are assessed, e.g. for different sorts of soils

(agricultural, woodland, municipal, topsoil, etc.), natural waters (ground, surface and precipitation), stream flat sediments, etc. However, in literature in regional studies Si contents in stream sediments are published rarely only. Consequently, the presented information about contents and distribution of Si in stream sediments of Slovakia can be important from the point of view of knowledge and mapping of silicon in stream sediments not just in Slovakia but world-wide as well.

### Literature

- Bodiš, D., Rapant, S., Khun, M., Klukanová, A., Lexa, J., Mackových, D., Marsina, K., Pramuka, S. & Vozár, J. 1999: *Geochemical Atlas of Slovak Republic-part VI.- Stream sediments*. Monography, Geol. Survey of Slovak Republic, Bratislava, 145 p.
- Čurlík, J. & Šefčík, P. 1999: *Geochemical Atlas of Slovak Republic – part V. – Soils*, Monography, VÚPOP, Bratislava. 99 p.
- Koljonen, T. (ed.) 1992: *The Geochemical Atlas of Finland, part 2: Till*. Geological Survey of Finland, Espoo, 218 p.
- Marsina, K., Bodiš, D., Havrila, M., Janák, M., Káčer, Š, Kohút, M., Lexa, J., Rapant, S. & Vozárová, A. 1999: *Geochemical Atlas of Slovak Republic-part III.- Rocks*. Monography, Geol. Survey of Slovak Republic, Bratislava, 134 p.
- Rapant, S., Vrana, K. & Bodiš, D. 1996: *Geochemical Atlas of Slovakia-part I.-groundwater*. Monography, Geol. Survey of Slovak Republic, Bratislava, 127 p.
- Reimann, C. & Caritat, P. 1998: *Chemical Elements in the Environment*. Springer, Berlín, 397 p.
- Taylor, S. R. & McLennan, S. M. 1985: *The continental crust: Its composition and Evolution*. Blackwell Scientific Publications, 312 p.
- Veselý, J. 1995: *Drainage sediments in environmental and exploration geochemistry*. Vestník Českého geologického ústavu 70, 3, p. 1–8.
- Vrana, K., Rapant, S., Bodiš, D., Marsina, K., Lexa, J., Pramuka, S., Maňkovská, B., Čurlík, J., Šefčík, P., Vojtaš, J., Daniel, J. & Lucivianský, L. 1997: *Geochemical Atlas of Slovak Republic at a scale 1 : 1 000 000*. Journal of Geochemical Exploration, 60, p. 7–37.



## Instructions for authors

Slovak Geological Magazine – periodical of the Geological Survey of Slovak Republic is quarterly presenting the results of investigation and researches in wide range of topics: regional geology and geological maps, lithology and stratigraphy, petrology and mineralogy, paleontology, geochemistry and isotope geology, geophysics and deep structure, geology of deposits and metallogeny, tectonics and structural geology, hydrogeology and geothermal energy, environmental geochemistry, engineering geology and geotechnology, geological factors of the environment, petroarcheology.

The journal is focused on problems of the Alpine-Carpathian-Balkan region

### General instructions

The Editorial Board of the Geological Survey of Slovak Republic – Dionýz Štúr Publishers accepts manuscripts in correct English. The papers that do not have sufficient accuracy in language level will be submitted back for language correction.

The manuscript should be addressed to the Chief Editor or the Managing Editor.

Contact address:

Geological Survey of Slovak Republic – Dionýz Štúr Publishers,  
Mlynská dolina 1, 817 04 Bratislava, Slovak Republic  
e-mail addresses: hok@gssr.sk  
gabina@gssr.sk  
http://www.gssr.sk

The Editorial Board accepts or refuses a manuscript with regard to the reviewer's opinion. The author is informed of the refusal within 14 days from the decision of the Editorial Board. Accepted manuscript is prepared for publication in an appropriate issue of the Magazine. The author(s) and the publishers enter a contract establishing the rights and duties of both parties during editorial preparation and printing, until the time of publishing of the paper.

### Text layout

The manuscript should be arranged as follows: TITLE OF THE PAPER, FULL NAME OF THE AUTHOR(S); NUMBER OF SUPPLEMENTS (in brackets below the title, e.g. 5 figs., 4 tabs.), ABSTRACT (max. 30 lines presenting principal results) – KEY WORDS – INTRODUCTION – TEXT – CONCLUSION – ACKNOWLEDGEMENTS – APPENDIX – REFERENCES – TABLE AND FIGURE CAPTIONS – TABLES – FIGURES. The editorial board recommends to show a localisation scheme at the beginning of the article.

The title should be as short as possible, but informative, compendious and concise. In a footnote on the first page, name of the author(s), as well as his (their) professional or private address.

The text of the paper should be logically divided. For the purpose of typography, the author may use a hierarchic division of chapters and sub-chapters, using numbers with their titles. The editorial board reserves the right to adjust the type according to generally accepted rules even if the author has not done this.

**Names of cited authors** in the text are written without first names or initials (e.g. Štúr, 1868), the names of co-authors are divided (e.g. Andrusov & Bystrický, 1973). The name(s) is followed by a comma before the publication year. If there are more authors, the first one, or the first two only are cited, adding et al. and publication year.

**Mathematical and physical symbols** of units, such as %, ‰, °C should be preceded by a space, e.g. 60 %, 105 °C etc. Abbreviations of the units such as second, litre etc. should be written with a gap. Only SI units are accepted. Points of the compass may be substituted by the abbreviations E, W, NW, SSE etc. Brackets (parentheses) are to be indicated as should be printed, i.e. square brackets, parentheses or compound. Dashes should be typed as double hyphens.

If a manuscript is typed, 2 copies are required, including figures. The author should mark those parts of a text that should be printed in different type with a vertical line on the left side of the manuscript. Paragraphs are marked with 1 tab space from the left margin, or by a typographic symbol. Words to be emphasized, physical symbols and Greek letters to be set in other type (e.g. *italics*) should be marked. Greek letters have to be written in the margin in full (e.g. *sigma*). Hyphens should be carefully distinguished from dashes.

### Tables and figures

**Tables** will be accepted in a size of up to A4, numbered in the same way as in a text.

Tables should be typed on separate sheets of the same size as text, with normal type. The author is asked to mark in the text where the table should be inserted. Short explanations attached to a table should be included on the same sheet. If the text is longer, it should be typed on a separate sheet.

**Figures** should be presented in black-and-white, in exceptional cases also in colour which must be paid approx. 100 EUR per 1 side A4. Figures are to be presented by the author simultaneously with the text of the paper, in two copies, or on a diskette + one hard copy. Graphs, sketches, profiles and maps must be always drawn separately. High-quality copies are accepted as well. Captions should be typed outside the figure. The graphic supplements should be numbered on the reverse side, along with the orientation of the figures. Large-size supplements are accepted only exceptionally. Photographs intended for publishing should be sharp, contrast, on shiny paper. High quality colour photographs will only be accepted depending on the judgement of the technical editors.

If a picture is delivered in a digital form, the following formats will be accepted: \*.cdr, \*.dxf, \*.bmp, \*.tiff, \*.wpg, \*.fga., \*.jpg \*.gif, \*.pcx. Other formats are to be consulted with the editors.

### References

Should be listed in alphabetical and chronological order **according to annotation in the text** and consist of all references cited.

Standard form is as follows: 1. Family name and initials of author(s), 2. Publication year, 3. Title of paper, 4. Editor(s), 5. Title of proceedings, 6. Publishers or Publishing house and place of publishing, 7. Unpublished report – manuscript should be denoted MS. Unpublished paper can appear as personal communications only. 8. Page range

Quotations of papers published in non-Latin alphabet or in languages other than English, French, Italian, Spain or German ought to be translated into English with an indication of the original language in parentheses, e.g.: (in Slovak).

Example:

Andrusov, D., Bystrický, J. & Fusán, O., 1973: *Outline of the Structure of the West Carpathians*. Guide-book for geol. exc. of X<sup>th</sup> Congr. CBGA. Bratislava: Geol. Úst. D. Štúra, 44 p.

Beránek, B., Leško, B. & Mayerová, M., 1979: Interpretation of seismic measurements along the trans-Carpathian profile K III. In: Babuška, V. & Plančár, J. (Eds.): *Geodynamic investigations in Czecho-Slovakia*. Bratislava: VEDA, p. 201-205.

Lucido, O., 1993: A new theory of the Earth's continental crust: The colloidal origin. *Geol. Carpathica*, vol. 44, no. 2, p. 67-74.

Pitoňák, P. & Spišiak, J., 1989: Mineralogy, petrology and geochemistry of the main rock types of the crystalline complex of the Nízke Tatry Mts. MS – Archiv GS SR, Bratislava, 232 p. (in Slovak).

### Proofs

The translator as well as the author(s) are obliged to correct the errors which are due to typing and technical arrangements. The first proofs are sent to author(s) as well as to the translator. The second proof is provided only to the editorial office. It will be sent to authors upon request.

The proofs must be marked clearly and intelligibly, to avoid further errors and doubts. Common typographic symbols are to be used, the list and meaning of which will be provided by the editorial office. Each used symbol must also appear on the margin of the text, if possible on the same line where the error occurred. The deadlines and conditions for proof-reading shall be stated in the contract.

### Final remarks

These instructions are obligatory to all authors. Exceptions may be permitted by the Editorial Board or the managing editor. Manuscripts not complying with these instructions shall be returned to the authors.

1. Editorial Board reserves the right to publish preferentially invited manuscript and to assemble thematic volumes,
2. Sessions of Editorial Board – four times a year and closing dates for individual volumes will be on every 31<sup>th</sup> day of March, June, September and December.
3. To refer to one Magazine please use the following abbreviations: *Slovak Geol. Mag.*, vol. xx, no. xx. Bratislava: D. Štúr. Publ. ISSN 1335-096X.

